

88-16

Edm.  
77008

# **WRIGHT-PATTERSON AIR FORCE BASE**

## **DYNAMIC TERRAIN INPUTS TO PREDICT STRUCTURAL INTEGRITY OF GROUND VEHICLES**

**M. W. Sayers**

**April 1988**

**UMTRI**

**The University of Michigan  
Transportation Research Institute**



Technical Report Documentation Page

|   |  |  |   |                            |           |
|---|--|--|---|----------------------------|-----------|
| 1. Report No.   |  | 2. Government Accession No.                  |   | 3. Recipient's Catalog No. |           |
| 4. Title and Subtitle<br>Dynamic Terrain Inputs to Predict Structural Integrity of Ground Vehicles  |  |  | 5. Report Date<br>April 1988  |                            |           |
|   |  |  | 6. Performing Organization Code   |                            |           |
| 7. Author(s)<br>M. W. Sayers  |  |  | 8. Performing Organization Report No.<br>UMTRI-88-16                        |                            |           |
| 9. Performing Organization Name and Address<br>The University of Michigan<br>Transportation Research Institute<br>2901 Baxter Road, Ann Arbor, Michigan 48109   |  |  | 10. Work Unit No. (TRAIS)   |                            |           |
|   |  |  | 11. Contract or Grant No.<br>F3615-87-M-3021                                |                            |           |
| 12. Sponsoring Agency Name and Address<br>US Air Force<br>Wright-Patterson Air Force Base, Ohio   |  |  | 13. Type of Report and Period Covered<br>Final<br>January 1988 — March 1988 |                            |           |
|   |  |  | 14. Sponsoring Agency Code  |                            |           |
| 15. Supplementary Notes   |  |  |   |                            |           |
| 16. Abstract<br><p>This report presents a study and evaluation of the technology and methodologies available for predicting the response of mobile ground equipment to dynamic input from terrain roughness. The purpose of the report is to develop a technical foundation for the subsequent formulation of military specifications for durability of ground vehicles used at air bases.</p> <p>The report reviews the techniques and methods that have been used successfully to (1) model and analyze vehicle response to road roughness, (2) characterize pavement inputs to various vehicle models, (3) develop a standard roughness scale—the International Roughness Index (IRI), and (4) measure pavement profile, road roughness, and vehicle response. Specialized instruments are described for the measurement of road profile. The modeling of road inputs is further developed, based in part on extensive measured profile data. In particular, the correlation between the left- and right-hand wheeltrack profiles is modeled to match actual road data.</p> <p>The report concludes by relating technology and methods to the Air Force environment. A standard road representation is tentatively proposed, with several types of roughness that are most relevant for predicting vehicle response and possible failure. Considerations are given for measuring profile, adopting a roughness index, and validating vehicle analyses.</p> |  |  |   |                            |           |
| 17. Key Words<br>road roughness, vehicle simulation, vehicle dynamics, profile measurement, PSD, correlated inputs, International Roughness Index (IRI), vehicle testing  |  |  | 18. Distribution Statement<br>Unlimited                                     |                            |           |
| 19. Security Classif. (of this report)<br>none  |  | 20. Security Classif. (of this page)<br>none |   | 21. No. of Pages<br>114    | 22. Price |



# TABLE OF CONTENTS

|   |     |
|---|-----|
| 1. INTRODUCTION.....  | 1   |
| 2. VEHICLE ANALYSIS METHODS.....                              | 3   |
| 2.1 Time-Domain Analyses.....                                 | 4   |
| 2.2 Frequency-Domain Analyses .....                           | 6   |
| 2.3 State Space Analyses .....                                | 16  |
| 2.4 Summary of Input Requirements.....                        | 19  |
| 3. RELATIONS BETWEEN ALTERNATIVE INPUT DESCRIPTIONS.....      | 21  |
| 3.1 Statistics for Random and Deterministic Signals .....     | 21  |
| 3.2 Correlation Between Multiple Wheeltrack Profiles.....     | 22  |
| 3.3 Conversions Between Statistics and Profiles .....         | 29  |
| 3.4 Speed Relationships .....                                 | 32  |
| 4. STANDARDIZED ROAD INPUTS.....                              | 34  |
| 4.1 Stationary Wheeltrack Profiles .....                      | 34  |
| 4.2 Models for Two Wheeltracks.....                           | 45  |
| 4.3 Corrugations.....   | 50  |
| 4.4 Localized Roughness .....                                 | 50  |
| 5. MEASURING ROAD ROUGHNESS.....                              | 54  |
| 5.1 Overview of Roughness Measures Used for Public Roads..... | 54  |
| 5.2 The International Roughness Index (IRI) .....             | 59  |
| 5.3 Roughness Measures and Vehicle Response .....             | 66  |
| 6. VALIDATION AND MEASUREMENT.....                            | 68  |
| 6.1 Basis for Comparisons .....                               | 68  |
| 6.2 Data Recording Requirements.....                          | 71  |
| 6.3 Measurement of Vehicle Response.....                      | 73  |
| 6.4 Measurement of "True Profile".....                        | 73  |
| 7. CONSIDERATIONS FOR AIR FORCE SPECIFICATIONS.....           | 93  |
| 7.1 Roughness Scale.....                                      | 93  |
| 7.2 Standardized Road Inputs .....                            | 94  |
| 7.3 Validation and Measurement.....                           | 98  |
| 7.4 Recommendations.....                                      | 102 |
| APPENDIX A—PSD COMPUTATION.....                               | 105 |
| APPENDIX B—SOURCE OF ROAD DATA.....                           | 108 |
| REFERENCES.....   | 109 |



## LIST OF FIGURES

|       |   |     |
|-------|---|-----|
| 2-1   | Quarter-car vehicle model.....  | 3   |
| 2.1-1 | Example of “wheelbase filtering” on a tandem suspension.....                    | 7   |
| 2.2-1 | PSD of vertical acceleration.....   | 11  |
| 2.2-2 | Relationship between input and output PSD functions.....                        | 14  |
| 2.3-1 | White noise.....  | 17  |
| 3.2-1 | Measured coherence functions between left- and right-hand wheeltrack profiles . | 23  |
| 3.2-2 | The “ribbon road” model.....  | 28  |
| 4.1-1 | PSDs of elevation, slope, and acceleration profile.....                         | 35  |
| 4.1-2 | Typical PSD functions for asphalt roads.....                                    | 37  |
| 4.1-3 | Typical PSD functions for surface treatment roads.....                          | 38  |
| 4.1-4 | Typical PSD functions for concrete roads.....                                   | 39  |
| 4.1-5 | Comparison between model PSD function and measurements.....                     | 41  |
| 4.1-6 | Distribution of low-wavenumber PSD model coefficients for measured data.....    | 43  |
| 4.1-7 | Distribution of high-wavenumber PSD model coefficients for measured data.....   | 44  |
| 4.1-8 | Effect of anti-aliasing filter on high wavenumbers.....                         | 46  |
| 4.2-1 | Use of a single-pole “shaping filter” to ratio PSD functions.....               | 48  |
| 4.3-1 | PSD functions showing corrugations on surface treatment roads.....              | 51  |
| 4.4-1 | Localized roughness in a PCC road.....  | 53  |
| 5.1-1 | A Profilograph.....   | 56  |
| 5.1-2 | The response-type system.....   | 57  |
| 5.2-1 | Response of the IRI quarter-car analysis.....                                   | 63  |
| 5.2-2 | Overview of the IRI roughness scale.....  | 65  |
| 5.3-1 | Response plots for acceleration, suspension rate, and tire load.....            | 67  |
| 6.1-1 | Comparison of simulated and measured vehicle response PSDs.....                 | 70  |
| 6.4-1 | The TRRL Beam profiling device.....   | 76  |
| 6.4-2 | The Dipstick profiling device.....  | 77  |
| 6.4-3 | The GM-type profiling system.....   | 78  |
| 6.4-4 | Comparison of mechanical and optical road followers in a GM-type system.....    | 80  |
| 6.4-5 | The Selcom laser height sensor.....   | 82  |
| 6.4-6 | The French APL profiling system.....  | 91  |
| 7.3-1 | Conceptual overview of tire enveloping.....                                     | 100 |





# 1. INTRODUCTION

This report presents a study and evaluation of the technology and methodologies available for predicting the response of mobile ground equipment to dynamic input from terrain roughness. The purpose of the report is to develop a technical foundation for the subsequent formulation of military specifications for durability of ground vehicles used at air bases. Contractors should be able to combine computer models of their candidate vehicle designs with standardized ground inputs to predict resulting motions and forces, which can be used to assess durability on typical paved terrain.

Pavement roughness encompasses all variations that cause vibrations in traversing vehicles. These variations include distinct localized pavement failures, such as potholes and slab misalignment, and also random deviations that reflect the practical limit of precision to which a pavement can be constructed and maintained. When travelling in a straight line, the input to each wheel is described by a longitudinal profile of the pavement. Thus, the ground input is normally treated as one or more longitudinal profiles.

A vehicle specification for pavement input involves three topics that are addressed in this report: (1) characterization of pavement roughness in a form suitable for the vehicle analysis, (2) a simple roughness scale that can be used to rank pavements, both real and simulated, and (3) the measurement requirements for experimental validation of the computer analyses.

The report is divided into seven sections, the first of which is this Introduction. The next three sections summarize the analytical methods used to predict vehicle response to road roughness. Section 2 reviews techniques for mathematically representing the dynamics of ground vehicles drawn from the fields of dynamics, control, vibrations, and random signal analysis. Section 3 describes how equivalent ground inputs can be represented for the various analyses covered in Section 2. Section 4 presents models of road roughness from the literature and from data collected by UMTRI in several recent research projects.

Section 5 reviews the testing and instrumentation requirements for validation of the vehicle analyses. A full-scale validation exercise requires the measurement of the input to the vehicle, which in this context is the road profile. Measurement of road profile is a highly specialized field that includes several new methods introduced in the past two years. This section reviews the valid methods that are known to the author as being in current use.

Section 6 departs from the vehicle dynamics viewpoints of the early sections, and looks at roughness from the perspective of the highway community. It summarizes the methods in use for measuring roughness, and describes the considerations behind the design of the first (and so far, the only) standard roughness scale, the International Roughness Index (IRI).

Section 7 concludes the report by discussing how the preceding material is pertinent to the development of a vehicle durability specification for standard ground inputs.

Recommendations are made for applying the material in the report toward the formulation of specifications.

Two appendices are attached with related material. Appendix A presents step-by-step details for a power spectral density (PSD) computation method recommended for road profiles. Appendix B describes the sources of road data used in the report.

## 2. VEHICLE ANALYSIS METHODS

This section reviews the general analytical techniques relevant to the analysis of vehicles responding to pavement roughness. To organize the following presentation, the methods are divided into three groups:

- time-domain analyses,
- frequency-domain analyses, and
- state-space analyses.

The following review is intended to provide an appreciation of how terrain inputs must be formulated for each type of analysis. It is also used to determine measurement requirements for validation activities.

The analyses are illustrated using the quarter-car representation of a ground vehicle shown below.

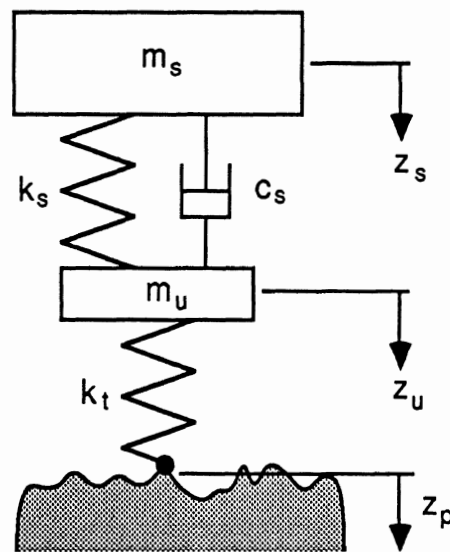


Figure 2-1. Quarter-car vehicle model.

The quarter-car example has two rigid bodies that move vertically, giving it two degrees of freedom. Two generalized coordinates and their derivatives are needed to describe the state of the system. The coordinates that will be used are the positions of the sprung and unsprung masses, designated  $z_s$  and  $z_u$ . In each type of analysis, generalized coordinates and other variables are defined such that the "state" of the system is specified by these variables.

## 2.1 Time-Domain Analyses

This category includes all analyses that simulate a real-world test on the computer or in the laboratory. For computer simulation, the response of a dynamic system is predicted using differential and algebraic equations that describe dynamic equilibrium at an instant in time. These equations are commonly called the equations of motion. The equations of motion are solved analytically or numerically to predict how the system variables change with time in response to inputs. Simulated responses are interpreted in the same manner as experimentally measured responses.

Most simulation work is performed via software running on a digital computer. The same basic methodology also applies to simulation by hardware, using an analog computer and/or a laboratory simulator. For example, prototype vehicles are sometimes tested for structural integrity using a road simulator. The simulator consists of servo-controlled hydraulic actuators that replicate vertical movements under a wheel that would be seen by a vehicle travelling over an uneven surface. The input requirements for this type of setup are identical to those of a computer-based time-domain analysis.

For the quarter-car example, the equations of motion can be obtained by summing the vertical forces acting on each of the two bodies in the system, and applying Newton's law  $F = ma$ . The resulting two equations are second-order, linear, ordinary differential equations:

$$m_s \ddot{z}_s + k_s (z_s - z_u) + c_s (\dot{z}_s - \dot{z}_u) = 0 \quad (2.1-1)$$

$$m_u \ddot{z}_u - k_s (z_s - z_u) - c_s (\dot{z}_s - \dot{z}_u) = k_t (z_p - z_u) \quad (2.1-2)$$

In these two equations, the quantities  $z_s$ ,  $\dot{z}_s$ ,  $\ddot{z}_s$ ,  $z_u$ ,  $\dot{z}_u$ ,  $\ddot{z}_u$ , and  $z_p$  vary with time. For such a simple model, a closed-form analytical solution for the variables can be derived. However, most vehicle models include more degrees of freedom, and may include nonlinear elements. Computer solution of the equations by numerical integration is required to obtain simulated time histories of the state variables.

Numerical integration of simultaneous, nonlinear, ordinary differential equations normally requires that the equations of motion be provided in the form of single-order, ordinary differential equations:

$$\dot{x}_i = f(t, x_1, x_2, \dots, x_n, u_1, \dots, u_m), i = 1, \dots, n \quad (2.1-3)$$

Where  $x_i$  ( $i=1\dots n$ ) are  $n$  state variables and  $u_j$  ( $j=1\dots m$ ) are  $m$  inputs. Given values of the state variables at time  $t$ , the values at a closely following time  $t + \Delta t$  can be estimated if the time interval  $\Delta t$  is sufficiently small. If the time interval is so small that the derivative is effectively constant over the interval, an approximate solution is

$$x_i(t+\Delta t) \approx x_i(t) + \Delta t \dot{x}_i(t) \quad (2.1-4)$$

A numerical integration solution proceeds as follows: the initial values of the state variables are specified at the starting time. The equations of motion, expressed in the form of eq. 2.1-3, are used to compute the derivatives of the state variables. An approximate equation such as eq. 2.1-4 is used to compute the values of the state variables at the new

## 2.1 Time-Domain Analyses

time. The process is repeated, “stepping” through time. Values of the state variables and their derivatives are obtained at closely spaced intervals of time.

Various strategies are used for obtaining accurate solutions of the differential equations with minimal computation. Eq. 2.1-4, shown to illustrate the concept, is not particularly efficient and would not be used for most simulation codes. Some of the numerical methods commonly used for the solution of ordinary differential equations with known initial values are the Runge-Kutta and Predictor-Corrector methods. Other methods are used for systems whose equations are “sparse” or “stiff.” Example algorithms for solving ordinary differential equations are provided in reference [1].

For the example quarter-car, the two second-order ordinary differential equations can be expressed as four first-order ordinary differential equations by defining the following state variables:

$$x_1 = z_s \quad x_2 = \dot{z}_s \quad x_3 = z_u \quad x_4 = \dot{z}_u \quad (2.1-5)$$

The equations of motion, expressed in terms of the input  $z_p$  and the four state variables, are:

$$\dot{x}_1 = x_2 \quad (2.1-6)$$

$$\dot{x}_2 = \frac{k_s}{m_s}(x_3 - x_1) + \frac{c_s}{m_s}(x_4 - x_2) \quad (2.1-7)$$

$$\dot{x}_3 = x_4 \quad (2.1-8)$$

$$\dot{x}_4 = \frac{k_s}{m_u}(x_1 - x_3) + \frac{c_s}{m_u}(x_2 - x_4) + \frac{k_t}{m_u}(z_p - x_3) \quad (2.1-9)$$

To simulate a quarter-car, eqs. 2.1-6 — 2.1-9 could be coded in a computer language such as FORTRAN for use with existing integration software.

The quarter-car model requires the vertical position of the road under the tire as a function of time, in order to compute the derivative of  $x_4$ . A minimal  $\Delta t$  interval is .005 sec (200 sample/sec), and typically shorter intervals are used. For a travel speed of 20 mi/h (32 km/h), the minimal interval corresponds to a length of 45 mm. Thus, the input profile must be provided for intervals closer than 45 mm for that simulated speed.

More comprehensive vehicle models include more wheels, and thus they require more inputs. The inputs for each wheel are related, because they are all caused by the same pavement surface. For wheels following the same track (e.g., wheels on the left side of the vehicle), the input to a rear wheel is the same as the input to the front wheel, after a time delay determined by wheelbase and speed. The dynamical equations for the vehicle are valid for any vertical inputs under the wheels. However, in order for the simulation to be representative of inputs from the ground, it is essential that the inputs to the rear wheels are the same as the inputs to the front, with the correct time delay.

The delay between inputs at the front and rear wheels affects the overall dynamics of the vehicle, because frequencies are filtered by the wheelbase effect. This effect is

## 2.1 Time-Domain Analyses

illustrated in Figure 2.1-1 for a wheelbase typical of tandem truck suspensions. Wavelengths equal to wheelbase always produce inputs to the two wheels that are in-phase, whereas wavelengths equal to twice the wheelbase always produce inputs that are out-of-phase. Thus, bouncing motions of the vehicle receive maximum excitation for wavelengths equal to the wheelbase, while pitching motions receive minimal input. Wavelengths that are twice the wheelbase produce maximum pitch input and minimal bounce.

Simulation software is available for analyzing classes of generic mechanical structures and dynamic systems. With these computer codes, engineers need not derive the equations of motion for the vehicle. Instead, they describe the configuration in terms of the number of bodies, the types of connections, and so forth. ADAMS [2] and DADS [3] are two commercial codes used by the motor vehicle industry and the military to simulate ground vehicles. They can handle large-scale motions, nonlinear elements, and a variety of complicated kinematics that arise from mechanical linkages. Also, extensive pre-processing and post-processing software is available to aid in the preparing of input data sets and viewing of simulation results. They handle flexible bodies, but are mainly designed for simulating systems composed of rigid bodies. The NASTRAN code, designed for general structural analysis, can also be used for time-domain simulation [4]. It limits the dynamic model to linear motions, and restricts the types of nonlinear elements that can be included.

The main problem with the general-purpose simulation codes is that they are computationally intensive, and require much more computation time than a special-purpose code written for the equations of a particular system. However, they save so much development time that they are often the most economical approach.

When a single vehicle model will be used extensively, an other alternative is to derive equations of motion for that system using one of several possible dynamics formalisms such as Kanes equations or Lagrange multipliers [5, 6].

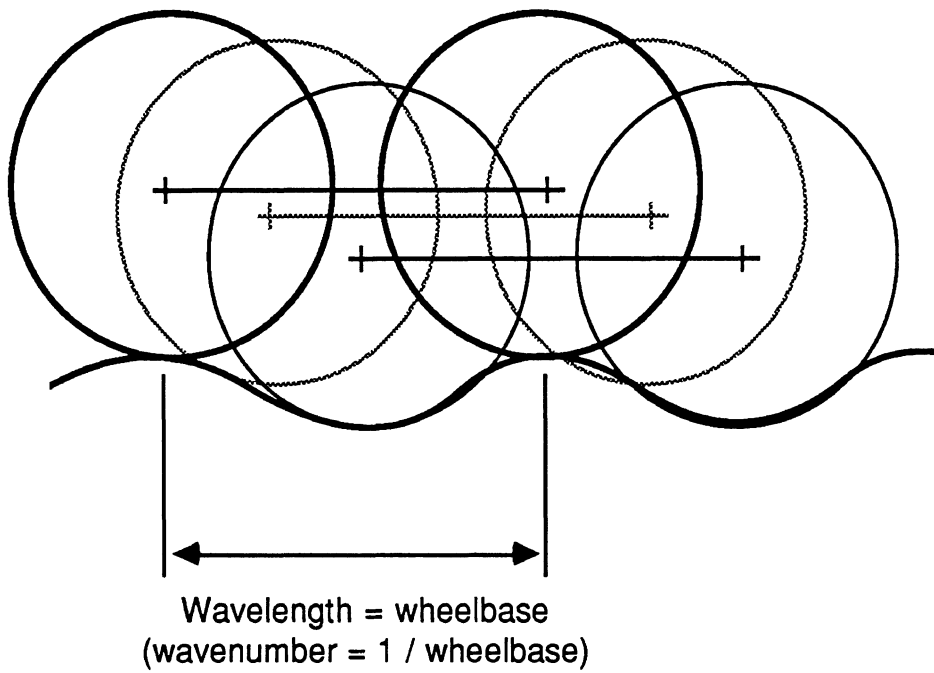
## 2.2 Frequency-Domain Analyses

Direct interpretation of vibration time histories is often difficult, whether the data are measured from tests or simulated by computer. Transformation of the time histories into the frequency domain is a useful method for viewing the frequency content of the vibrations, particularly when the vibrations are essentially random in nature. The frequency domain is also useful for identifying modal resonances in a dynamic system. The transformation is made with a Fourier transform.

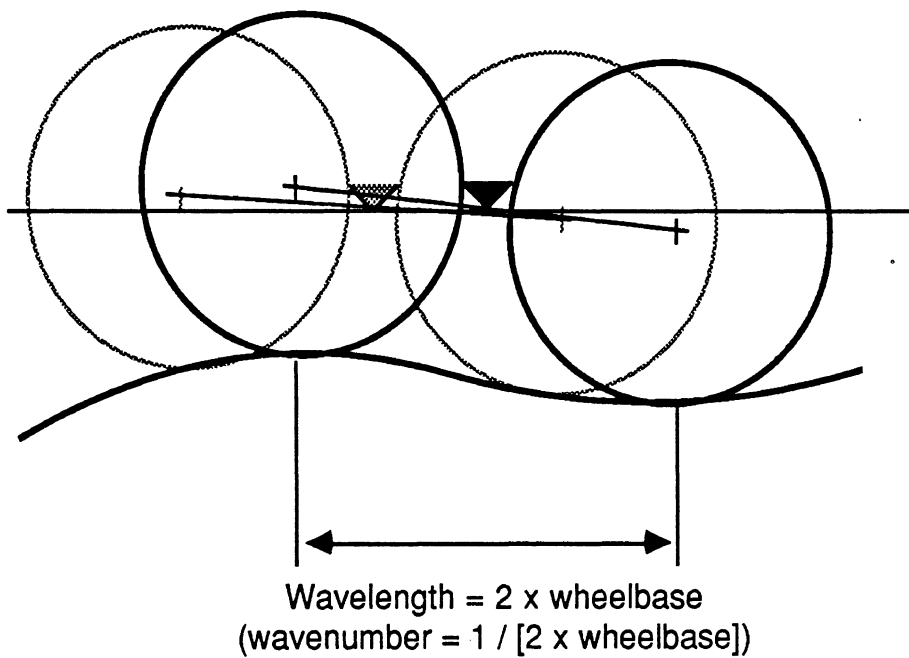
### *Fourier Transforms*

A classical method for analyzing linear equations of motion is through the Laplace transform, defined as follows:

$$F(s) \triangleq \int_0^{\infty} f(t) e^{-st} dt \triangleq \mathcal{L} [f(t)] \quad (2.2-1)$$



a. Full bounce response, no pitch



b. Full pitch response, no bounce

Figure 2.1-1. Example of “wheelbase filtering” on a tandem suspension.

## 2.2 Frequency-Domain Analyses

A special case of the Laplace transform is the Fourier transform, which is defined by making the substitution  $s = j\omega$ , where  $\omega$  is circular frequency (rad/sec) and  $j = \sqrt{-1}$ .

A property of the Laplace transforms is that the derivative operator in ordinary differential equations can be replaced by the Laplace variable, transforming ordinary differential equations into algebraic equations. To obtain a frequency-domain response directly, the substitution can be made

$$\frac{d}{dt} \rightarrow s \rightarrow j\omega \rightarrow j2\pi f \quad (2.2-2)$$

where  $s$  is the Laplace variable (1/sec),  $\omega$  is circular frequency (rad/sec), and  $f$  is cyclical frequency (cycle/sec).<sup>1</sup>

The above substitution can be easily verified for a variable that is periodic:

$$x = A e^{j\omega t} \quad (2.2-3)$$

where  $A$  is an amplitude parameter and the complex expression  $e^{j\omega t}$  represents a sinusoidal vector whose real part is a cosine function with circular frequency  $\omega$ . Note that

$$\begin{aligned} \dot{x} &= \frac{d}{dt}(x) = j\omega A e^{j\omega t} \\ \dot{x} &= j\omega x \end{aligned} \quad (2.2-4)$$

Laplace transforms can be used to solve the differential equations describing a dynamic system. The nature of the transform is such that convolution in the time domain corresponds to multiplication in the frequency domain. If the Laplace transform of the input is known, it can be multiplied by the Laplace transform of the dynamic system to yield the Laplace transform of the output. Theoretically, an inverse Laplace transform can be computed for the output to obtain a close-form equation for the response time history. With the availability of computers and numerical integration programs, inverse Laplace transforms are seldom, if ever, performed to obtain time-domain responses these days.

In the special case of the Fourier transform, viewing the output in this form reveals the vibrational nature of the mechanical system in convenient form. The Fourier transform is a building block that can be used to compute transfer functions and power spectral density (PSD) functions.

The basic theory for the following relations is developed in Reference [7], and example computer codes for obtaining Fourier transforms are presented in [1].

---

<sup>1</sup> In the following material, the equations are somewhat simpler when expressed in terms of circular frequency ( $\omega$ ). However, cyclical frequency ( $f$ ) is more commonly used for experimental data. Both forms are used in this report, and the word "frequency" is used for both forms.



## 2.2 Frequency-Domain Analyses

### Transfer Functions

For a linear system, the steady-state response to a sinusoidal input is a sinusoidal output at the same frequency, but possibly with a different amplitude and phase. The dynamics of the system determine the amplitude and phase relationship between input and output at any given frequency. For the quarter-car, the output variables can be written

$$z_s = A_s e^{j\omega t - \phi_s} \quad z_u = A_u e^{j\omega t - \phi_u} \quad (2.2-5)$$

Eq. 2.2-4 can be substituted into the quarter-car equations (eqs. 2.1-1 and 2.1-2) to yield algebraic equations involving  $j\omega$ :

$$-\omega^2 m_s z_s + k_s (z_s - z_u) + j\omega c_s (z_s - z_u) = 0 \quad (2.2-6)$$

$$-\omega^2 m_u z_u - k_s (z_s - z_u) - j\omega c_s (z_s - z_u) = k_t (z_p - z_u) \quad (2.2-7)$$

By combining the above equations, the phase and amplitude relationships between any two variables can be derived as a function of frequency. For example, the relation between acceleration of the sprung mass ( $\ddot{z}_s$ ) and pavement elevation under the tire ( $z_p$ ) is

$$\frac{\ddot{z}_s}{z_p} = \frac{-\omega^2 k_t (k_s + j c_s \omega)}{m_s m_u \omega^4 - j c_s (m_s + m_u) \omega^3 - [k_t m_s + k_s (m_s + m_u)] \omega^2 + j \omega c_s k_t + k_t k_s} \quad (2.2-8)$$

The ratio  $\frac{\ddot{z}_s}{z_p}$  defines a vector called a complex transfer function. (As a complex function, it contains both amplitude and phase information in a “real” part and an “imaginary” part). In a general case, a transfer function is written as  $H_{xy}(j\omega)$ , where  $x$  is the input and  $y$  is the output. In this example, it is designated  $H_{z_p \ddot{z}_s}(j\omega)$ .

Since the Fourier transform is a special case of the Laplace transform, it holds that the Fourier transform of an output can be obtained by multiplying the Fourier transform of the input by the transfer function of the dynamic system. This is particularly useful when considering the response of vehicles to inputs that can be characterized by a power spectral density (PSD) function.

Transfer functions can be obtained for a variety of analytical models. In addition to rigid-body systems such as the example quarter-car, transfer functions can be computed for systems with flexible bodies. The NASTRAN computer code produces transfer functions that include both rigid-body and flexible-body behavior. Transfer functions can also be measured experimentally with spectrum analyzers or equivalent equipment.

When using transfer functions to predict vehicle response, the same methods are used regardless of whether the transfer functions were derived from a rigid-body model, a flexible-body model, or measured from an actual physical system. Thus, the frequency-domain approach is well suited for combining analyses from a variety of sources.

## 2.2 Frequency-Domain Analyses

### Power Spectral Density (PSD) Function

The power spectral density (PSD) is a statistical measure developed to characterize random signals, such as the vibrations of a vehicle responding to a random road input. It is also used as a means for describing the surface properties of a road. The material provided below is covered more fully in Reference [7], and follows the same notational conventions as the reference.

Conceptually, a PSD of a signal is the partial derivative of the mean square of the signal with respect to frequency, such that

$$\int_0^{\infty} G_{xx}(f) df = \sigma_x^2 + u_x^2 \quad (2.2-9)$$

where  $G_{xx}$  is the PSD of a variable  $x$ ,  $f$  is circular frequency,  $\sigma_x^2$  is the variance of  $x$ , and  $u_x$  is the mean value of  $x$ . When considering vehicle responses, the mean values of the variables of interest are either zero by definition, or they are set to zero as a part of routine data processing. With  $u_x$  identically zero, the mean square value is equal to the variance, and the root-mean-square (RMS) value is equal to the standard deviation. Throughout this report, all signals are assumed to have zero mean values unless it is stated otherwise.

Figure 2.2-1 shows a PSD for the vertical acceleration at a particular location in a vehicle. Eq. 2.2-9 states that total area under the PSD is equal to the mean square of acceleration. The area under a portion of the PSD curve gives the portion of the variance due to the frequency range covered, as indicated in the figure.

All PSD functions used in this report are “single-sided,” meaning that the integral in eq. 2.2-9 goes from 0 to  $\infty$ . Another form, the “double-sided” PSD, is defined for an integral going from  $-\infty$  to  $+\infty$ . The double-sided version has half the amplitude of the single-sided PSD, such that the integral yields the variance.

Mathematically, the PSD for a function of time can be defined as a limit:

$$G_{xx}(f) \triangleq \lim_{T \rightarrow \infty} \frac{2}{T} |X(f,T)|^2 \quad (2.2-10)$$

where  $X(f,T)$  is the finite Fourier transform of  $x(t)$  over a time interval  $T$ , as defined in the equation:

$$X(f,T) \triangleq \int_0^T x(t) e^{-j2\pi f t} dt \quad (2.2-11)$$

$X(f,T)$  is generally a complex function, with both a real and imaginary part. However, the PSD, computed from the magnitude, is always real when computed for a single variable.

The finite Fourier transform is usually computed using the Fast Fourier Transform (FFT) algorithm for efficiency, and as a result computer software will often require that the number of data samples be a power of 2 (1024, 2048, 4096 ...). (Data processing

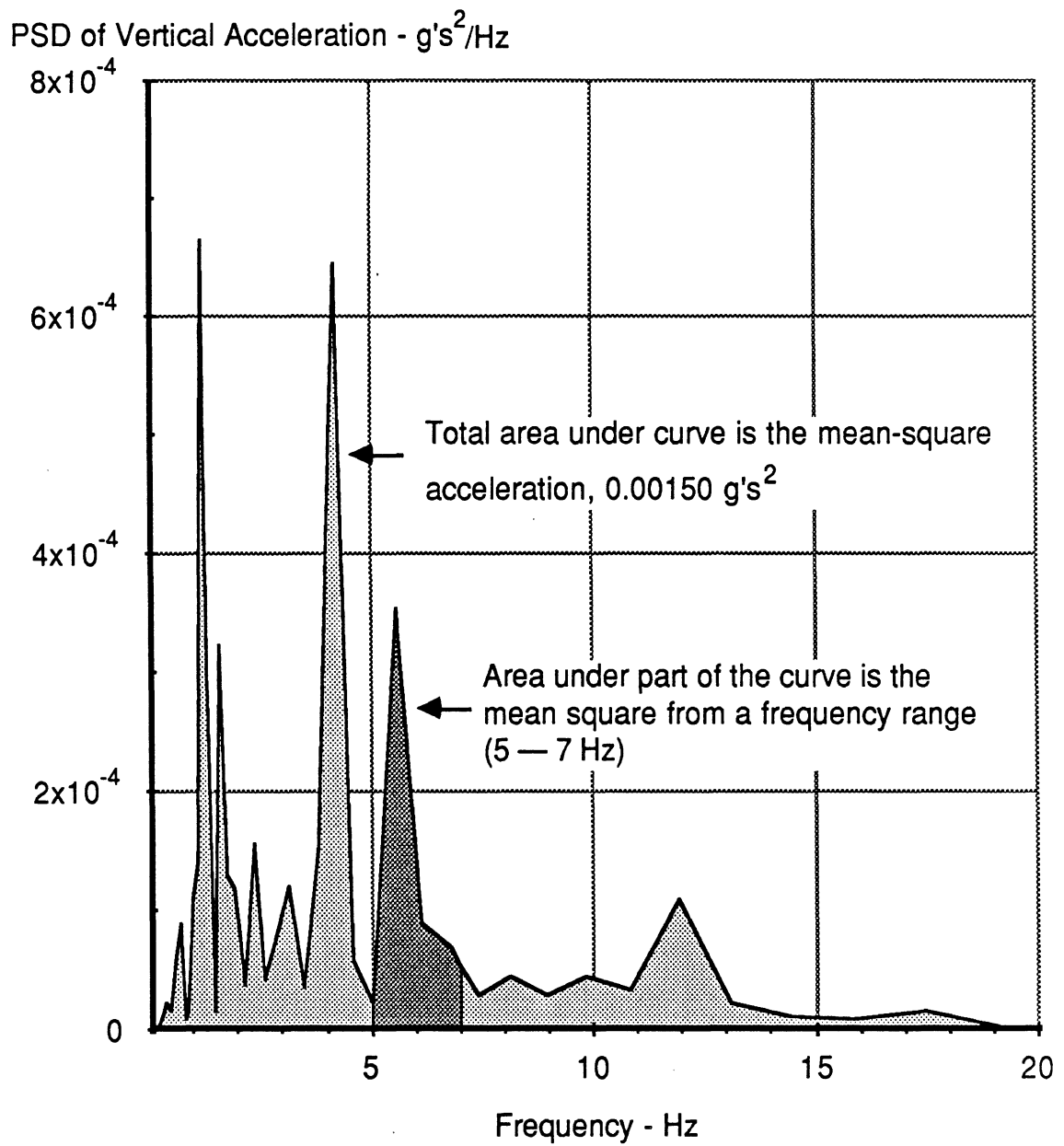


**Figure 2.2-1. PSD of vertical acceleration in a vehicle**

## 2.2. Frequency-Domain Analyses

considerations for computing PSDs and other frequency-domain transforms are provided in an appendix.)

The PSD function is more generally defined for two variables:

$$G_{xy}(f) \triangleq \lim_{T \rightarrow \infty} \frac{2}{T} X^*(f, T) Y(f, T) \quad (2.2-12)$$

When used for one variable ( $G_{xx}$ ), the PSD is usually called the autospectral density, and when used for two different variables ( $G_{xy}$ ) it is called the cross-spectral density. Note that the autospectral density function is a special case of the cross-spectral density when both variables ( $x$  and  $y$ ) are the same. The cross-spectral density can include phase information, and may have an imaginary component.

An alternate definition for the PSD function is that of the Fourier transform of the correlation function between two signals:

$$G_{xy}(f) = 2 \int_{-\infty}^{+\infty} R_{xy}(\tau) e^{-j2\pi f \tau} d\tau \quad (2.2-13)$$

where the correlation function,  $R_{xy}(\tau)$ , is defined as

$$R_{xy}(\tau) \triangleq \lim_{T \rightarrow \infty} \frac{1}{T} \int_0^T x(t) y(t + \tau) dt \quad (2.2-14)$$

The alternate PSD definition is useful for deriving PSD functions from theoretical random signals, whereas the first definition is more directly related to how the PSD is computed. The two definitions are mathematically equivalent.

A PSD based on spatial frequency (cycle/ft) rather than temporal frequency (cycle/sec) is used for characterizing road profiles and other functions of distance. To do this, substitute  $\xi$  (distance) for  $t$  (time),  $L$  (length of data) for  $T$  (time limit for data), and  $\nu$  (wavenumber, spatial cyclic frequency) for  $f$  (temporal cyclic frequency). For example, the finite Fourier transform and cross-spectral density definitions become

$$X(\nu, L) \triangleq \int_0^L x(\xi) e^{-j2\pi \nu \xi} d\xi \quad (2.2-15)$$

$$G_{xy}(\nu) \triangleq \lim_{L \rightarrow \infty} \frac{2}{L} X^*(\nu, L) Y(\nu, L) \quad (2.2-16)$$

### *Coherence Function*

Correlation between two signals is defined in the frequency domain with the coherence function

## 2.2 Frequency-Domain Analyses

$$\gamma_{xy}^2(f) \triangleq \frac{|G_{xy}(f)|^2}{G_{xx}(f) G_{yy}(f)} \quad (2.2-17)$$

The coherence function ranges from 0 (the two signals have no fixed phase relationship at that frequency) to unity (the two signals are related perfectly by a gain and phase). Coherence is analogous to the squared correlation coefficient ( $r^2$ ) between two variables, except that it applies for a particular frequency. It is always expressed as a squared quantity. Signals commonly have high coherence over one range of frequencies, and low coherence over another.

In order to measure coherence, it is necessary to perform averaging when computing PSDs. The averaging reduces effects of uncontrolled aspects of the measurement process. One averaging method involves computing PSD functions for repeated tests, and averaging across the ensemble at each frequency (ensemble averaging). A second method involves averaging adjacent PSD values over a small frequency range (frequency averaging). In either method, random phase relationships cause cancellation in the resulting averaged  $G_{xy}$  values, whereas a consistent phase does not. (Averaging strategy is discussed further in the Appendix describing frequency-domain computation details.)

### *Input-Output Relations*

Two very useful relationships for linear systems subjected to broad-band inputs are

$$G_{xy} = G_{xx} H_{xy} \quad (2.2-18)$$

$$G_{yy} = G_{xx} |H_{xy}|^2 + G_{nn} \quad (2.2-19)$$

where  $G_{nn}$  is that part of the output PSD not linearly related to the input. This component arises due to other sources of excitation (noise) and nonlinearities in the system. (Note: the explicit dependence of a PSD function on frequency [ $G_{xx}(f)$ ] has been dropped to simplify the notation.)

Figure 2.2-2 shows this relationship for the quarter-car example. The PSD of the acceleration is obtained by weighting the PSD of a road input by the transfer function of the quarter-car, as defined in eq. 2.2-8. The PSD of the output acceleration can be integrated to give the mean-square acceleration, and thus RMS acceleration. The PSD plot itself shows how the structural modes of vibration in the vehicle contribute to the mean-square acceleration.

Eq. 2.2-19 is also very useful for analyzing measured data when both inputs and outputs are measured. It is rearranged to define transfer function from PSDs computed via the Fourier transforms of the data:

$$H_{xy} = \frac{G_{xy}}{G_{xx}} \quad (2.2-20)$$

When  $G_{xy}$  is computed using an averaging technique, effects of noise, nonlinearities, and other parts of the response that are not linearly related to the input are averaged out and therefore these factors do not contribute to  $H_{xy}$ .

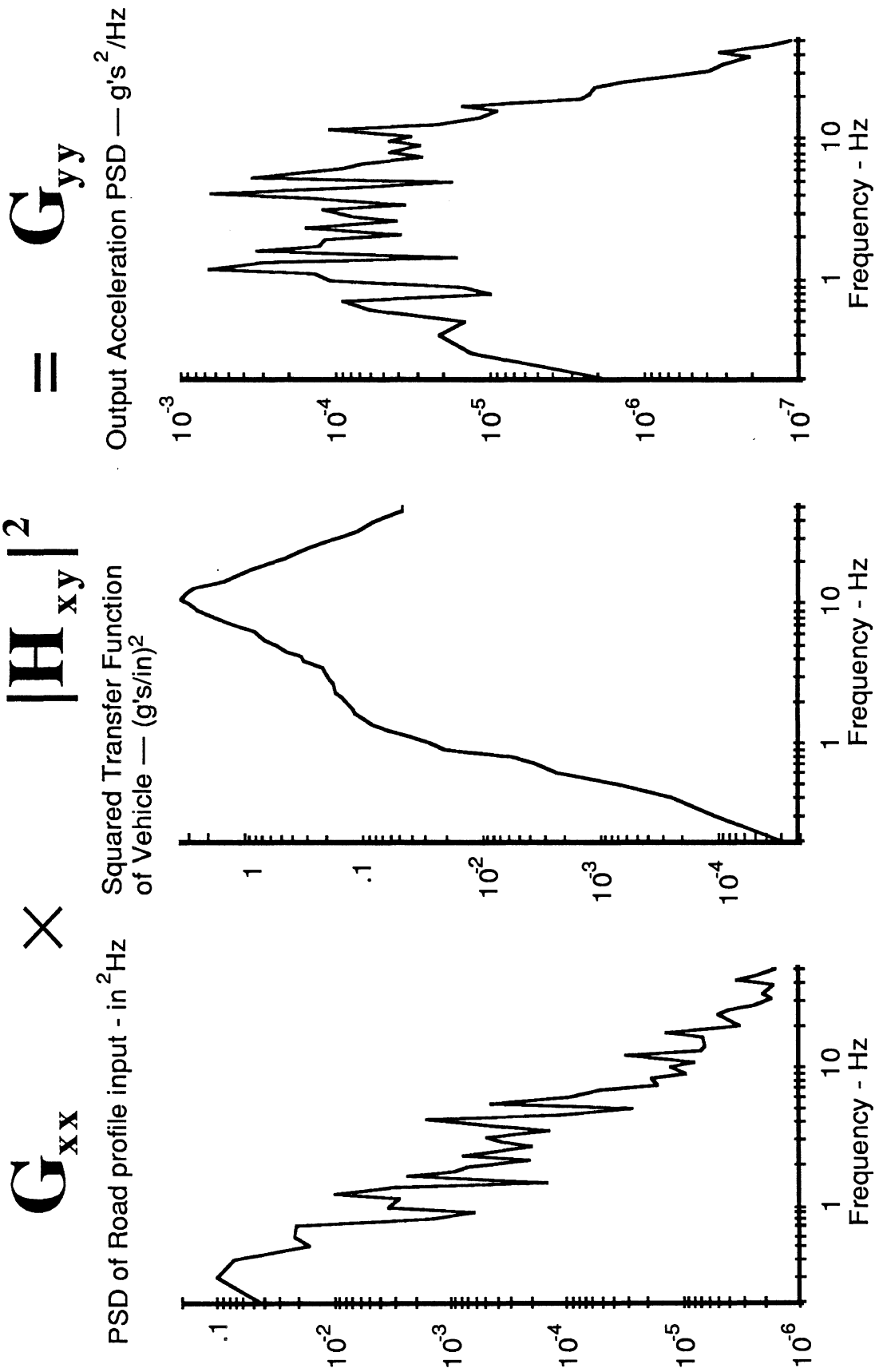


Figure 2.2-2. Relationship between input and output PSD functions.

## 2.2 Frequency-Domain Analyses

The coherence function should always be computed when  $H_{xy}$  is computed from experimental data via eq. 2.2-20 to determine the quality of the linear relationship. Coherence above 0.95 is usually obtained over the frequency range of interest when the instrumentation is working and the system is somewhat linear. A low coherence can be caused by transducer error, a highly nonlinear system, or additional inputs to the system that are uncorrelated to the measured input (e.g., engine vibration, wind, etc.).

For frequency-domain analyses, the PSD of the road profile is required as input. If the vehicle model includes several wheels, the inputs to each wheel are related, since they are all caused by the same pavement surface. As noted earlier, for wheels following the same track (e.g., wheels on the left side of the vehicle), the input to a rear wheel is the same as the input posed to the front wheel, after a time delay determined by wheelbase and speed. This time delay has a simple transfer function:

$$\begin{aligned} z_p(t + \tau) &= A e^{j\omega(t + \tau)} \\ &= e^{j\omega\tau} A e^{j\omega t} \\ &= e^{j\omega\tau} z_p \end{aligned} \quad (2.2-21)$$

That is, the transfer function for a delay of  $\tau$  seconds is  $e^{j\omega\tau}$ .

When the delay is included in the vehicle dynamics, the inputs for all wheels following the same track (wheeltrack) are characterized by a single input PSD function. The “wheelbase filtering” illustrated earlier derives from the inclusion of eq. 2.2-21 in the vehicle transfer functions.

When considering wheels that do not follow the same wheeltrack (e.g., wheels on the left and right side of the vehicle), the vehicle model can no longer be considered a single-input system. The model must deal with multiple inputs, which are, in general, correlated at some frequencies more than at others. For a two-input system ( $x_1$  and  $x_2$ ), an output PSD is obtained with the relationship

$$G_{yy} = |H_{x_1y}|^2 G_{x_1x_1} + |H_{x_2y}|^2 G_{x_2x_2} + H_{x_1y}^* H_{x_2y} G_{x_1x_2} + H_{x_2y}^* H_{x_1y} G_{x_2x_1} + G_{nn} \quad (2.2-22)$$

This equation requires the cross-spectral densities of the inputs. If the inputs are uncorrelated, such that the cross-spectral density is zero over the frequency range of interest, the relationship is simplified:

$$G_{yy} = |H_{x_1y}|^2 G_{x_1x_1} + |H_{x_2y}|^2 G_{x_2x_2} + G_{nn} \quad (2.2-23)$$

When a multiple-input model is necessary, it should be formulated in terms of inputs that have zero cross-spectral densities, if possible, to take advantage of the above simplification.

When a variable is defined as the weighted sum of two other variables, eq. 2.2-22 can be applied with the simplifications that (1) the transfer functions are identically unity at all frequencies, and (2) the “noise” PSD ( $G_{nn}$ ) is zero. That is, if

$$y = a x_1 + b x_2 \quad (2.2-24)$$

## 2.2 Frequency-Domain Analyses

where  $a$  and  $b$  are constants, then

$$G_{yy} = a^2 G_{x_1x_1} + b^2 G_{x_2x_2} + ab G_{x_1x_2} + ab G_{x_2x_1} \quad (2.2-25)$$

If the two inputs have zero coherence at all frequencies, then the PSD of the sum of the variables is simply the weighted sum of the PSDs of the individual variables:

$$G_{yy} = a^2 G_{x_1x_1} + b^2 G_{x_2x_2} \quad (2.2-26)$$

## 2.3 State Space Analyses

Techniques have been developed under modern control theory to compute RMS values of response variables directly for linear systems subjected to random inputs, if the inputs have certain statistical properties. (For example, see References [8, 9].) The equations of motion are expressed in matrix form as

$$\dot{\mathbf{x}} = \mathbf{A} \mathbf{x} + \mathbf{\Gamma} \mathbf{w} \quad (2.3-1)$$

where  $\mathbf{x}$  is an  $n \times 1$  matrix of the state variables,  $\mathbf{w}$  is an  $m \times 1$  matrix of “noise” inputs,  $\mathbf{A}$  is an  $n \times n$  matrix whose coefficients define the dynamics of the system, and  $\mathbf{\Gamma}$  is an  $n \times m$  matrix whose coefficients define the distribution of the noise inputs. In this formulation, the noise inputs are modeled as “white noise,” which means that the PSD is constant over the entire frequency range. A property of white noise is that  $R_{xx}(\tau)$ —the autocorrelation function—is a delta function at  $\tau=0$ . That is,

$$R_{xx}(\tau) = E [x(t) x(t + \tau)] = \sigma_x^2 \delta(0) \quad (2.3-2)$$

where the operator  $E[ ]$  indicates the expected value of the quantity enclosed in the brackets.

The variance for a true theoretical white noise is infinite, as indicated by the delta function, because it includes an infinite range of frequencies. Although most noise sources do not have infinite amplitudes, the concept of white noise can be applied if they have a uniform PSD over the frequency range of interest. (Or, stated another way, a variable can be considered as white noise if the width of the autocorrelation function is much less than the shortest response time of interest.) Figure 2.3-1 shows an input that could be modelled as white noise. Although the true PSD is not constant over all frequencies, it is a constant over the frequencies of interest. Also, the width of the autocorrelation function is not zero, but it is much smaller than the response times of interest.

The magnitudes of the noise inputs can be expressed in matrix form, using a matrix  $\mathbf{Q}$  defined as

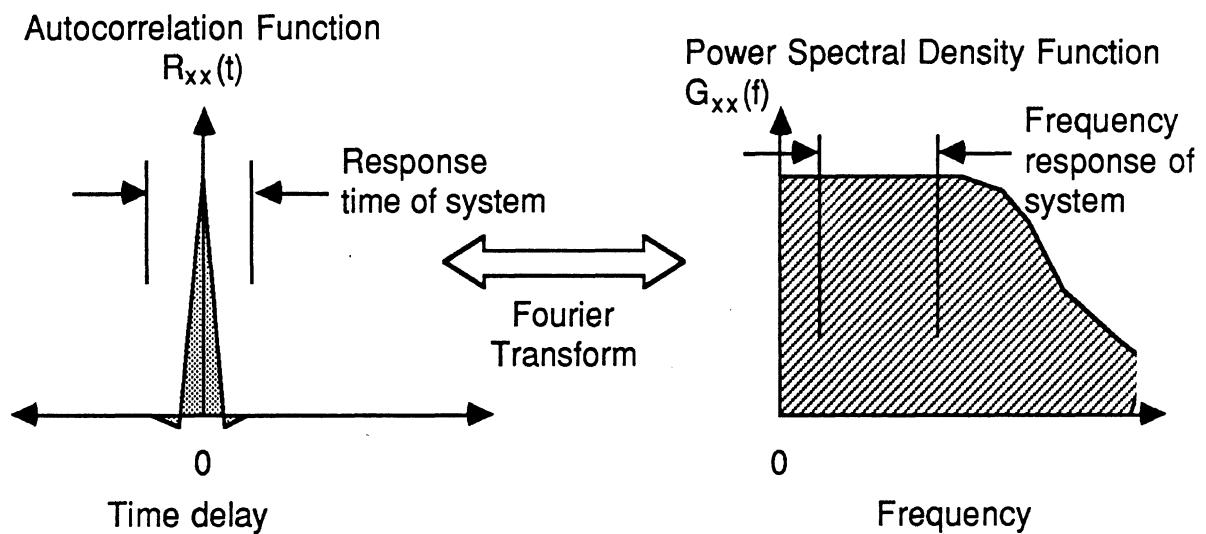
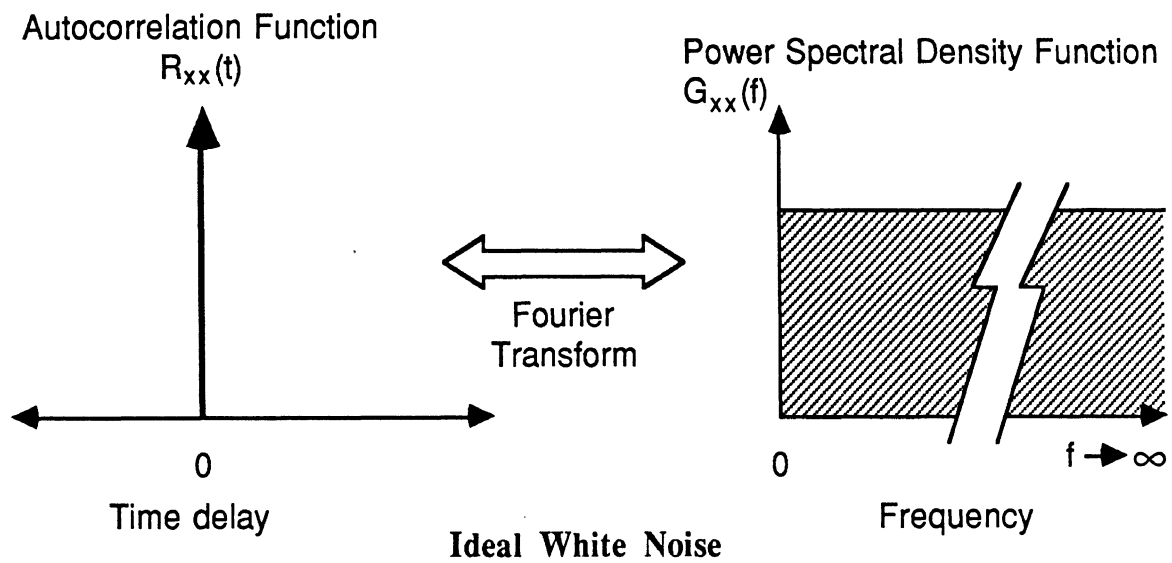
$$\mathbf{Q} \delta(0) = E [ \mathbf{w}(t) \mathbf{w}^T(t+t) ] \quad (2.3-3)$$

The variances and covariances of the state variables can also be expressed in matrix form:

$$\mathbf{X} \delta(0) = E [ \mathbf{x}(t) \mathbf{x}^T(t+t) ] \quad (2.3-4)$$

For statistically stationary input noise, the output variables are also stationary. The variances in the matrices are related by the “Covariance Propagation Equation.”





Broad-band signal that can be approximated as white noise

Figure 2.3-1. Autocorrelation and PSD functions for white noise.

### 2.3 State Space Analyses

$$\mathbf{A} \mathbf{X} + \mathbf{X} \mathbf{A}^T + \mathbf{\Gamma} \mathbf{Q} \mathbf{\Gamma}^T = 0 \quad (2.3-5)$$

This equation can be solved numerically to provide the variances and covariances of the state variables in terms of the variances of the noise inputs.

When the PSDs of random inputs are not uniform, the state-space approach can still be used if the inputs can be shaped by filters to yield the proper PSD function. The dynamics of the filters must be expressible by linear, first-order, ordinary differential equations. Those equations are then added to the matrix formulation of eq. 2.3-1 by adding to the  $\mathbf{A}$  matrix.

For example, consider a theoretical road input PSD function of the form

$$G_{z_p z_p}(f) = \frac{A}{(2\pi f)^2} \quad (2.3-6)$$

where  $A$  is a roughness amplitude parameter determined by road roughness and travel speed. This theoretical form is obtained if white noise is integrated. This is seen by considering the transfer function of the integration operation,

$$H_{z_p \dot{z}_p}(f) = \frac{1}{j2\pi f} \quad (2.3-7)$$

Thus, the desired PSD for profile elevation is obtained if the derivative (profile vertical velocity) is white noise with PSD amplitude  $A$ . That is,

$$\begin{aligned} G_{z_p z_p}(f) &= |H_{z_p \dot{z}_p}(f)|^2 G_{\dot{z}_p \dot{z}_p}(f) \\ &= \frac{A}{(2\pi f)^2} \end{aligned} \quad (2.3-8)$$

The matrix formulation of eq. 2.3-1 is obtained by adding profile elevation to the four state variables defined earlier in eq. 2.1-5 and used in eqs. 2.1-6 through 2.1-7, to yield five state variables:

$$\mathbf{x} = \begin{Bmatrix} z_s \\ \dot{z}_s \\ z_u \\ \dot{z}_u \\ z_p \end{Bmatrix} \quad (2.3-9)$$

The  $\mathbf{A}$  and  $\mathbf{\Gamma}$  matrices are

### 2.3 State Space Analyses

$$A = \begin{bmatrix} 0 & 1 & 0 & 0 & 0 \\ -\frac{k_s}{m_s} & -\frac{c_s}{m_s} & \frac{k_s}{m_s} & \frac{c_s}{m_s} & 0 \\ 0 & 0 & 0 & 1 & 0 \\ \frac{k_s}{m_u} & \frac{c_s}{m_u} & -\frac{k_s + k_t}{m_u} & -\frac{c_s}{m_u} & \frac{k_t}{m_u} \\ 0 & 0 & 0 & 0 & 0 \end{bmatrix} \quad (2.3-10)$$

$$\Gamma = \begin{Bmatrix} 0 \\ 0 \\ 0 \\ 0 \\ 1 \end{Bmatrix} \quad (2.3-11)$$

and the  $Q$  matrix is  $1 \times 1$  with a value of  $A$ , representing the vertical velocity input as white noise with PSD amplitude  $A$  ( $\text{in}^2\text{sec}^{-2}\text{Hz}^{-1}$ ).

### 2.4 Summary of Input Requirements

The input requirements for time-domain, frequency-domain, and state-space analyses can now be summarized for the context of ground vehicles subjected to roughness inputs from the ground.

Time-based simulations require that ground elevation be provided for each wheel position, at each instant of time covered by the simulation. Conceptually, the model is used to simulate an experimental test on the computer. The outputs of the simulation are the same variables that might be measured in a test (with “perfect” transducers). A time-domain simulation is deterministic, with the predicted variables defined by the dynamic properties of the model, the initial conditions, and the explicit values provided as time-varying inputs.

Of the three types of analysis reviewed here, the time-domain approach generally can handle the widest range of conditions. It works for any vehicle model described by equations that can be solved by computer, which need not be linear. (Also, with advanced hardware, “real-time simulation” can be used to exercise a mixture of theoretical equations and physical hardware.) The inputs and outputs of a time-domain simulation can be processed to yield virtually any form of statistics, not just PSDs and RMS values. The major disadvantage of this approach is that it requires the most computation. A great deal of computer time is often required for a single simulation when general-purpose codes such as NASTRAN or ADAMS are used,

If a simulation is used when actual road elevation values are not available, a method is needed for synthesizing artificial inputs. In order for the simulated results to be

## 2.4 Summary of Input Requirements

representative of typical conditions, the road inputs must be generated in such a way that they have statistical properties representative of actual ground inputs.

Frequency-based analyses typically require inputs in the form of one or more PSD functions. When considering multiple wheels following the same track, a single PSD is sufficient as input because the wheels see the same input at different times (the delay between inputs is a part of the vehicle dynamic response). When considering different wheeltracks, the coherence and phase relationships between the inputs must also be provided. Predictions made using frequency-domain analyses usually restrict the vehicle model to be linear. However, the method does not restrict the manner in which the transfer functions are obtained. This allows the analysis to include dynamic characterizations from a variety of sources, including rigid and flexible models, and experimental data.

The frequency analysis methods are often preferable to time-domain simulation due to computational efficiency, and because the frequency plots present information simply and compactly. Because they operate on statistics directly, they eliminate the work needed to obtain a statistically valid range of samples as required by the time-domain methods. The output statistics are representative if the input statistics are representative and the modeling assumptions are valid. Further, a few transfer functions for a vehicle can be used to evaluate a variety of road inputs.

The major limitation of frequency-domain analyses is that the theory is based on linear systems. Difficulties can be encountered for vehicles with significant nonlinear response properties.

State-space analyses assume that all inputs can be approximated as random, uncorrelated white noise sources, and that the vehicle model is linear. Inputs that are not white noise can also be accommodated if they can be obtained by filtering white noise. (The properties of the filters are lumped with the dynamics of the vehicle to perform the analysis.) These analyses are the most efficient computationally, but provide the least information. They are commonly used for performing fundamental sensitivity analyses and performing control system optimizations.

### 3. RELATIONS BETWEEN ALTERNATIVE INPUT DESCRIPTIONS

Due to the apparent randomness of the longitudinal profiles, roughness inputs are nearly always described statistically. Longitudinal profiles fit the general category of “broad-band random signals,” and are well suited for characterization by the PSD function defined in the preceding section. Further development is presented here to deal with the correlation that exists between profiles of parallel wheeltracks used at inputs for the left- and right-hand side of a vehicle. This section presents mathematical relationships that can be used to convert between PSDs, profiles, and white-noise sources.

#### 3.1 Statistics for Random and Deterministic Signals

The “randomness” of a measured road profile is a topic that deserves some consideration when dealing with statistical analyses. A longitudinal profile is not random. Measures of longitudinal profile are repeatable for a given pavement, providing that the same wheeltrack position is used for all measurements and that the time interval between measurements is fairly short.<sup>1</sup> The only random element is the measurement error, which can be held to a negligible level with modern profiling equipment. Nonetheless, the concept of a random input is useful for vehicle analyses. In many cases, actual measurements are not available as inputs for vehicle models, so “representative” inputs must be used. The basis for determining the validity of an input is typically by comparing its statistics to statistics obtained from measured roads.

Most textbooks and references dealing with random signal analysis consider the statistics of the statistics, such as expected value of a PSD function at each frequency, variance of a PSD function at each frequency, etc. (For example, see Reference [7].) When computed for a deterministic signal such as a measured road profile, the “statistics” are also deterministic. Estimates of statistical error based on assumptions of random signals are irrelevant because the statistics are precisely defined by the profile. That is, error analyses developed for random signals are not appropriate for road profile data.

---

<sup>1</sup> The profile could be viewed as random from the perspective of a vehicle because variations in profile cannot be predicted prior to reaching them with the front wheels. However, it is definitely not random from the overall system view used in most analyses.

### 3.2 Correlation Between Multiple Wheeltrack Profiles

Most ground vehicles travel over two wheeltracks, and are thus subjected to two simultaneous input profiles. A surprisingly large number of vehicle analyses use a “bicycle model” representation, in which the width of the vehicle is ignored and all motions occur in the “pitch plane” of the vehicle. (That is, they include bouncing and pitching, but no roll or longitudinal twisting.) A single-profile description of the road surface is the single input required for these models.

Analyses involving two-track vehicle models require valid inputs from two profiles. Further, vehicle models involving unusual configurations (e.g., a tricycle layout) may involve even more wheeltrack profiles. When measured profiles are used, this is straightforward if the measurements are made in parallel paths with a separation equal to the track width of the vehicle. For time-domain analyses, these profiles are used directly as inputs to the vehicle model. Frequency-domain models require computation of the PSD of each profile and the cross-spectral density between them.

When theoretical inputs are used, or a mixture between experimental data and extrapolated data are used, a model of the surface characteristics must be used to generate the profiles or PSD functions. The model must predict coherence between profiles to qualitatively match coherence functions observed for measured data. Two of the most simple models that one might consider to relate the left- and right-hand wheeltracks are: (1) the profiles are perfectly correlated, and thus related by a linear transformation such as a scale factor and/or phase delay; or (2) the profiles are completely uncorrelated. Both models have been used and are reported in the literature, but neither matches the real world. Coherence functions between measured wheeltrack profiles always vary with wavenumber<sup>1</sup>, with a limit of unity applying for very low wavenumbers (the profiles are identical when considering long wavelengths such as hills and valleys) and zero for very high wavenumbers (the profiles are uncorrelated when considering very short wavelengths such as texture). Over the range of wavenumbers to which a vehicle responds, the coherence lies between these two limits. The upper-left plot in Figure 3.2-1 shows a typical measured coherence function for an asphalt road.

#### *Modal Profile Components*

Modal profiles can be used to simplify the representation of two wheeltrack inputs by isolating uncorrelated roughness components. The following two modal inputs can be defined:

$$z_V = \frac{z_L + z_R}{2} \qquad z_C = \frac{z_L - z_R}{2} \qquad (3.2-1)$$

---

<sup>1</sup> Wavenumber is the reciprocal of wavelength and is a spatial equivalent of frequency. It has units of cycle/length.

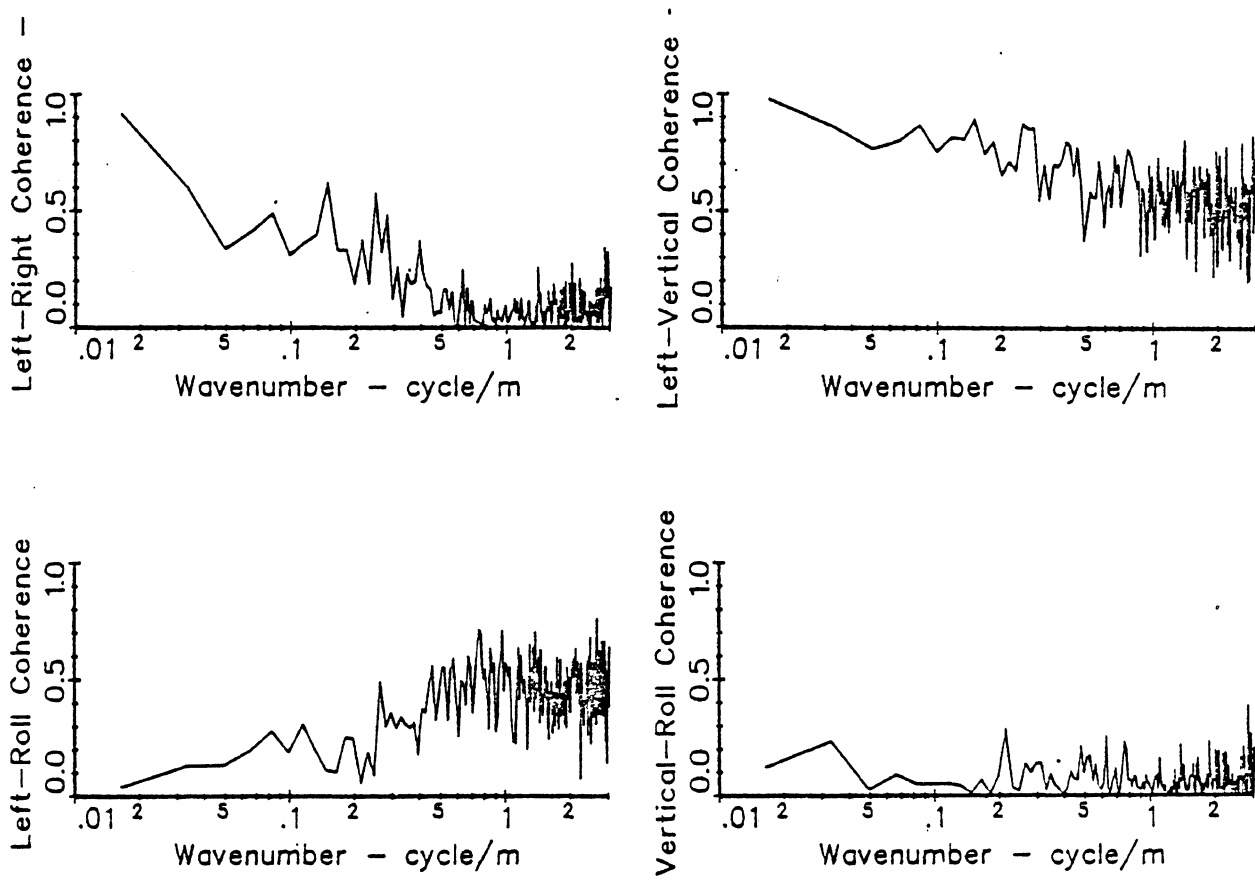


**Figure 3.2-1. Measured coherence functions between left- and right-hand wheeltrack profiles.**

### 3.2 Correlation Between Multiple Wheeltrack Profiles

where  $z_L$  and  $z_R$  are the elevations in the left- and right-hand wheeltracks,  $z_V$  is the average vertical elevation (the input which primarily excites pitch-plane vehicle motions), and  $z_C$  is a cross-level profile (the input which primarily excites rolling and torsional motions). The inverse equations define the wheeltrack profiles in terms of the modal profiles:

$$z_L = z_V + z_C \qquad z_R = z_V - z_C \qquad (3.2-2)$$

When roads have left- and right-hand wheeltracks with similar levels of roughness, the vertical and cross-level modal profiles are nearly always uncorrelated. That is, there is no consistent phase relationship between the two, such that the coherence between  $z_L$  and  $z_R$  is zero for all wavenumbers. The bottom-right plot in Figure 3.2-1 shows that the coherence function is nearly zero for the vertical and cross-level profiles. Physically, this means that when the average of the two elevation profiles ( $z_V$ ) goes up, the difference between the two ( $z_C$ ) is equally likely to be positive or negative. The vehicle analysis can be simplified substantially if the model is formulated in terms of uncorrelated modal inputs (compare eqs. 2.2-22 and 2.2-23).

It can be seen from eq. 3.2-1 that when one of the wheeltrack profiles is significantly rougher than the other, the rough profile contributes more than half to both the vertical and roll modal profiles, such that the two are not independent. It sometimes happens that one wheeltrack is rougher than the other, particularly on narrow roads where the edge of the road is more susceptible to damage by erosion of the sub-grade. This type of input has not been addressed in the literature.

#### *Relationships Between the Statistics of Modal and Wheeltrack Profiles*

When the vertical and cross-level profiles are uncorrelated, the PSD of a single wheeltrack is the sum of the vertical and cross-level PSD functions:

$$G_{zz} \triangleq G_{z_L z_L} \triangleq G_{z_R z_R} = G_{z_V z_V} + G_{z_C z_C} \qquad (3.2-3)$$

Relations between the PSD functions of the various profiles can be developed. First, consider the ratio between the PSDs of the cross-level and vertical profiles:

$$\beta = \frac{G_{z_C z_C}}{G_{z_V z_V}} \qquad (3.2-4)$$

Eqs. 3.2-3 and 3.2-4 imply the following relationships:

$$G_{zz} = G_{z_V z_V} (1 + \beta) \qquad (3.2-5)$$

$$G_{z_V z_V} = G_{zz} \frac{1}{(1 + \beta)} \qquad (3.2-6)$$

$$G_{z_C z_C} = G_{zz} \frac{\beta}{(1 + \beta)} \qquad (3.2-7)$$



### 3.2 Correlation Between Multiple Wheeltrack Profiles

The PSD definition (eq. 2.2-12) and the fact that  $z_V$  and  $z_C$  are uncorrelated leads to expressions for the cross-spectral density and the coherence between the wheeltrack profiles:

$$G_{z_L z_R} = G_{z_V z_V} (1 - \beta) \quad (3.2-8)$$

$$\gamma_{z_L z_R}^2 = \frac{|1 - \beta|^2}{\beta} \quad (3.2-9)$$

At this point, some insight into how these relationships relate to pavement properties can be gained by considering the limit, when wavenumbers approach zero and infinity. Table 1 summarizes the limiting relationships for a travelled lane whose left- and right-hand wheeltracks have about the same roughness levels, and whose roughness derives from random variations in the surface.

Table 1. Limiting conditions for PSD and coherence functions for very low and very high wavenumbers.

| <i>Function</i>      | <i>Low wavenumbers</i>             | <i>High wavenumbers</i> |
|----------------------|------------------------------------|-------------------------|
| $G_{z_L z_L}$        | $G_1$                              | $G_2$                   |
| $G_{z_R z_R}$        | $G_1$                              | $G_2$                   |
| $\gamma_{z_L z_R}^2$ | 1                                  | 0                       |
| $G_{z_V z_V}$        | $G_1$                              | $\frac{G_2}{2}$         |
| $G_{z_C z_C}$        | $G_\epsilon \ll G_1$               | $\frac{G_2}{2}$         |
| $\beta$              | $\frac{G_\epsilon}{G_1} \approx 0$ | 1                       |

In the above table,  $G_1$ ,  $G_2$ , and  $G_\epsilon$  designate arbitrary PSD amplitudes for very small and very large wavenumbers. For very low wavenumbers, the profiles of the left- and right-hand wheeltracks are nearly identical—both go up and down the hills and valleys together. Thus the PSD functions for the wheeltracks are shown in the table as having the same value, designated  $G_1$ . Because the wavenumber amplitudes and phases of the wheeltrack profiles are essentially identical at this limit, the coherence between the wheeltrack profiles is unity, the vertical average is the same as either wheeltrack ( $G_1$ ), and the cross-level component is orders of magnitude smaller. The PSD ratio  $\beta$  is very small, and approaches zero as the amplitude of the vertical profile grows with decreasing wavenumber.

For very high wavenumbers, surfaces that do not have a directional orientation in texture (e.g., asphalt) are expected to exhibit random phase between the two wheeltrack

### 3.2 Correlation Between Multiple Wheeltrack Profiles

profiles, such that the coherence approaches zero. As noted in Section 2.2, the PSD of a variable defined as a linear combination of uncorrelated variables can be computed from the PSDs of the components. Thus,

$$\begin{aligned} G_{z_v z_v} &= \left(\frac{1}{2}\right)^2 G_{z_L z_L} + \left(\frac{1}{2}\right)^2 G_{z_R z_R} \\ &= \frac{G_2}{2} \end{aligned} \quad (3.2-10)$$

and

$$\begin{aligned} G_{z_c z_c} &= \left(\frac{1}{2}\right)^2 G_{z_L z_L} + \left(-\frac{1}{2}\right)^2 G_{z_R z_R} \\ &= \frac{G_2}{2} \end{aligned} \quad (3.2-11)$$

The relationships shown in the table are drawn from two characteristics that nearly all pavements have in common: (1) PSD functions of elevation profiles always increase in amplitude as wavenumber decreases (this characteristic will be covered extensively in Section 4.1); and (2) profiles of parallel wheeltracks become uncorrelated in the limit as wavenumber increases relative to the spacing between the profiles. The possible exception to this is the special case when roughness is caused mainly by slab joints that cross both wheeltracks at the same point.

The vertical and cross-level modal profiles apply for a specific spacing between wheeltracks. Thus, modal inputs developed for a large vehicle with a wide track are probably incorrect for a small vehicle with a narrow track. Two models have been proposed to allow inputs to be generated for a variety of wheeltrack spacings.

#### *“Ribbon Road” Model of Parkhilovskii*

Parkhilovskii proposed a variation of the modal profiles, in which a wheeltrack profile is comprised of a vertical component and an angular roll component

$$z_p = z_v + b \phi \quad (3.2-12)$$

where  $z_p$  is the elevation in a wheeltrack profile,  $\phi$  is a roll component, and  $b$  is the transverse distance between the wheeltrack and the center of the lane. The left- and right-hand wheeltrack profiles can be defined for a reference vertical profile that might or might not lie halfway between the two profiles

$$z_L = z_v + b_1 \phi \quad z_R = z_v - b_2 \phi \quad (3.2-13)$$

where  $b_1$  and  $b_2$  are the distances between the left- and right-hand wheeltrack and the reference vertical profile. When  $b_1$  and  $b_2$  are set equal to each other, the roll component is a rescaled version of the cross-level profile:

$$z_C = b \phi \quad (3.2-14)$$

### 3.2 Correlation Between Multiple Wheeltrack Profiles

Because the model includes track spacing as a parameter, a family of wheeltrack profiles can be generated simply by varying  $b$ . In addition, the model can be used to generate two wheeltrack profiles with different roughness levels by setting  $b_1$  and  $b_2$  to different values.

The Parkhilovskii model defines a full surface that has been called the “ribbon road” [10]. The contribution from the roll component is zero at the center and grows for wheeltracks spaced further from the center, as illustrated in Figure 3.2-2 for a simple case with negligible vertical roughness. This geometry occurs frequently in the literature, possibly because it is a simple model which includes track width as a parameter. However, the model is not representative of most public roads, and therefore the particular formulation of Parkhilovskii is not recommended except for occasional winding, hilly roads that have the appearance of a ribbon.

#### *Isotropic Surface Model*

The assumption of an isotropic surface has been developed extensively as a means for generating multiple wheeltrack profiles from a single measured PSD function [10, 11]. The assumption of isotropy is appealing because the complete topography of a road surface can be determined from the PSD of a single measured wheeltrack profile. Physically, the isotropy assumption means that the statistical properties of any wheeltrack on the surface match those of any other wheeltrack—as if lane markers are painted on a large uniformly rough parking lot.

The spatial autocorrelation function of a profile varies with the distance between two points on that profile. For an isotropic surface, the orientation of the line connecting those points is irrelevant—only the distance matters. The distance between two points on parallel wheelpaths is

$$s = \sqrt{\xi^2 + (2b)^2} \quad (3.2-15)$$

where  $\xi$  is the distance component parallel to the wheeltracks and  $b$  is half of the track spacing. The cross-correlation function can now be written in terms of the autocorrelation function of a wheeltrack profile

$$R_{z_L z_R}(x) = R_{z_L z_L}(s) = R_{z_R z_R}(s) = R_{zz}(s) \quad (3.2-16)$$

This model has been used when a PSD function is available for a single wheeltrack, and a vehicle analysis requires inputs from two or more. Starting with a single profile PSD function, the autocorrelation function is computed via a discrete Fourier transform. That transform is then converted to a cross-correlation function using eq. 3.2-16. Finally, the cross-spectral density function is computed by a discrete Fourier transform of the cross-correlation function (eq. 2.2-13).

The end result is that the road is represented by a PSD for each wheeltrack (the two PSDs are identical), and a cross-spectral density function between the two wheeltracks, which is specific to the wheeltrack spacing. Due to symmetry, the cross-spectral density function is always positive and real.

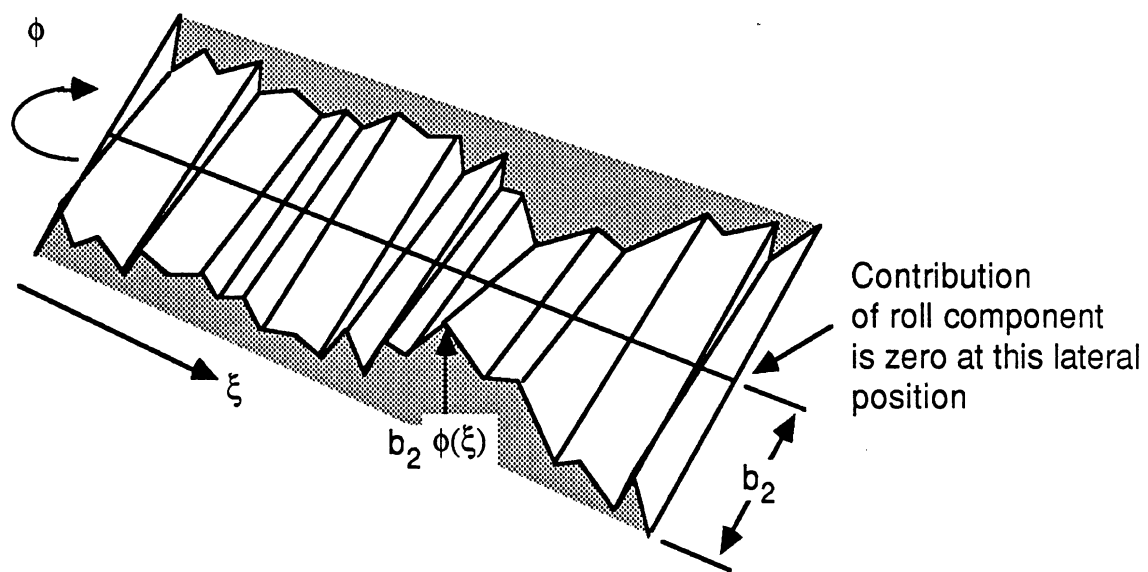


Figure 3.2-2. The "ribbon road" model.

### 3.2 Correlation Between Multiple Wheeltrack Profiles

Comparisons between the cross-spectral densities predicted by the isotropic road model and measured profiles have shown that many public roads are not isotropic [12, 13], although some are [11, 14].

### 3.3 Conversions Between Statistics and Profiles

As noted earlier, different vehicle analyses require different forms of input descriptions:

- Time-domain analyses require a longitudinal profile for each wheel.
- Frequency-domain analyses require PSD functions for the profiles.
- State-space analyses require one or more “white-noise” amplitude levels, and optionally, shaping filters.
- Hardware simulations require a continuous signal proportional to profile for each wheel, sometimes generated with white-noise sources and filters.

There are three descriptions commonly used: longitudinal profile, PSD, and filtered white-noise. Of the three, the profile contains the most information, and a white-noise amplitude contains the least. A PSD function succinctly shows roughness as a distribution of mean-square variations over wavenumber. Because the different representations do not contain the same amount of information, it is not always possible to convert reversibly. For example, it is possible to generate an infinite number of profiles that have the same PSD. When converting to a representation that contains more information—say, from a PSD to a profile—information must be added artificially. It is important that this be done in such a way that the inputs remain representative of real pavements.

Statistical representations of the profile that address characteristics other than the mean-square value may be sometimes necessary. In particular, it may be important to distinguish roads whose roughness is spread uniformly over their length due to a generalized unevenness, and roads whose roughness is caused by localized features such as potholes. For example, consider two road profiles with identical mean-square summary roughness levels and similar PSD functions. One is a smooth profile with a single large pothole; the other is a slightly rougher profile with no singular features. Although both roads have the same “average” roughness properties, the one pothole on the smooth road damages vehicles, whereas the distributed roughness on the other road does not.

#### *Conversion from White-Noise Sources to PSD*

Conversion from white-noise sources to a PSD is performed by multiplying the transfer functions of the shaping filters (if used) by the amplitude of the white-noise sources. If the input is built by adding several shaped noise sources together, the PSD of the input is the sum of the PSDs of the components:

$$G_{zz} = \sum_{i=1}^n |H_i|^2 Q_i \quad (3.3-1)$$

### 3.3 Conversions Between Statistics and Profiles

where  $H_i$  is the transfer function of the shaping filter for the  $i^{\text{th}}$  noise source and  $Q_i$  is the (constant) PSD amplitude for that source. Assuming that unnecessary (redundant) noise sources were not used, this transformation is reversible. (That is, white-noise amplitudes can be deduced from the PSD functions.)

#### *Conversion from White-noise Sources to Profile*

A random signal can be generated digitally using a random number algorithm. In using such an algorithm, several parameters must be specified: a type of distribution, a mean value, and a standard deviation. When generating profiles, a Gaussian distribution should be used, the mean value should be zero, and the standard deviation should be

$$\sigma = \sqrt{\frac{G_0}{2\Delta}} \quad (3.3-2)$$

where  $G_0$  is the amplitude of the noise PSD and  $\Delta$  is the interval between samples, expressed in the (inverse) units used for wavenumber. (For example, if wavenumber is cycle/ft, then  $\Delta$  should be specified in ft.)

A profile defined as a sum of filtered white-noise sources is generated by (1) creating an independent sequence of random numbers for each white-noise source, scaled according to eq. 3.3-2 to match a model PSD amplitude, (2) feeding those sequences into digital shaping filters with the desired response properties, and (3) summing the outputs of the filters.

The same process can be performed electronically, for use in laboratory simulators. Instead of numerical methods, electronic components are used to perform the same functions. Independent white-noise generators are fed into analog filters, whose outputs are summed to obtain a voltage signal with the desired statistical properties of the profile. That voltage can be used as excitation to laboratory shakers or an analog computer simulation.

#### *Conversion from PSD to White-Noise Sources*

Characterizing a PSD as a sum of filtered white-noise sources involves curve fitting. Given a relationship as defined in eq. 3.3-1, the job is to determine values for  $Q_i$  and functions for  $H_i$  such that the PSD built from the noise sources matches the original PSD with an acceptable level of agreement. This conversion is not exact, and usually only a ballpark agreement is sought. Filters that can be described by simple differential equations are integrators and one-pole high-pass and low-pass filters.

It is helpful to plot the profile PSD on log-log paper, and to consider approximations of the slope of the elevation PSD to powers of 2. A white-noise source for profile elevation is constant with frequency; a source for profile slope decreases with the second power of frequency; a source for profile acceleration decreases with the fourth power of frequency. The PSD model presented in Section 4.1 was developed using this approach, to allow the generation of profiles via eqs. 3.3-1 and 3.3-2.

### 3.3 Conversions Between Statistics and Profiles

#### *Conversion from PSD to Profile*

Profiles are usually handled in sections that are approximately stationary over their length. A popular method for generating a random profile that is approximately stationary from a PSD function is by summing a large number of sinusoids. The amplitudes are determined by the PSD function and a frequency interval, and the phase angles are random. That is,

$$z(\xi) = \sum_{i=1}^n \left[ \sqrt{\Delta v_i G_{zz}(v_i)} \cos(2\pi v_i \xi + \phi_i) \right] \quad (3.3-3)$$

where

$$\Delta v_i = \frac{v_{i+1} - v_{i-1}}{2} \quad (3.3-4)$$

$\xi$  is longitudinal distance,  $n$  is the number of sinusoidal components used to generate the profile,  $v_i$  is the spatial frequency associated with the  $i^{\text{th}}$  component of the summation,  $\Delta v_i$  is the bandwidth of the  $i^{\text{th}}$  component, and  $\phi_i$  is a random phase angle, generated such that it has a uniform distribution over the range  $-180^\circ$  to  $+180^\circ$ . The number of components should be large enough that the exact values of the frequency within a frequency window  $\Delta v$  is not significant. Typically, the components should cover the wavenumber range of .0033 to 1 cycle/ft (wavelengths from 1 to 300 ft/cycle), with a  $\Delta v$  interval of 0.0033 cycle/ft for the low frequencies and .01 for the higher frequencies.

The profile obtained with this method is approximately stationary (due to the uniform distribution of random phase) and Gaussian (due to the central limit theorem). For computational efficiency, the sum of sinusoids can be replaced with the FFT [14].

If the PSD can be expressed as a sum of filtered white-noise sources, the conversion from white-noise to profile (eqs. 3.3-1 and 3.3-2) is a second alternative that requires much less computation.

The transformation is reversible if the PSD computation software is insensitive to details such as the number of samples and the stationarity of the signal. (See Appendix A.)

#### *Generating Correlated Profile with Cross-Spectral Densities*

Profiles that have a coherence ranging between zero and unity can also be generated from PSD functions using eqs. 3.3-3 and 3.3-4. The approach is to build the profile from several uncorrelated components, and to use the cross-spectral density function to determine the relative contribution of each. When two profiles are needed, three spectral densities are used: the PSD of each profile and the cross-spectral density. One of the profiles is generated from the PSD as described above. Assuming the first profile was for the left-hand wheeltrack, the profile for the right-hand wheeltrack is generated using the summation

### 3.3 Conversions Between Statistics and Profiles

$$z_R(\xi) = \sum_{i=1}^n \left[ \sqrt{\Delta v_i G_{z_{LZ}}(v_i)} \cos(2\pi v_i \xi + \phi_i) + \sqrt{\Delta v_i (G_{zZ}(v_i) - G_{z_{LZ}}(v_i))} \cos(2\pi v_i \xi + \theta_i) \right] \quad (3.3-5)$$

where  $\phi_i$  is from the same series of phase angles used for the first (left-hand) profile, and  $\theta_i$  is from a second series of uniformly distributed phase angles. The correlated component of the second profile is produced by the first term, and the uncorrelated component is produced by the second term.

A simpler method can be used when the profiles are summed from the two uncorrelated profile components  $z_V$  and  $z_C$  (eq. 3.2-1). The PSDs of the modal profiles are converted to profiles, and those modal profiles are combined to yield wheeltrack profiles with the proper correlation by applying eq. 3.2-2.

#### *Conversion from Profile to White-Noise Sources*

Reduction of a profile signal to one or more noise amplitudes is not normally performed. One way to perform the conversion is to first compute the PSD from the profile, and then determine equivalent noise amplitudes from the PSD function.

#### *Conversion from Profile to PSD*

Conversion from a measured profile to a PSD is accomplished by conventional spectral analysis software that applies eqs. 2.2-10 and 2.2-11. Additional steps are involved to handle numerical problems that can occur for real-world data. The steps used for computing PSDs at UMTRI are provided in Appendix A.

This conversion is not reversible—a profile cannot be reconstructed from a PSD.

## 3.4 Speed Relationships

Ground surface properties are described as functions of spatial variables, independent of the vehicle speed. To the moving vehicle, the variations in a surface appear as time-varying inputs under each wheel, with the specific input being a function of speed.

When the inputs are represented by elevation profiles, the transformation from space to time is simply to multiply the time by speed to obtain the corresponding distance:

$$z_p(t) = z_p(\xi) \quad \xi = t V \quad (3.4-1)$$

where  $z_p$  is elevation along a profile. When the input is represented by a spatial slope profile, the chain rule can be applied to obtain a vertical velocity input

$$\begin{aligned} \dot{z}_p(t) &= \frac{d}{dt} z_p(t) \\ &= \frac{d\xi}{dt} \frac{d}{d\xi} z_p(\xi) \end{aligned}$$



### 3.3 Conversions Between Statistics and Profiles

$$= V z'_p(\xi) \quad (3.4-2)$$

If the profile is described by a PSD of elevation, the spatial frequency (wavenumber) is converted to temporal frequency (Hz) by the speed.

$$f = vV \quad (3.4-3)$$

$$\left\{ \frac{\text{cycle}}{\text{sec}} = \frac{\text{cycle}}{\text{length}} \frac{\text{length}}{\text{sec}} \right\}$$

The PSD amplitudes must be comparably rescaled, such that the integral over temporal frequency yields the mean-square elevation:

$$G_{zz}(f) = \frac{1}{V} G_{zz}(v) \quad (3.4-4)$$

When the PSD is developed for the slope of profile, the conversion to yield a PSD of vertical velocity is

$$G_{\dot{z}\dot{z}}(f) = V G_{z'z'}(v) \quad (3.4-5)$$

If a road is approximated as a white-noise slope input ( $G_{z'z'}$  is constant over wavenumber), then eq. 3.4-5 implies that the mean-square (PSD) input increases approximately with speed and the vibration levels (RMS, etc.) increases approximately with  $\sqrt{V}$ .

## 4. STANDARDIZED ROAD INPUTS

An “average pavement” model ensures that predictions of vehicle response are representative over a range of actual conditions. A standardized input is obtained with a mathematical model of a road input, generally in the form of an equation specifying a PSD function. The roughness properties are then completely defined by the values of coefficients in the PSD equation.

There has been some interest in establishing such a standard, including a draft proposal that was once considered by an ISO subcommittee[15]. Such efforts have been hampered by the relatively small amount of profile data available to vehicle dynamicists. Measures of both wheeltrack profiles, needed to determine the correlation between the right- and left-hand inputs, are even more scarce.<sup>1</sup>

In the following material, the modeling of a single profile via a PSD equation is considered for roads whose roughness is caused by seemingly random variations in the profile. Next, models for creating the proper correlation between two wheeltracks are considered. Finally, sources of roughness that are not well represented by PSD functions are addressed.

### 4.1 Stationary Wheeltrack Profiles

Early measures of longitudinal profiles of airport runways and other traveled surfaces were processed to obtain plots of PSD functions, and the PSD was proposed as a convenient means for characterizing ground inputs to vehicles [16, 17]. Example PSD functions for two profiles are shown in Figure 4.1-1. In addition to the PSD of elevation, the figure shows the first and second derivatives (slope and spatial acceleration), obtained by multiplying by the factor  $(2\pi v)^2$  for each level of differentiation. Notice that when the PSD is shown for profile slope, the scaling can be set to show the greatest detail. In contrast, the plots of elevation PSD are necessarily compressed to fit on the paper, so that details are lost. For this reason, all profile PSD functions that follow are based on slope. A similar convention has been used in other publications involving numerous measured road PSDs [18, 19, 20].

Since the first profile PSDs were computed, the most popular model for a wheeltrack profile is a profile whose slope is “white-noise” with a constant amplitude roughness A,

$$G_{z'z'}(v) = A \quad (4.1-1)$$

---

<sup>1</sup> Nearly all of the profile data measured today are obtained for use in the highway community, where there is little or no interest in establishing standard pavement roughness models. (Rather, the interest is in defining standard vehicle dynamics responses, so that alternative pavement characteristics can be evaluated.) Advances in technology have resulted in a number of high-speed systems that are routinely used to measure road profile. However, the PSD analyses needed to develop input models are seldom performed. Profile data shown in this report are drawn from two UMTRI research projects, described in Appendix B.

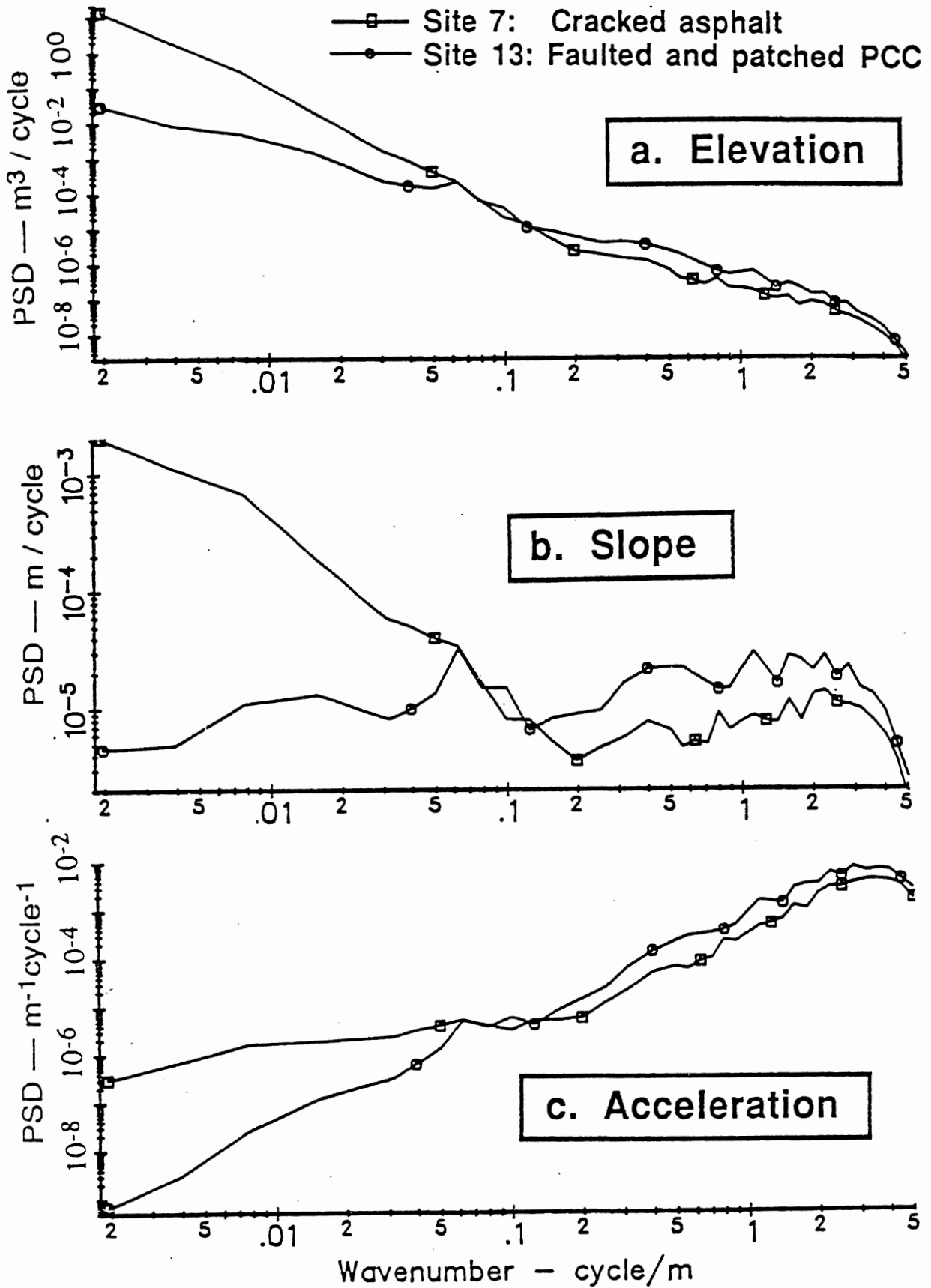


Figure 4.1-1. PSDs of elevation, slope, and acceleration profile.

#### 4.1 Stationary Wheeltrack Profiles

where  $z'$  is the longitudinal slope of the road in the wheeltrack. The PSD function of elevation (the integral of slope) is obtained by dividing by a factor of  $(2\pi v)^2$

$$G_z(v) = \frac{A}{(2\pi v)^2} \quad (4.1-2)$$

The “white-noise slope” model is an appealing road model, because it involves only the single roughness parameter,  $A$ . Also, it is simple enough to be compatible with all analyses described in this report, and even closed-form solutions for simple vehicle analyses.

Figures 4.1-2 through 4.1-4 show example PSD plots measured for three types of pavements: asphalt (Figure 4.1-2), surface treatment (Figure 4.1-3), and Portland cement concrete (Figure 4.1-4). These plots were prepared using the PSD of profile slope. Thus, the model of eq. 4.1-2 is represented by a horizontal line at the level  $A$ . Figure 4.1-2 shows example lines of white-noise slope, elevation, and acceleration for reference. Although the PSDs of measured profile come closer to matching a model of white-noise slope better than they do models of white-noise elevation or white-noise acceleration, the agreement could be better.

Alternate PSD model equations have been proposed to provide closer agreement with measured data than the white-noise slope model. One of these is a straight line on log-log paper, with the form:

$$G_z(v) = A v^\alpha \quad (4.1-3)$$

When a PSD cannot be reasonably characterized by a single straight line, then a piece-wise fit has been used, with different values of  $A$  and  $\alpha$  selected to cover two or more wavenumber ranges [11]. This model was proposed for analyses in the frequency domain and is not particularly well suited for state-space analyses or other applications in which it is necessary to model the road as filtered white-noise.

To describe this general type of PSD signature in a form compatible with all of the vehicle analyses described earlier, it is convenient if the profile can be defined using white-noise sources and “shaping filters.” If possible, the shaping filters should be defined by simple equations for use with state-space analyses and for hardware implementations. One such approach was demonstrated in Reference [9]; a more general approach is developed later in Section 4.2.

PSD functions of profile slope were prepared for a variety of roads in several recent research projects (see Appendix B or References [19, 20]). As shown in Figures 4.1-2 through 4.1-4, PSD functions of measured slope profiles generally have a minimum value between .1 to .5 cycle/m. Systematic decreases in PSD slope amplitude outside that band are nearly always due to limitations in the profile measuring equipment. Because the roads do not seem to show any “roll-off” (within the limitations of the measuring equipment), the use of high-pass filters or low-pass filters to shape a model PSD function is not indicated. A model that matches the measured data has been defined using three independent white-noise sources and integrators

PSD of L. Wheeltrack - m/cycle

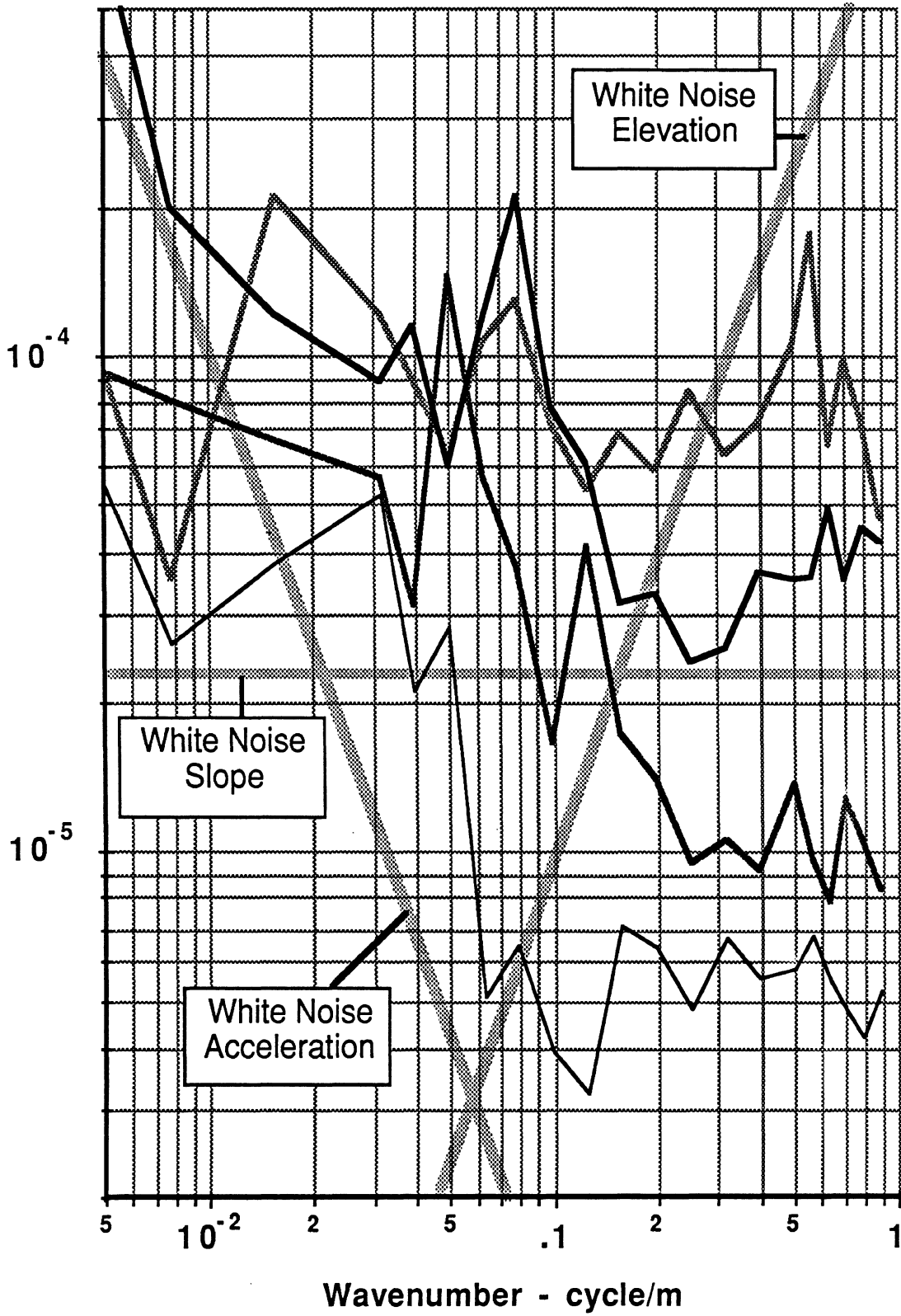


Figure 4.1-2. Typical PSD functions for asphalt roads.

PSD of L. Wheeltrack - m/cycle

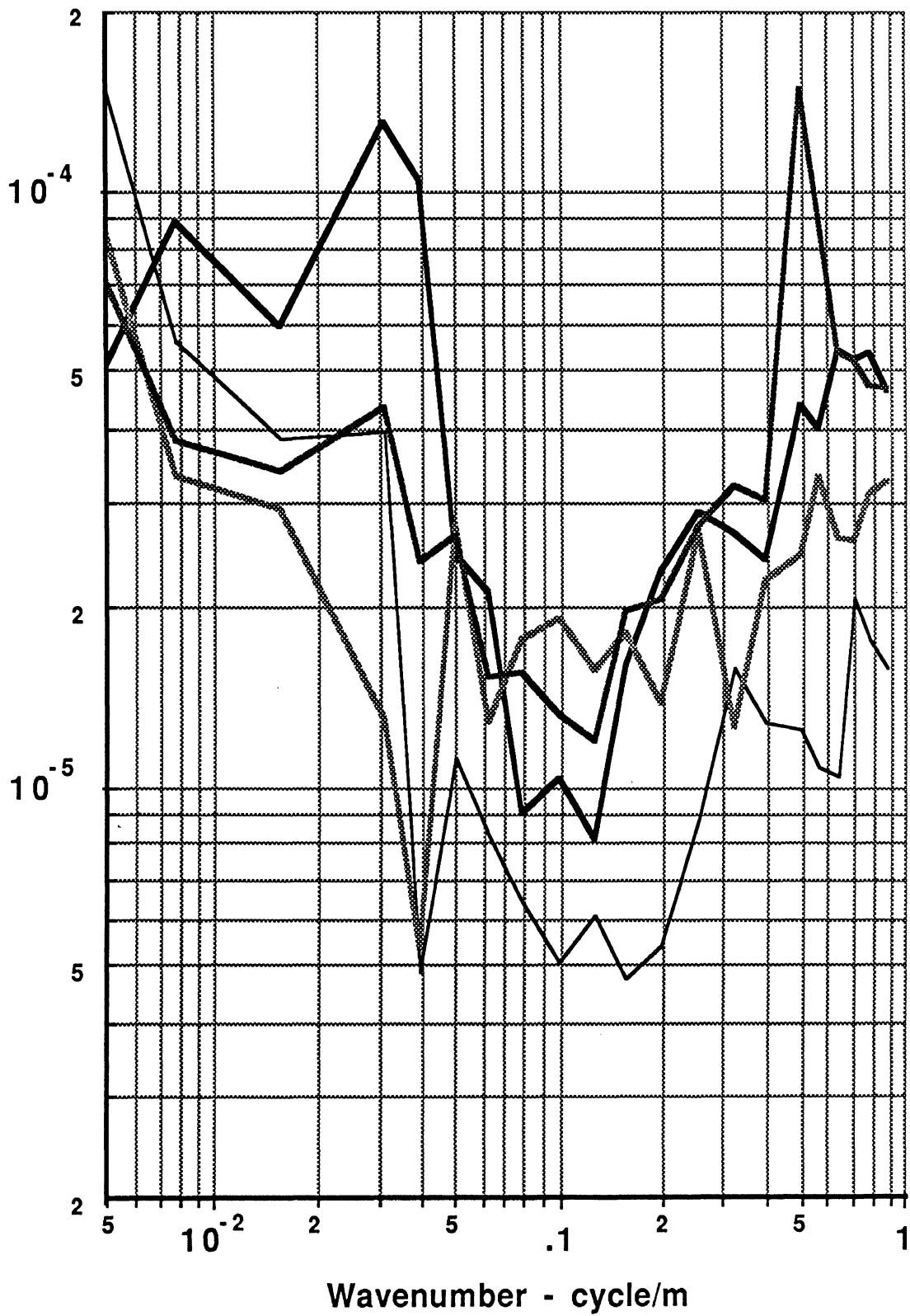


Figure 4.1-3. Typical PSD functions for surface treatment roads.

PSD of L. Wheeltrack - m/cycle

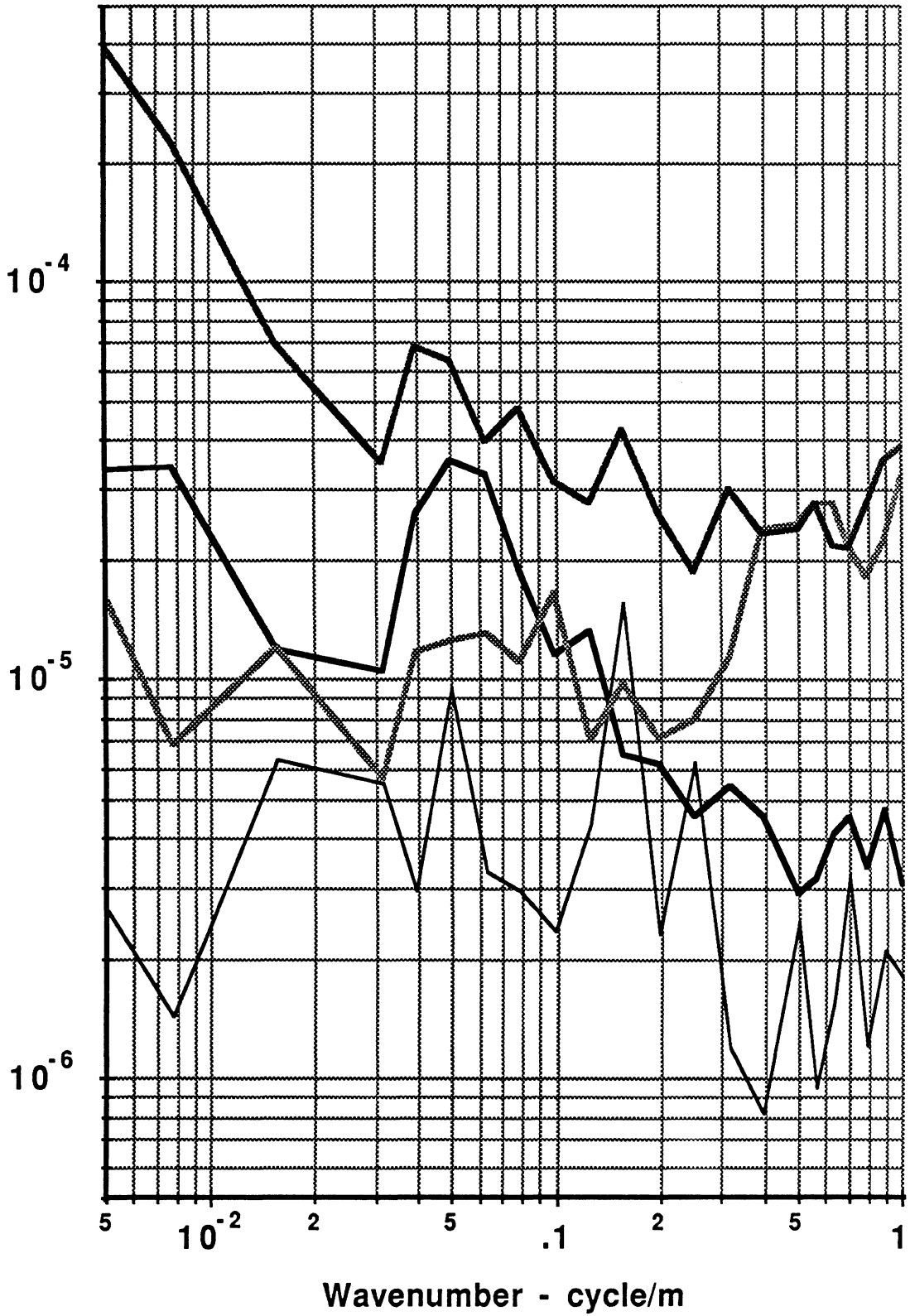


Figure 4.1-4. Typical PSD functions for concrete roads.

#### 4.1 Stationary Wheeltrack Profiles

$$G_z(v) = G_a (2\pi v)^{-4} + G_s (2\pi v)^{-2} + G_e \quad (4.1-4)$$

This formulation allows an input profile to be generated using up to three independent white-noise sources. The first component, with the amplitude  $G_a$ , is a white-noise acceleration that is integrated twice. The second, with amplitude  $G_s$ , is a white-noise slope that is integrated once. The third, with amplitude  $G_e$ , is a white-noise elevation. More details concerning the generation of profiles using this model are presented in Section 7.1. The same model can be written to define the PSD of profile slope by looking at the derivative of eq. 4.1-4

$$G_z'(v) = G_a (2\pi v)^{-2} + G_s + G_e (2\pi v)^2 \quad (4.1-5)$$

Figure 4.1-5 shows comparisons between the model and measured PSD functions for two profiles. Virtually all published PSD functions also fit this model form, including numerous plots for European roads [18] and Texas roads [21].

A characteristic shown in some published data is a roll-off at high and low wavenumbers. All profiling instruments have limited bandwidth, and more often than not, the bandwidth is not specified. Extensive data collected with a variety of instruments in the 1984 Ann Arbor Road Profilometer Meeting showed that the roll-off was due to the instrumentation in every case. That is, there were no sites where the road PSDs roll-off as if subject to a high-pass or low-pass filter for wavenumbers between 0.002 and 4 cycle/m (wavelengths between 0.25 m and 500 m). (The roll-off due to the instrument is shown later for the high-wavenumber limit.)

A number of profiles measured for paved roads were processed to determine the three coefficients needed for the above model using a step-wise curve-fitting method. The ranges of values for these coefficients are summarized below for four classes of surface type:

Table 2. Roughness parameters for white-noise PSD model.

| Surface Type               | $G_s$<br>$m/cycle \times 10^{-6}$ | $G_a$<br>$1/(m \cdot cycle) \times 10^{-6}$ | $G_e$<br>$m^3/cycle \times 10^{-6}$ |
|----------------------------|-----------------------------------|---|-------------------------------------|
| Asphalt (Ann Arbor)        | 1 — 300                           | 0 — 7                                       | 0 — 8                               |
| Asphalt (Brazil)           | 4 — 100                           | .4 — 4                                      | 0 — .5                              |
| PCC (Ann Arbor)            | 4 — 90                            | 0 — 1                                       | 0 — .4                              |
| Surface Treatment (Brazil) | 8 — 50                            | 0 — 4                                       | .2 — 1.2                            |

The range of values shown for the slope coefficient  $G_s$  mainly reflects the roughness range covered by the roads in each category. The broadest range existed within the category of asphalt roads, which included a very smooth section of interstate and a badly damaged urban road with potholes and large patches. The other two coefficients describe additional roughness increasing for very short and very long wavelengths. Amplitudes of very long wavelengths, indicated by non-zero values of  $G_a$ , might be associated with the quality of



Slope PSD functions — m/cycle

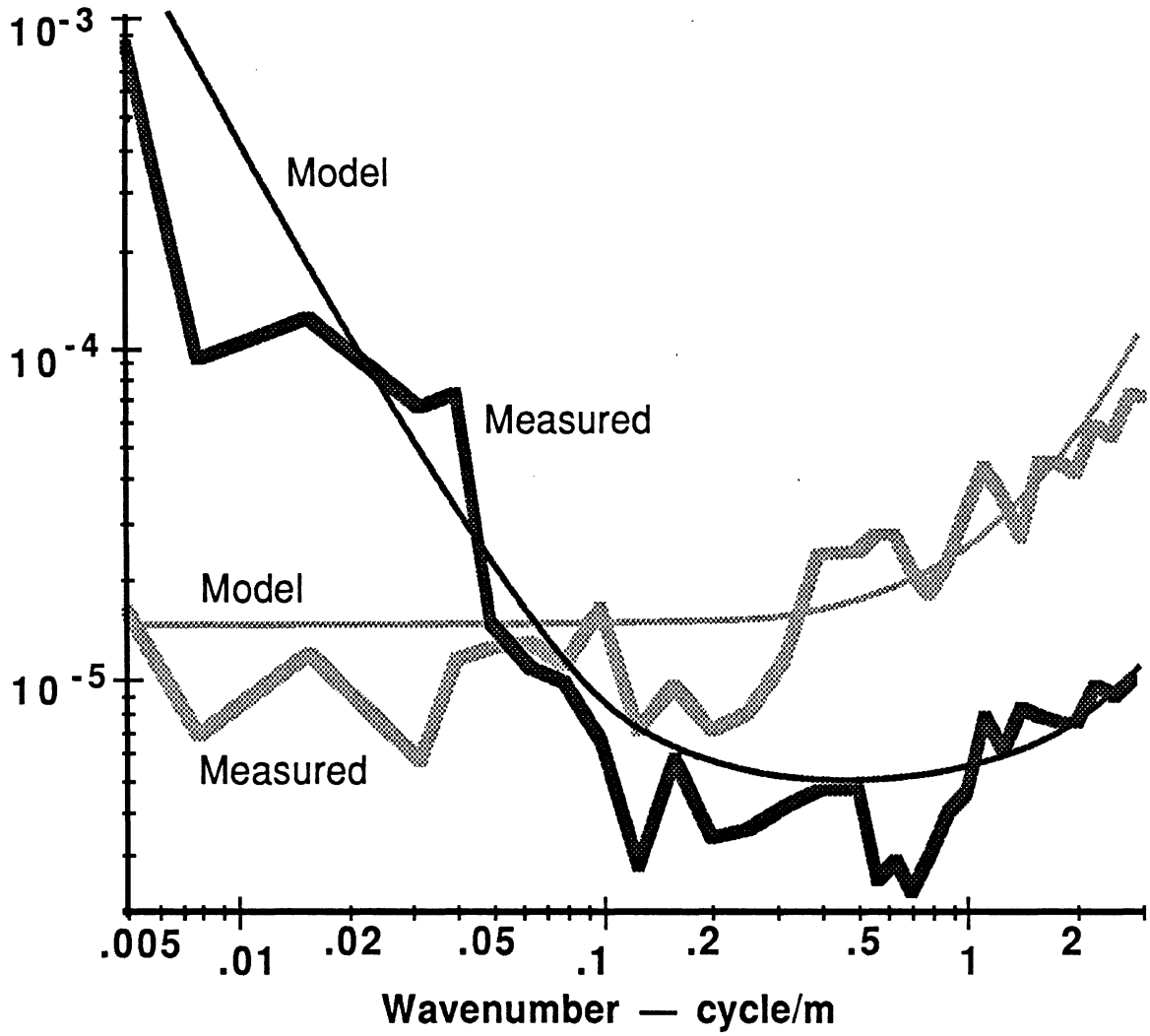


Figure 4.1-5. Comparison between model PSD function and measurements.

#### 4.1 Stationary Wheeltrack Profiles

grading performed in building the road. High amplitudes of very short wavelengths, typified by non-zero values of  $G_e$ , are commonly caused by surface defects that are extremely localized such as faults, tar strips, potholes, etc. Localized roughness is common on unpaved roads, and appears to be carried over when dirt roads are given surface treatments.

The data used to prepare Table 2 are shown graphically in Figures 4.1-6 and 4.1-7, to better indicate the distribution of the roughness parameters. Figure 4.1-6 shows that there is little correlation between the  $G_s$  and  $G_a$  coefficients. The maximum acceleration coefficients are found on roads with moderate slope values. This is to say that the roads with very low  $G_s$  values are not likely to have the highest  $G_a$  values.

Figure 4.1-7 shows that roads with low  $G_s$  values nearly always have low  $G_e$  values. That is, smooth roads with low  $G_s$  values are unlikely to have much of the localized surface failures that cause significant  $G_e$  values. Roads with high  $G_s$  values might or might not have high  $G_e$  values, meaning that the roughness may come from localized failures or from other causes.

Asphalt pavements generally show the highest  $G_a$  coefficients, and PCC pavements show the lowest. This indicates that, on the average, asphalt roads have proportionately more of their roughness at very long wavelengths and less at short wavelengths. However, the figures also show that individual PCC roads can have the same coefficients as individual asphalt roads. Surface type alone is not sufficient to determine the relative distribution of roughness as characterized by the three coefficients of the model. Overall, the figures indicate that there is no hard and fast rule relating surface type to specific PSD signatures. Instead, they show the limits of PSD signatures that are encountered, based on the model. Any combination of coefficients shown in the figures represents a road that has been measured.

Eq. 4.1-5 is valid only for the range of wavenumbers shown in the figures. As noted earlier, the model is valid up to the bandwidth limitations of the profile measurements. This range greatly exceeds the bandwidth of most vehicle analyses. If a greater frequency range is required, an extrapolation is probably not valid for reasons given below.

None of the PSD models are valid for wavenumber approaching zero, as this would imply a profile with a mean-square elevation approaching infinity. This does not limit the practical use of the models, because the mean-square elevation approaches infinity only for roads of infinite length. If a vehicle analysis involves very low frequencies or long time durations, a high-pass filter can be used to attenuate the roughness amplitudes for very long wavelengths that are outside the bandwidth of a vehicle. For example, a one-pole high-pass filter with a cut-off set for a wavelength of 1000 ft will prevent the elevation levels from drifting to infinity, while retaining all of the roughness characteristics that could ever influence a vehicle. (A shorter cut-off of 200 ft. is adequate for most analyses.)

At the upper frequency limit, the mean-square elevation reaches a limiting value if the elevation PSD decrease with wavenumber with a negative exponent of one or greater ( $\alpha < -1$ ). This condition is not satisfied if eq. 3.3-5 is used and  $G_e$  is non-zero, as it is for most concrete pavements. When  $G_e$  is non-zero, the mean-square value of elevation increases in proportion to the upper wavenumber bound. Given that the mean-square

(Wheeltrack Profile)

Accel. Coef  
 $G_a - 1/(m \cdot \text{cycle})$

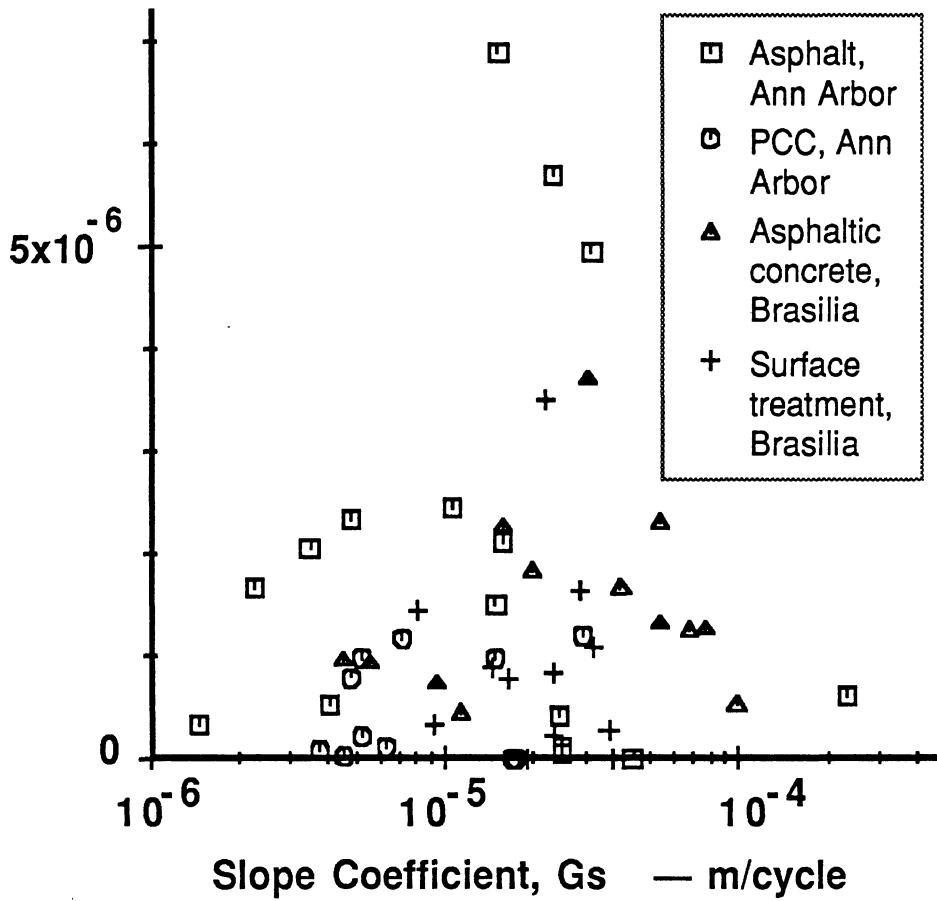


Figure 4.1-6. Distribution of low-wavenumber PSD model coefficients for measured data.

(Wheeltrack Profile)

Elev. Coef  
 $G_e - m^3/cycle$

Note: One site had a  $G_e$  coefficient of  $7.7 \times 10^{-6}$

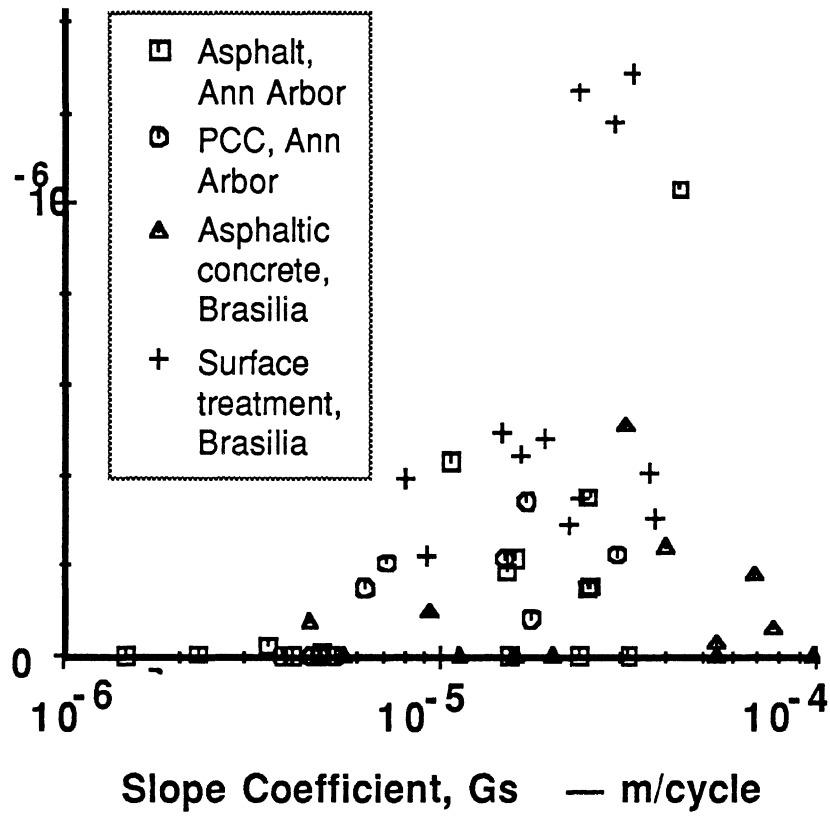


Figure 4.1-7. Distribution of high-wavenumber PSD model coefficients for measured data .

## 4.1 Stationary Wheeltrack Profiles

elevation levels of real roads should not grow without limit as the sample interval decreases (thereby increasing the upper wavenumber), the PSD functions of real roads must roll off at high wavenumbers.

Most profile measurements that have been made in the United States are not accurate for wavenumbers above 3 cycle/m. To prevent aliasing problems, low-pass filters are used to attenuate the measurements for wavenumber with a cut-off at about one-fourth of the sample frequency. Figure 4.1-8 shows the PSDs for the left-hand wheeltrack of eleven concrete pavements. In every case, the PSD is increasing with wavenumber for wavenumbers above 1 cycle/m, until 3 cycle/m where the anti-aliasing filter was set. The sample frequency for these measures was 13.1 sample/m (3 inch interval). The only way to determine the roughness properties for wavenumbers above 3 cycle/m is to make new measurements with a higher sampling rate and a higher cut-off for the anti-aliasing filter. If profiles are generated which will have higher frequencies, they should be filtered with at least a one-pole low-pass filter, with the cut-off set for 3 cycle/m, in order to prevent extrapolations beyond the range of measured data.

## 4.2 Models for Two Wheeltracks

A number of relationships were presented in Section 3.2 involving the correlation between the left- and right-hand wheeltracks, and the vertical and cross-level modal profiles. The modal profiles are defined by the point-by-point sum and difference of the wheeltrack profiles. When the two wheeltracks have identical roughness levels, the modal profiles are uncorrelated and can be used to develop wheeltrack profiles with realistic correlation. The correlation can be summarized by a function of wavenumber,  $\beta$ , defined as the ratio of the cross-level profile to the vertical profile. Recall that  $\beta$  must approach zero for very low wavenumbers and unity for very high wavenumbers.

Inputs for two parallel wheeltrack profiles can be generated from the PSD function of a single wheeltrack profile and a prescribed  $\beta$  function. The relationships in Section 3.2 and 3.3 can be used to generate stationary profiles with the appropriate correlation for time-domain simulations, or cross-spectral densities for frequency-domain analyses.

The modeling of multiple wheeltrack inputs of equal roughness essentially reduces to a choice of how the  $\beta$  function is defined. Two methods for defining this function are by (1) an arbitrary shaping filter, and (2) the assumption that the surface is isotropic.

### *The Shaping Filter Approach*

In this method,  $\beta$  is defined by the squared transfer function of a high-pass filter. The filter should result in a  $\beta$  function that matches measurements for real roads, but it can also be chosen for simplicity and efficiency.

This approach has been presented for a white-noise slope as the modal vertical profile [9]. It is further developed below for an arbitrary wheeltrack PSD, using a one-pole low-pass filter with the transfer function

PSD of L. Wheeltrack - m/cycle

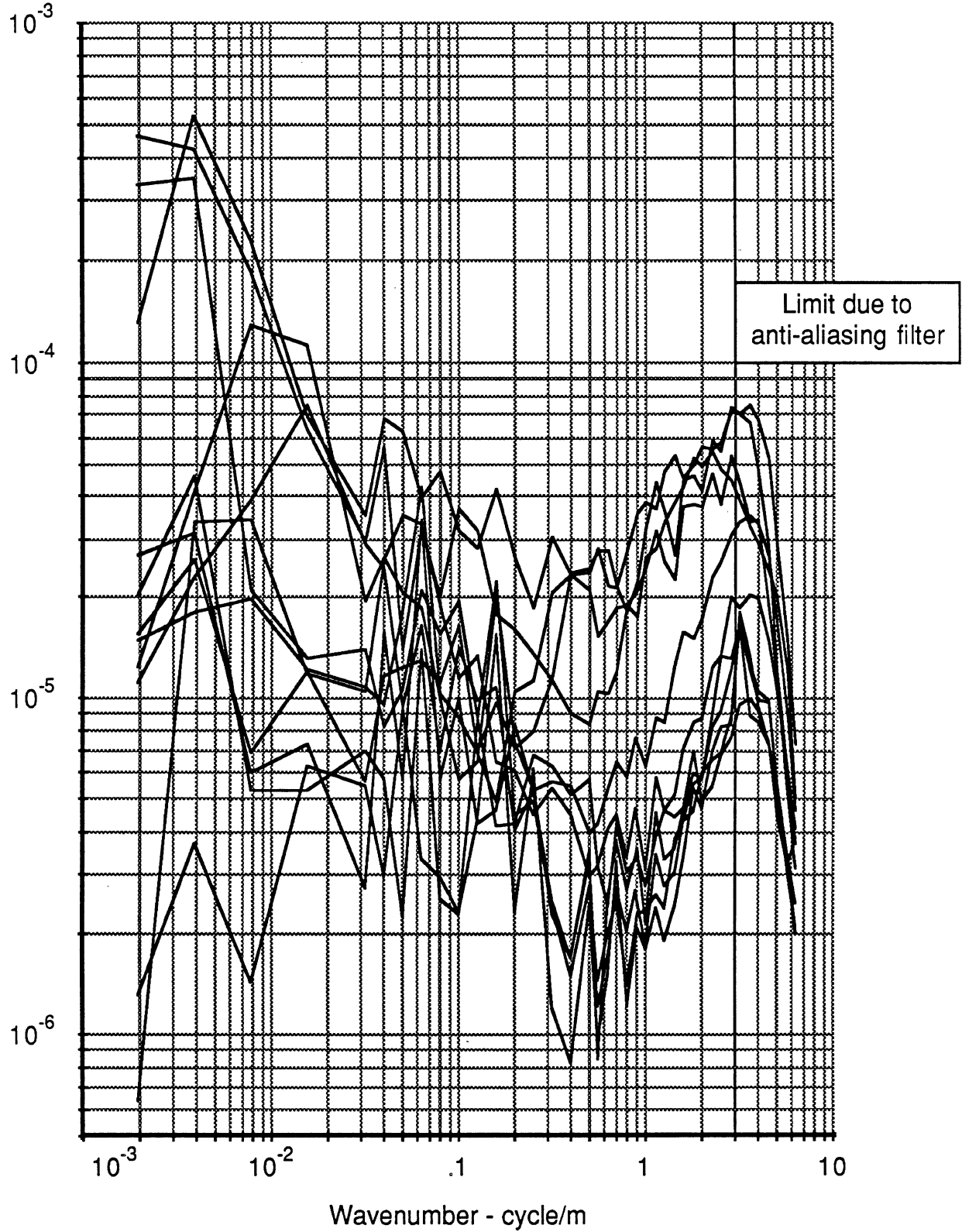


Figure 4.1-8. Effect of anti-aliasing filter on high wavenumbers

## 4.2 Models for Two Wheeltracks

$$H_{\text{low}}(\omega) = \frac{\omega_1}{\omega_1 + j\omega} \quad (4.2-1)$$

where  $\omega_1$  is the cut-off frequency. The corresponding high-pass filter has the transfer function

$$H_{\text{hi}}(\omega) = \frac{j\omega}{\omega_1 + j\omega} \quad (4.2-2)$$

$\beta$  is defined by the squared amplitude of the high-pass transfer function

$$\beta(\omega) = |H_{\text{hi}}(\omega)|^2 = \frac{\omega^2}{\omega_1^2 + \omega^2} \quad (4.2-3)$$

A spatial equivalent of the filter is obtained by substituting longitudinal distance ( $\xi$ ) for time ( $t$ ), to obtain the transfer function in terms of spatial frequency. By also converting from circular to cyclical frequency, the  $\beta$  function becomes

$$\beta(v) = |H_{xy}(v)|^2 = \frac{v^2}{v_1^2 + v^2} \quad (4.2-4)$$

Figure 4.2-1 shows that a one-pole high-pass filter with a cut-off wavenumber ( $v_1$ ) of 0.2 cycle/m (5-m wavelength) provides a good match for measured profiles from asphalt roads with a track spacing of 1.5 m.

For this shaping filter, the relation between the wheeltrack and vertical PSD (eq. 3.2-6) becomes

$$\begin{aligned} G_{z_v z_v} &= G_{zz} \frac{1}{(1 + \beta)} \\ &= G_{zz} \frac{v_1^2 + v^2}{v_1^2 + 2v^2} \\ &= \frac{1}{2} G_{zz} \left( 1 + \frac{v_1^2}{v_1^2 + v^2} \right) \end{aligned} \quad (4.2-5)$$

where

PSD Ratio:  $G_c / G_v = \beta$

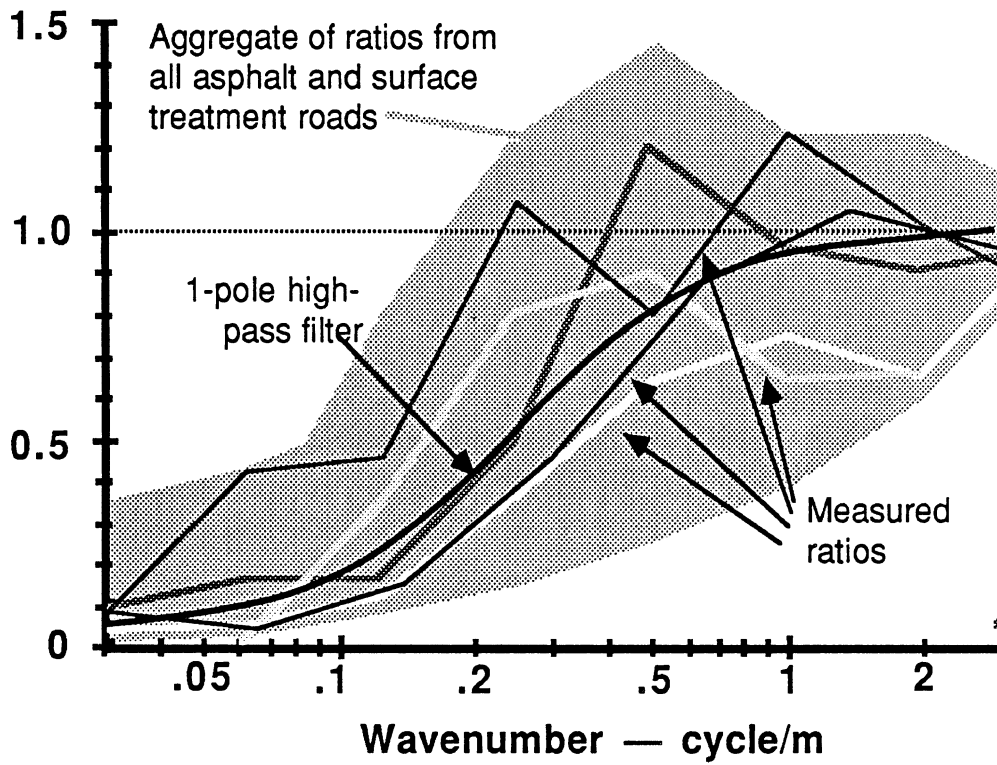


Figure 4.2-1. Use of a single-pole “shaping filter” to define ratio between cross-level and vertical PSD functions.



## 4.2 Models for Two Wheeltracks

$$v_2 = \frac{v_1}{\sqrt{2}} \quad (4.2-6)$$

In order to generate profiles using this shaping filter, it is useful to further decompose the profiles such that the vertical modal profile is the sum of two uncorrelated components:

$$z_V = z_{V_1} + z_{V_2} \quad (4.2.7)$$

The PSD component  $G_{z_{V_1}z_{V_1}}$  will now be defined as

$$G_{z_{V_1}z_{V_1}} = \frac{G_{zz}}{2} \quad (4.2-8)$$

By combining eqs. 4.2-5 and 4.2-8, the PSD component  $G_{z_{V_1}z_{V_1}}$  is also defined:

$$G_{z_{V_1}z_{V_1}} = \frac{1}{2} G_{zz} \left( \frac{v_2^2}{v_2^2 + v^2} \right) \quad (4.2-9)$$

The cross-level PSD can also be written in terms of the wheeltrack PSD and the cut-off wavenumber

$$G_{z_C z_C} = \frac{1}{2} G_{zz} \left( \frac{v^2}{v_2^2 + v^2} \right) \quad (4.2-10)$$

Eqs. 4.2-6 through 4.2-10 suggest a procedure to generate profiles from a wheeltrack PSD, when the wheeltrack PSD can be generated from white-noise sources shaped by filters.

1. Three uncorrelated profiles are generated by filtering and summing white-noise sources such that they are described statistically by the specified wheeltrack PSD. They should be scaled such that their PSD amplitudes are half of the wheeltrack PSD.
2. The first of these is designated  $z_{V_1}$ . It is not filtered further.
3. The second is filtered with a low-pass filter with a cut-off wavenumber of  $v_2$ . The result is the profile  $z_{V_2}$ .
4. The third is filtered with the high-pass filter with a cut-off wavenumber of  $v_2$ . The result is the profile  $z_C$ .
5. The left- and right-hand wheeltrack profiles are now obtained from these three components:

$$z_L = z_{V_1} + z_{V_2} + z_C \quad z_R = z_{V_1} + z_{V_2} - z_C \quad (4.2-11)$$

## 4.2 Models for Two Wheeltracks

The suggested value for  $v_2$  is  $\frac{0.2}{\sqrt{2}} = 0.14$  cycle/m.

This approach is simple to apply and it is efficient for all of the vehicle analyses that are in use. However, it does not have an underlying theoretical foundation to accommodate arbitrary lateral spacings. For example, what would be the proper cut-off wavenumbers  $v_1$  and  $v_2$  if the spacing between profiles were 0.5 m instead of 1.5 m? We expect that the cut-off wavenumber should increase as the lateral spacing between wheeltracks decreases, such that the vertical PSD approaches the wheeltrack PSD, and the cross-level PSD approaches zero.

### *Isotropy*

The isotropic road model defines  $\beta$  as a function of the PSD of a wheeltrack and the lateral spacing between wheeltracks. Unlike the arbitrary filter, this relation is based on a well-defined physical property that a surface might have. Unfortunately, measured data for public roads indicate that most roads are not isotropic. The assumption of isotropy is not valid for pavements whose roughness properties are directional. Roads with ruts in the wheeltracks and concrete roads are obviously not isotropic, and the paving machines used for asphalt construction may produce directional properties.

A practical drawback to the method is that it is computationally intensive and requires unconventional software to map the autocorrelation function into a cross-correlation function.

## 4.3 Corrugations

Country roads that were never graded to the same degree as highways during construction can have unusual roughness properties. This is particularly true for dirt roads which develop corrugations in response to vehicle dynamic response before they are paved. At speeds around 50 mi/h, the 10 Hz axle resonance exhibited by most highway vehicles corresponds to a wavenumber of 0.5 m (2-m wavelength). It is not uncommon to find roads with roughness concentrated about this wavenumber. Figure 4.3-1 shows measured PSD functions from two roads that have relatively high amplitudes at the 0.5 wavenumber.

Roads with corrugations can cause problems when studying vehicle response because vibrations jump up in amplitude when the travel speed is such that the corrugation corresponds to a temporal frequency at which the vehicle has a lightly-damped resonance. The effect is that the vehicle “tunes in” to the corrugation at some particular speed.

## 4.4 Localized Roughness

Most road profiles have the appearance of a stationary random signal, but some do not. A vehicle traversing a road that looks like a stationary random signal is subjected to a more or less continuous excitation. On a road where the roughness is caused by a few discontinuities or other source of localized roughness, the vehicle is subjected to relatively

PSD of L. Wheeltrack - m/cycle

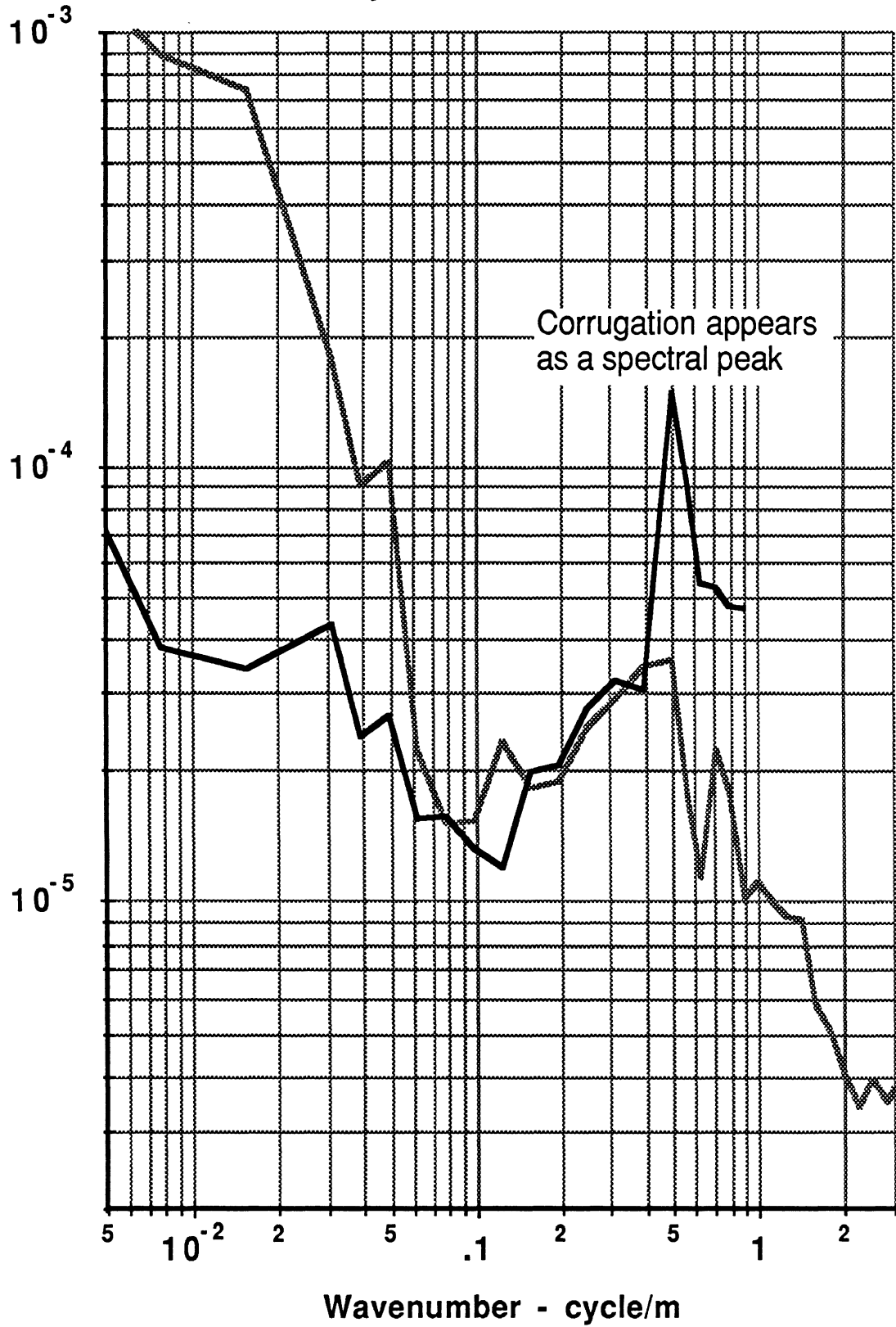


Figure 4.3-1. PSD functions showing corrugations on surface treatment roads.

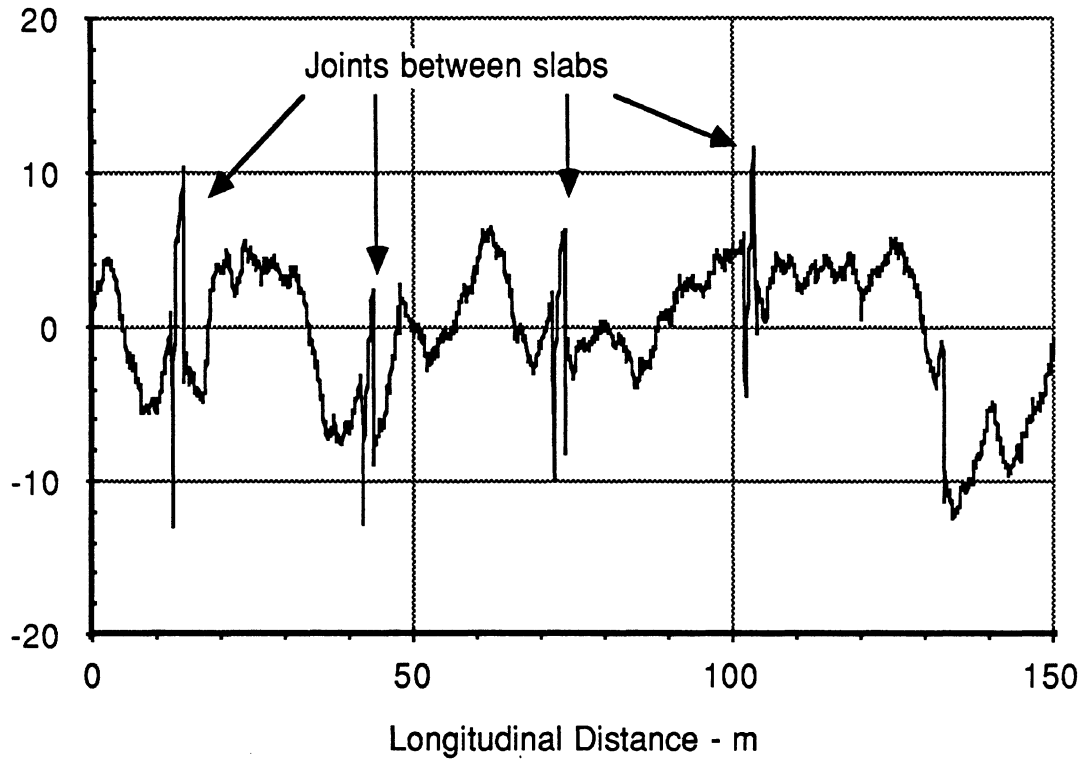
#### *4.4 Localized Roughness*

low levels of vibration most of the time and occasional high levels. The jolts and impacts are averaged out, so that the mean-square vibration levels might be quite reasonable for a pavement/speed/vehicle combination that is not at all reasonable.

The PSD representation of road roughness does not indicate how the roughness is distributed over the length of the road. They can be computed for road sections that are not stationary, and will often give the correct results for a vehicle analysis in terms of mean-square response levels. The danger is that the mean-square summary produced by the analysis might not be an appropriate index to gauge the vehicle response.

Discontinuities are a fact of life for many Portland Concrete Cement (PCC) roads, due to their slab construction. For example, Figure 4.4-1 shows a profile for an old PCC road with gaps and patches at the joints and the corresponding PSD function. The joints are spaced at an interval of 29 m, and thus they define a periodic disturbance whose fundamental spatial frequency is 0.033 cycle/m. Although the spacing is periodic, the shape of the disturbance at each joint varies from joint to joint. The PSD function at the bottom of the figure does not indicate that the surface is perceived as a series of harsh impacts, rather than a continuous noise. It does not even show the spikes that normally identify a truly periodic signal. The only clue that the roughness might be caused by repeating discontinuities is a high concentration of roughness at the second harmonic (wavenumber of 0.06).

Left Elevation - mm



PSD of L. Wheeltrack - m/cycle

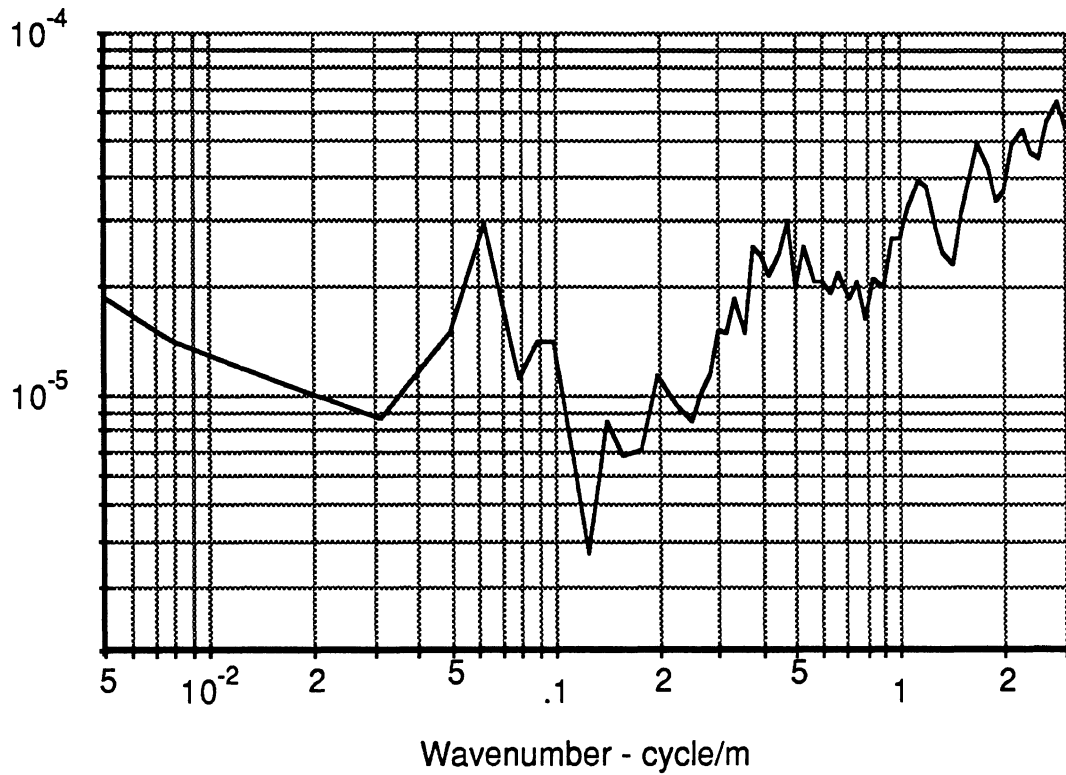


Figure 4.4-1. Localized roughness in a PCC road.

## 5. MEASURING ROAD ROUGHNESS

This section is partly at odds with the rest of the report, because rather than dealing with how roads are used as inputs for vehicle analyses, it presents the view of the highway community of how roughness measures are used to describe pavement condition. This perspective is relevant because many roughness measuring instruments and devices have been developed for use by highway engineers.

In the past few years, highway agencies have started converting to a standard roughness scale developed for The World Bank, called the International Roughness Index (IRI). A standard roughness scale could be useful for the Air Force as well, because it offers a simple and convenient way to rank different surfaces and compare them with computer inputs. The IRI is described, and the design considerations behind the IRI are summarized to provide background for later considering a similar scale for Air Force use.

### 5.1 Overview of Roughness Measures Used for Public Roads

Ever since an extensive AASHO research project conducted in the 1950's, road roughness has been identified as one of the most direct measures of the present serviceability provided by a road [22]. The history of a road's roughness is a primary indicator of its performance over time, and the analysis of roughness can aid in the diagnosis of roadway deterioration and the design of appropriate maintenance. Thus, roughness measures are used by engineers and planners to assess the present condition of a road network, and, in light of budget limitations, prioritize future construction and maintenance activities.

In developing countries, planners are faced not only with the management of existing roads, but also with the choice between quality and quantity in the development of a public road system. The planners must trade off vehicle operating costs and road costs, both of which are strongly related to roughness.

A persistent problem that has faced the highway community has been how to characterize road roughness in a universal, consistent, and relevant manner. To the public, the meaning of "roughness" is intuitive, based on the experience of using a variety of roads. A more technical and objective definition is difficult to obtain.

The material presented in preceding sections provides alternative descriptions of a measured profile, but nowhere is the quality of "roughness" defined. When the word is used in the context of an input to a vehicle model, it is usually a parameter in a PSD model or a white-noise amplitude that is meant. In that context, roughness parameters are usually associated with specifying the amplitude of a road model, rather than summarizing the condition of existing roads.

The American Society for Testing and Materials (ASTM) has defined road roughness rather loosely:

## 5.1 Overview of Roughness Measures Used for Public Roads

*“The deviations of a pavement surface from a true planar surface with characteristic dimensions that affect vehicle dynamics, ride quality, and dynamic pavement drainage, e.g., profile, transverse profile, cross slope, rutting” [23]*

This definition is often supplemented with a collection of other terms used by the highway engineer, such as cracking, faulting, raveling, corrugations, etc.

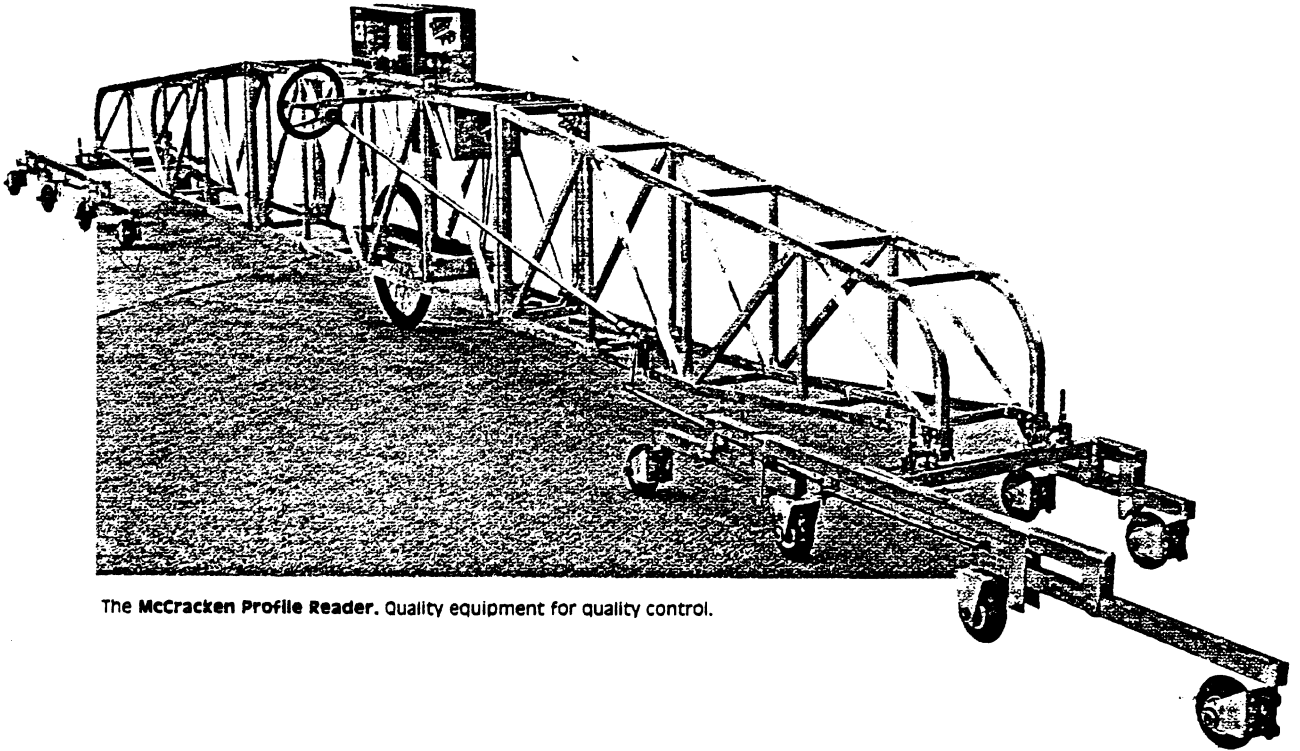
Multitudes of instruments have been devised that produce measures that correlate with the broad concept of “roughness” as described above. The popular methods now in use by the highway community are based on three categories of instruments: (1) “true profile” measurement, (2) measurement of the response of a “profilograph” to roughness, and (3) measurement of vehicle response to roughness. Until recently, direct profile measurement has been slow, expensive, and difficult. Most of the roughness measurements made by the highway community have fallen into the latter two categories. In the past few years, there have been substantial improvements in profiling technology, driven in part by a growing awareness of the limitations of the other methods. The present trend is toward profile measurement, and a description of profile measuring methods is covered later in Section 6.4. The other two categories are described below, because they have influenced the way in which roughness is perceived and defined within the highway community.

### *Profilographs*

Profilographs are multi-wheeled structures that are moved at very low speeds (2 mi/h or slower) over a pavement to measure roughness, and are most commonly used for newly poured concrete. One of these instruments is shown in Figure 5.1-1. They are sometimes called “profilometers” or profiling devices, because they produce a strip-chart with a line trace of a “roughness profile.” The line trace shows the movement of one component of the device relative to another, and has no simple relationship to the “true profile” that would be obtained with a direct rod and level survey.

### *Response-Type Systems*

By far, most of the roughness data collected over the past forty years have been measured with vehicles instrumented with “roadmeters” to produce a roughness index based on vibrations of the vehicle in response to roughness. The systems are called by several generic names, including: “response-type road roughness measuring system” (RTRRMS), “response-type system,” or “roadmeter system.” The term “roadmeter” refers to a transducer that accumulates suspension motions induced by road roughness in typical motor vehicles. Some of the currently popular models are the Mays meter, the PCA meter, the Cox meter, and various home-made models. Nearly all popular roadmeters follow the concept of the Bureau of Public Roads (BPR) Roughometer, and accumulate deflections of the vehicle suspension as it travels down the road. The BPR Roughometer is a single-wheel trailer with a one-way clutch mechanism that accumulates the suspension stroke in one direction. (The total stroke is twice that value.) Roadmeters are more commonly used in ordinary passenger cars, and Figure 5.1-2 shows a typical installation. The roughness measure that is obtained is “inches” of accumulated suspension stroke, which is reported as



The McCracken Profile Reader. Quality equipment for quality control.

**Figure 5.1-1. A Profilograph.**



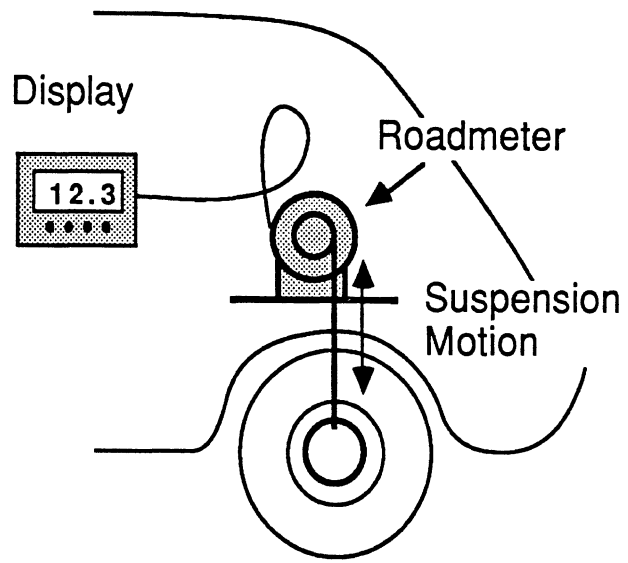


**Figure 5.1-2. The Response-type system.**

## 5.1 Overview of Roughness Measures Used for Public Roads

inches per mile of travel. Mathematically, this ratio is an “average rectified slope” (ARS). ARS can be reported with engineering units such as in/mi or m/km, although sometimes arbitrary units are used based on the instrumentation hardware, e.g., “counts/mi.”

Naturally, ARS measures from response-type systems are subject to each and every variable that influences vehicle response characteristics. Even when the vehicle is standardized, differences remain between nominally identical vehicles. Additionally, the response properties of the vehicles change with time. The consequences of this technology are two recurring problems:

1. Roughness measuring methods have not been stable with time. Roadmeter measures made today cannot be compared with confidence to those made several years ago.
2. Roughness measurements have not been transportable. Roadmeter measures made by one agency are seldom reproducible by another.

These problems exist in part because the roadmeters are typically inventions devised to be cheap, rugged, and easy to use. A rigorous understanding of how they function together with a vehicle, and what they actually measure lagged their development by several decades. A study funded by the National Cooperative Highway Research Program (NCHRP) provided the first comprehensive description of their operation and how it relates to the road profile [24].

A second source of difficulty has been the lack of a standard roughness scale. With a standard roughness scale, some of the problems inherent in a response-type system can be overcome by calibration. The lack of a standard measure was at first not seen as a serious problem by many of the users of roughness instruments. Roughness data for a city, county, or state could have arbitrary units, so long as the data base was internally consistent. However, even the repeatability of the instruments has been a problem. The technical limitations had a more visible impact on efforts by The World Bank to incorporate findings from major research projects in different parts of the world. As a result, The World Bank initiated a research effort that culminated in the development and adoption of the International Roughness Index (IRI), described in Section 5.2.

### *Profile Analyses*

High-speed profile measurement has been available for the past 20 years. The equipment now available is described in Section 6.4, so only the uses made of the measures are described here.

In the United States, the majority of the analyses have been intended to replicate the performance of the profilograph and response-type system, but without the sources of variation that plague those devices. Measured profiles are used as inputs to a simulated profilograph or response-type system. Because the simulated system is a fixed mathematical transform, it is not subject to the physical limitations and sources of variation in the physical system. Most profile analyses have been intended to produce an ARS measure compatible with a response-type system. The quarter-car model is the most common simulation, but other analyses are in use that have been found to produce

## 5.1 Overview of Roughness Measures Used for Public Roads

summary indices that correlate well with the response-type measures. For example, a mid-chord-deviation analysis, often called (incorrectly) RMS vertical acceleration, is used with an experimentally derived regression equation to produce an “in/mi” index [25].

Although most of the roughness data in the USA have been based in one way or another on the response-type system, European countries have made greater use of profiling devices. Several European roughness scales have been defined for profile measures. Most of these are obtained by computing the RMS or average rectified value of the elevation profile after it has been filtered to eliminate long wavelengths. In Belgium, a scale called CP (coefficient of smoothness) is defined by the following process:

1. The profile is smoothed by a moving average filter covering a specified baselength, B.
2. The smoothed profile is subtracted from the original, thereby removing long wavelengths.
3. The absolute value of the filtered profile is averaged, and the average is reported in arbitrary units of CP, where 1 CP is equivalent to 0.02 mm.

The CP statistic is highly dependent on the baselength used, and therefore the baselength is generally reported as a subscript, e.g., CP<sub>2.5</sub> indicates the baselength was 2.5 m. The CP scale is described in more detail in References [19, 26].

In France, a standard profiling device called the APL (longitudinal profile analyzer) trailer is used. The APL produces a voltage proportional to profile, which can be recorded on FM tape. The signal from the tape is played back into a bank of three Butterworth filters, to isolate roughness corresponding to short, medium, and long wavelengths. The output of each filter is squared and accumulated to yield mean-square values. This analysis is called the APL 72 waveband analysis, and is described in Reference [27].

Due to the characteristic shape of road PSDs, a summary statistic computed from an elevation profile is strongly influenced by the longest wavelength present in the signal. For example, the elevation profile for a smooth road with wavelengths up to 1000 ft will generally yield a higher summary amplitude than the elevation profile for a rough road with wavelengths up to 100 ft. The implication of this is that the CP and APL 72 roughness indices are defined primarily by the longest wavelengths included in the “filter” used. Although short wavelengths are also present, they are so small in amplitude relative to the long wavelengths that they have a negligible effect on the roughness statistic. Thus, the CP and APL 72 indices mainly show the roughness for a band of about one octave, where that band is defined by the longest wavelength passed by the filter.

## 5.2 The International Roughness Index (IRI)

The difficulties that existed in exchanging roughness data obtained by alternate methods motivated an experiment in Brasilia, Brazil in 1982, called the International Road Roughness Experiment (IRRE). The IRRE was a collaborative study initiated by The World Bank and undertaken by research teams from Brazil, France, England, the USA, and Belgium, under the technical direction of UMTRI. It was proposed to find the best

## 5.2 The International Roughness Index (IRI)

practices appropriate for the many types of roughness measuring equipment in use. At the same time, it was planned to provide means for comparing roughness data obtained by different procedures and instruments. The equipment included the categories of profile measurement and response-type systems.

Analyses of the data showed that measures from the response-type systems were correlated when the instruments were operated at the same test speed, and that all could be calibrated to a single roughness scale without compromising their accuracy. Analyses of the profile data demonstrated that the different measurement methods were compatible with some, but not all, of the common roughness indices when suitable data processing methods were applied. Thus, a single roughness index was proposed which would be called the International Roughness Index (IRI). The IRI can be measured by all of the equipment included in the experiment, and is also compatible with nearly all equipment used worldwide.

The experiment, the measured data, and results of analyses are reported in Reference [19]. Practical guidelines for measuring IRI are provided in Reference [28]. Pertinent information from these reports is summarized very briefly below.

### *Considerations in Defining the IRI*

Five criteria guided the selection of the IRI:

1. **Time Stable.** The IRI is defined by a roughness numeric that does not change with time, is valid on any type of road surface, and covers all levels of roughness. To achieve this goal, the IRI is defined as a mathematical function of the longitudinal profile of the road, independently of the hardware used to measure the profile.
2. **Transportable.** The IRI is measurable by generic profile measuring equipment available throughout the world. It is compatible with manual methods such as the rod and level, and also present and future high-speed profiling systems.
3. **Relevant.** The IRI is a meaningful measure of roughness that reflects road condition as it affects the public, in terms of vehicle operating cost, ride quality, and safety.
4. **Reproducible.** The procedures used to obtain IRI ensure that measures from different pieces of hardware result in the same measured roughness numeric when applied to the same road.
5. **Practical.** The procedures needed to measure IRI are understood by practitioners, who view the required effort as being reasonable. Otherwise, the IRI scale would not be widely accepted.

Due to the predominance of response-type systems, the IRI was designed for maximum compatibility with that generic type of system. Hence, the IRI has units of average rectified slope (ARS), normally reported as m/km or in/mi. The IRI was defined by selecting the best way to operate response-type systems, subject to the above criteria. For many systems, the only available choice is measurement speed. "Standard" speeds in use at the

## 5.2 The International Roughness Index (IRI)

time ranged from 32 km/h (20 mi/h) to 80 km/h (50 mi/h). The 32 km/h speed was standard for the original BPR Roughometer, and has been held over for many of the response-type systems based on the BPR design. The higher speed is preferred by the majority of users because it allows more efficient data acquisition. Data from the IRRE showed that most of the response-type instruments can be operated at any practical travel speed, even for systems such as the BPR trailer that had always been associated with lower speeds.

The data showed that all response-type systems were capable of the best reproducibility when operated at low speeds. However, a standard speed of 80 km/h (50 mi/h) was chosen for the IRI for three reasons:

1. 80 km/h is the most relevant speed. The ARS measured from an instrumented vehicle summarizes the vibrations caused by road roughness wavelengths that are most relevant to the travel speed. Most roads are travelled at speeds of 80 km/h or higher, even in developing countries with few paved roads.
2. 80 km/h was the most practical speed, and an IRI scale optimized for this speed would provide the best reproducibility for practitioners using this speed. For many of the practitioners, high-speed collection of data is absolutely necessary. The overwhelming consensus of practitioners was that, regardless of the “best” speed (for accuracy), most data from response-type systems would be measured at 80 km/h, even if it is converted to a roughness scale optimized for another speed.
3. The future trend in roughness instrumentation is towards profile measurement, rather than response-type systems. Optimizing the IRI to the currently popular response-type system hardware at the expense of relevance would have been short-sighted.

IRI must ultimately be defined by a mathematical transform of a measured profile, to ensure that the scale is stable with time and is transportable. When profile measurements are available, IRI is simply computed from the profile. For the majority of practitioners, IRI is obtained by calibrating a response-type system to IRI measures obtained from profile measurements. The calibration is achieved by performing a correlation experiment covering a number of test sites whose IRI values have been determined through profile measurement (manually, if necessary). The reproducibility of IRI measures obtained by calibrated response-type systems is thus limited to the degree of correlation between the IRI numeric computed from profile, and the ARS measure obtained by a roadmeter.

For maximum correlation with the response-type systems, the reference was defined as a mathematical model of a response-type system. The model is the quarter-car, used as a recurring example in Section 2 of this report. The ARS from a quarter-car model is computed as

$$\text{ARS} = \frac{1}{L} \int_0^{T=L/V} |\dot{z}_s - \dot{z}_u| dt \quad (5.2-1)$$

where  $L$  is the length of profile,  $V$  is the simulated speed, and  $\dot{z}_s$  and  $\dot{z}_u$  are the vertical velocities of the quarter-car sprung and unsprung masses. The vehicle parameters used for

## 5.2 The International Roughness Index (IRI)

the quarter-car model were taken from the earlier NCHRP research [24], where they had been selected to provide maximum correlation with a wide range of response-type systems. This is achieved by defining a roughness measure that covers the wavenumbers that are most important to all vehicles, yet does not “tune in” to a narrow band of wavenumbers. Parameters for the quarter-car were chosen that were representative of ground vehicles with high damping (i.e., stiff shock absorbers). These parameter values, normalized by the sprung mass, are:

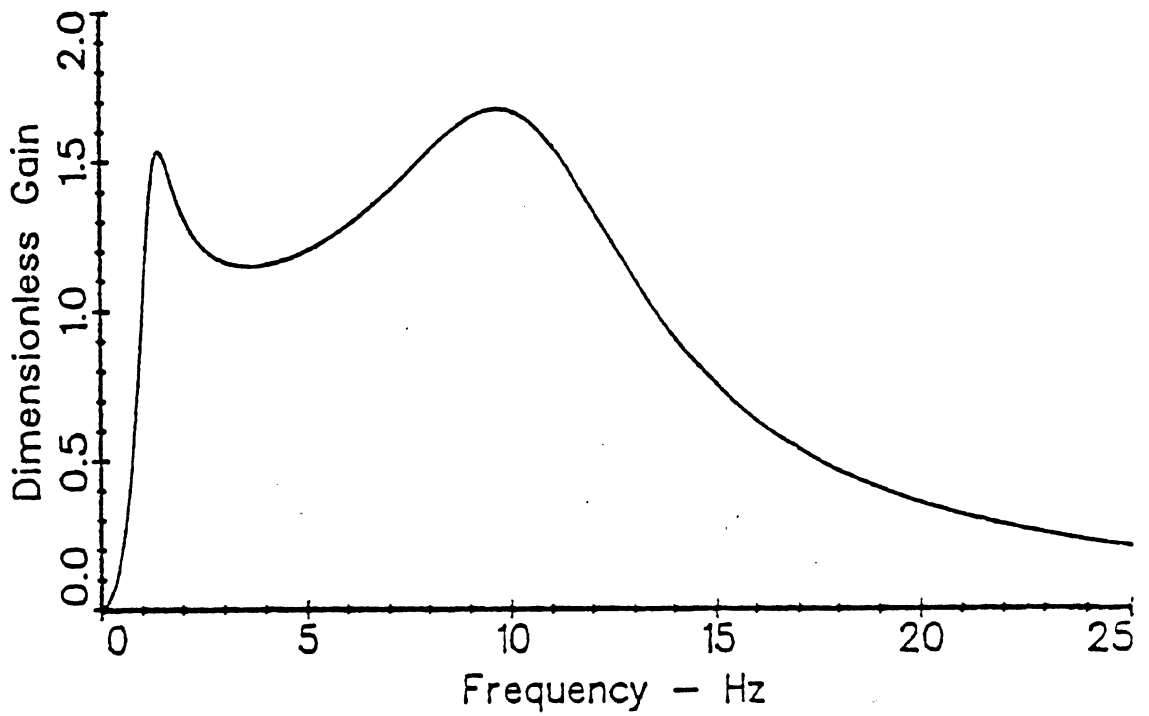
$$\frac{k_s}{m_s} = 63.3 \text{ sec}^{-2} \quad \frac{k_t}{m_s} = 653 \text{ sec}^{-2} \quad \frac{m_u}{m_s} = 0.15 \quad \frac{c_s}{m_s} = 6.0 \text{ sec}^{-1} \quad (5.2-2)$$

Figure 5.2-1 shows the response of the IRI quarter-car to wavenumber. The quarter-car is essentially a filter with properties shown in the figure. For typical roads, 80% of the mean-square slope used to compute IRI derives from wavenumbers between .05 and 0.56 cycle/m (wavelength from 1.8 to 20 m/cycle). The weighting is distributed over wavenumbers in that range, with somewhat more emphasis given to wavenumbers 0.07 and 0.4.

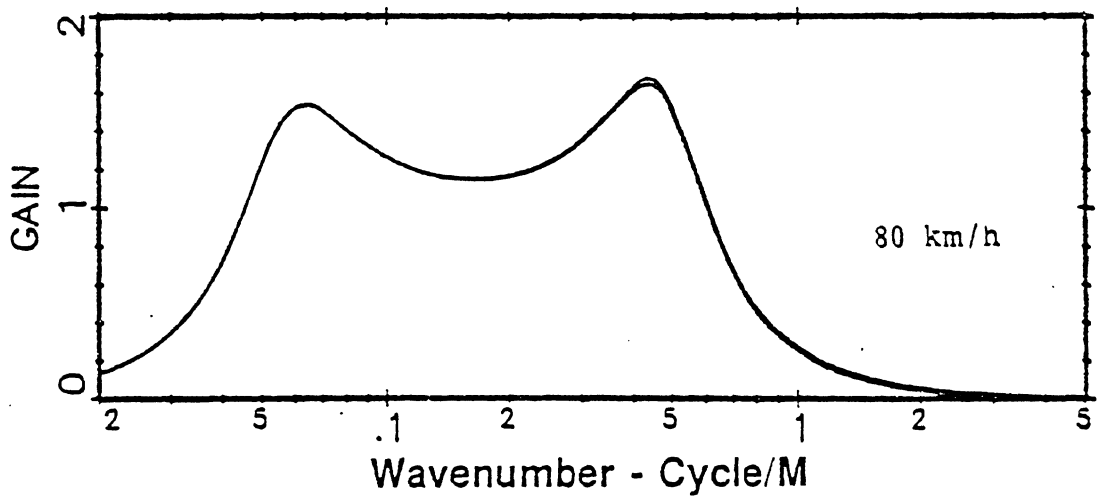
One other choice had to be made in defining the roughness scale—should the IRI be computed from a single profile or from two? Most road vehicles cover two wheeltracks, and thus involve two profile inputs. Most response-type systems are based on ordinary passenger cars or light trucks, and therefore respond to inputs from the right- and left-hand wheeltrack profiles. However, some of the instruments have but one wheel, and respond to a single profile input. Further, many of the profiling systems in use measure a single profile. As explained in Sections 3.2 and 4.2, some of the roughness from the right- and left-hand wheeltracks is out-of-phase, resulting in a reduction of the pitch-plane response of the vehicle. That is, vibrations at the center of a two-track vehicle are slightly less than those existing in a one-track vehicle with otherwise identical dynamic properties.

The quarter-car model developed in Section 2 can be extended to a half-car model with simultaneous inputs from both sides. When response-type systems are made by installing a roadmeter in a two-track vehicle, the roadmeter is nearly always installed at the center of a solid rear axle. When this configuration is modeled mathematically, it turns out that roll motions of the vehicle provide zero input to the ARS summary statistic. ARS is predicted correctly from the standard quarter-car model, if the input to the model is the point-by-point average of the left- and right-hand wheeltrack profiles (this is the modal profile  $z_v$  described in Sections 3.2 and 4.2).

As a part of the analyses for the IRRE, both the quarter-car and the half-car models were used to compute ARS values as candidate IRI numerics. When ARS was computed for a single wheeltrack, the summary ARS measures from the left- and right-hand sides were averaged to yield a single measure for the test site. The ARS measures from the half-car simulation were always lower than the averaged values from the quarter-car; however, the correlation between the two was nearly perfect. In other words, the data did not indicate a preference for either method with respect to offering better correlation with the response type systems.



a. Response of the IRI/NCHRP quarter-car in the frequency domain



b. Sensitivity of the IRI analysis to wavenumber

**Figure 5.2-1. Response of the IRI quarter-car analysis..**

## 5.2 The International Roughness Index (IRI)

The IRI was defined as a summary numeric applying to a single wheeltrack—the quarter-car model shown in Figure 2-1. When used to calibrate two-track response-type systems, the IRI is measured for both wheeltracks and the average is used.

### *Equipment Classifications*

The equipment and methods used to measure roughness are as diverse as the uses made of the data. In some applications, excellent accuracy and repeatability are needed to discern subtle changes in the roughness of a particular test site. In other cases, vast quantities of data are used to summarize the state of a road network. Less accuracy for individual measures is required, although it is important that systematic biases are not introduced into the data. There is a fundamental trade-off between cost and accuracy when measuring roughness, and the importance of these factors varies with each project. Thus, alternate procedures for measuring IRI are allowed so that practitioners can design a plan that fits the requirements for a particular project.

Roughness measuring methods applicable to IRI were classified according to accuracy and concept into four groups:

1. IRI is computed from a measured profile, and the profile measurement is so accurate that further improvements would not noticeably change the IRI value. Class 1 measures can be obtained by static methods such as rod and level, if suitable tolerances are placed on sampling interval (100 mm or less) and resolution (1 mm for average pavements, .5 mm for smooth pavements). They can also be obtained with high-speed profiling devices under certain conditions.
2. IRI is computed from a measured profile. The profile measurements are accurate enough to yield unbiased values of IRI on the average, but could be improved to yield higher accuracy for individual sites. Class 2 measures can be obtained with static methods using less stringent tolerances than class 1 (e.g., 500 mm sample interval) or high-speed profiling instruments.
3. IRI is estimated with a generic roughness-measuring device that has been calibrated to the IRI scale. The calibration is performed by a correlation with IRI measures made with a class 1 or class 2 method. Predicted values of IRI correlations with response-type systems are defined as Class 3 measures. Also, measures from profilographs and other roughness measuring systems that do not see the “true profile” over the range of wavenumbers required for the quarter-car model fall into this class if they are calibrated by correlation to the IRI scale.
4. IRI is estimated through subjective ratings or through roughness measures that have no verifiable link to IRI. For ballpark estimates, benchmark roughness levels can be used to convert roughness data to the IRI scale. Figure 5.2-2 provides an overview of the IRI scale that one might use to convert existing data. More extensive guidelines have also been prepared.



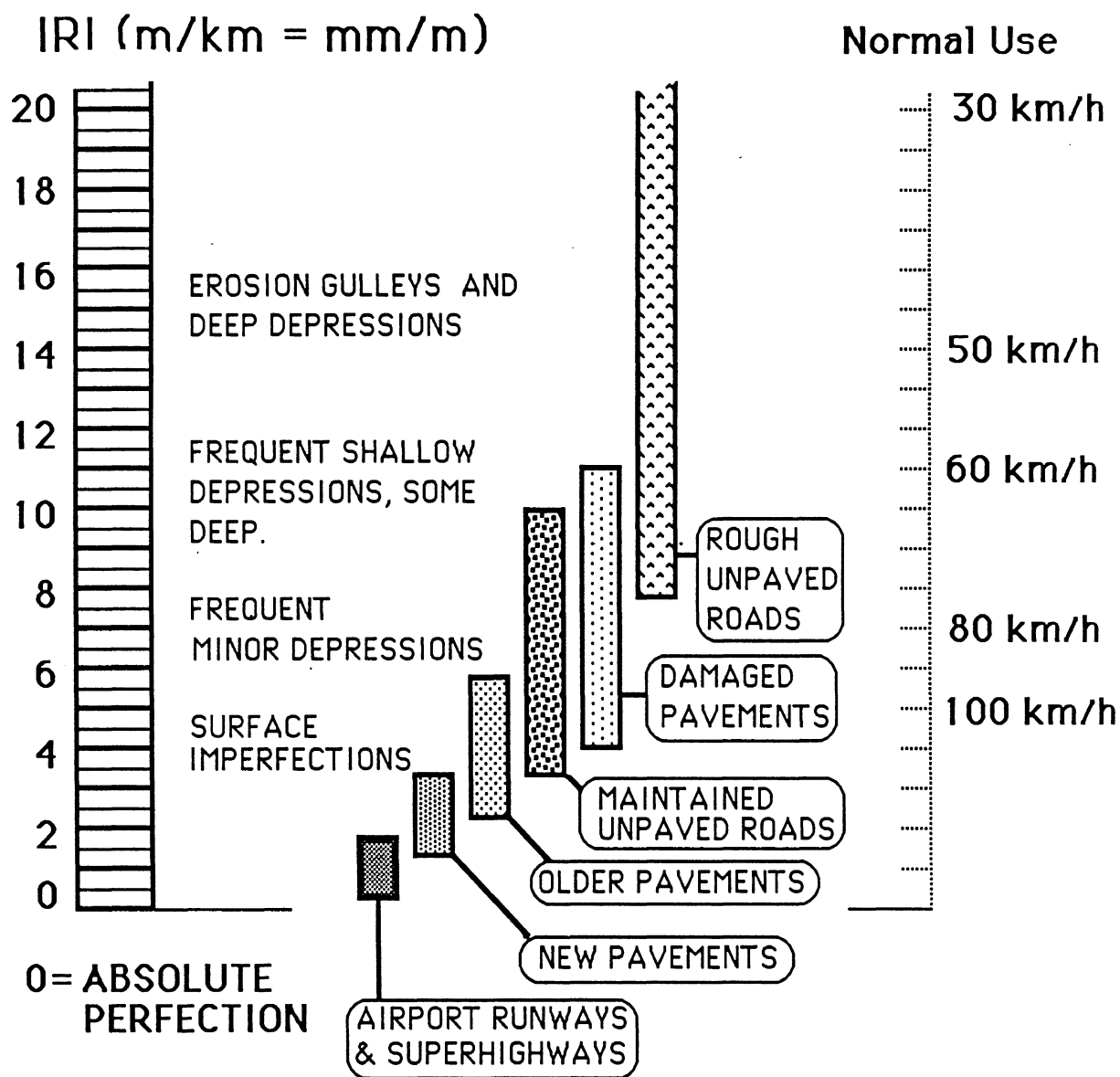


Figure 5.2-2. Overview of the IRI roughness scale.

### 5.3 Roughness Measures and Vehicle Response

Measuring roughness as it affects vehicles using the roads has been a motivating factor in the development of the measures described in Section 5.1, but cost and hardware simplicity are the factors that have been given greater priority. The IRI is compatible with most of the systems in use by the highway community, which are either response-type systems or profiling systems with a response-type system in software (e.g., the IRI). The following discussion considers how IRI relates to other vehicle responses.

Three common vehicle variables that are of interest have similar responses to roughness, as shown by the transfer functions in Figure 5.3-1.

1. **Vertical acceleration of the body.** This acceleration is the primary measure of ride quality when summarized as an RMS level.
2. **Suspension velocity.** This variable is used to compute IRI, and is related to the power dissipated in the suspension.
3. **Vertical tire force.** Vertical tire force is proportional to tire deflection. The RMS level of either force or deflection indicates how well the tire can utilize traction for braking and cornering, and thus it is linked to safety. For heavy vehicles, it is also linked to pavement damage.

The similarities in these variables are due to the combined effects of their locations and their units. For example, the vertical displacement of the body is dominated by motions near 1 Hz, with little effect of the axle resonance. Also, the acceleration of the axle is dominated by vibrations near 10 Hz, with little effect of the body resonance. However, it so happens that the above three variables are of most interest, and they are all highly correlated with IRI.

The response plots are shown as functions of wavenumber, based on a speed of 88 km/h (55 mi/h). The mapping between the time-based frequency (cycle/sec) and spatial wavenumber (cycle/m) is determined by the speed (eq. 3.4-3). The bottom plot in the figure shows how the same dynamic response translates into a different band of wavenumbers for a lower speed of 32 km/h (20 mi/h). For vehicles traveling at low speeds, the bottom plot shows that the IRI overlaps the significant wavenumbers. However, it includes wavenumbers that are too small to be seen by the vehicle ( $v < .04$  cycle/m, wavelengths  $> 25$  m), and omits high wavenumbers (1 cycle/m) that do contribute to the vehicle response.

A fourth variable, suspension deflection, might also be of interest. It is mainly dominated by the body resonance and not as strongly correlated to IRI as the others.

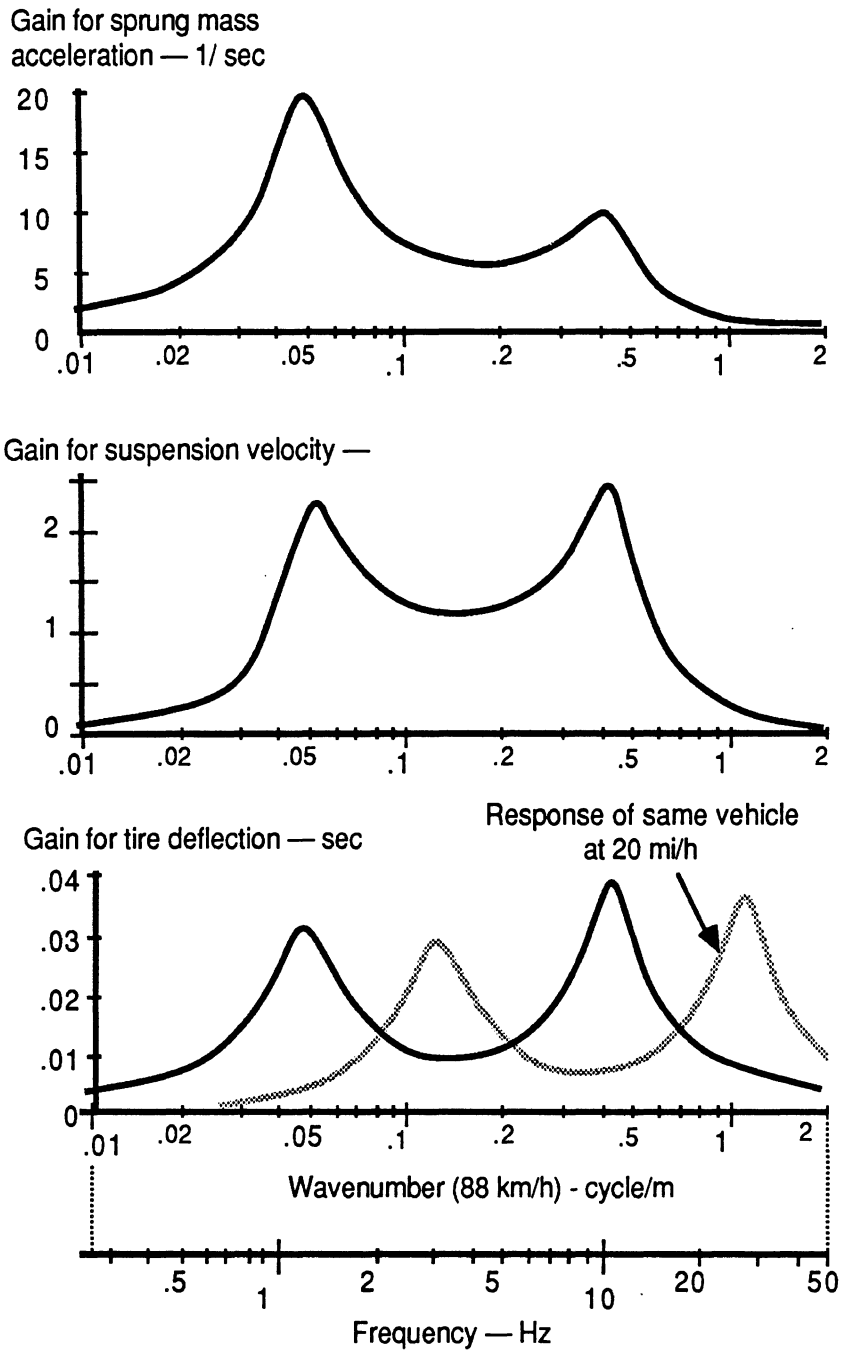


**Figure 5.3-1. Response plots for acceleration, suspension rate, and tire load.**

## 6. VALIDATION AND MEASUREMENT

Validation of vehicle analyses involves performing a few experiments whose conditions can be duplicated by the analysis, to allow comparison between measurement and theory. The process is complicated by measurement limitations, and by the need for a criterion to evaluate “how good” the comparison is.

Measurement of vehicle response is relatively straightforward and relies on conventional transducers and data acquisition systems that have been around for years. Therefore, only the basic considerations are reviewed here. Measurement of road profile, on the other hand, is a very specialized area that is still developing. Accordingly, the instruments available for measuring profile are described in much greater detail.

### 6.1 Basis for Comparisons

Measured and predicted responses are usually compared on the basis of graphs of time histories or frequency response. Evaluations are usually made subjectively by overlaying plots from the model with plots from the experiment. Simple RMS levels and other summary indices are not normally considered adequate for validation purposes because ballpark levels can be obtained too easily with incorrect models. When the purpose of the vehicle analysis is ultimately to predict histograms or summary index such as an RMS level, validation should involve the statistics of interest, in addition to the graphical comparisons of time histories or frequency response plots.

#### *Criteria for Validation*

Predictions from a valid model never match a measured response perfectly, due to a number of factors:

- Measurements include electronic noise and transducer error.
- The real vehicle exhibits high-frequency vibrational modes beyond the frequency range of interest for the model.
- The measures of input may not be perfect, particularly for road roughness inputs. Even if the profiles under each wheel are measured perfectly, an exact synchronization between the profiles and the on-vehicle measures is difficult to obtain unless the profile measures are made at the same time as the vehicle testing. Also, it is hard for test drivers to locate the vehicle in the precise lateral position used for previous profile measurements.
- The nominal vehicle equilibrium position is indeterminate when linkages include friction and free-play.

In comparing the predicted responses to the measurements, the engineer evaluates the agreement based on what the model is intended to predict. Is it sufficient to predict gross

## 6.1 Basis for Comparisons

motions resulting from potholes? Peak stresses in structural members? Exact transient waveforms in response to measured inputs?

Repeat runs should be made to determine the experimental repeatability. If there are factors that are suspected as causing the response of the vehicle to change, a few tests should be repeated periodically throughout the test program to demonstrate the reproducibility of the measurement.

The agreement between a model and test data can be no better than the test reproducibility. If the test data show that the test results are highly reproducible, but they show a different type of response than predicted by the model, then the reason for the discrepancy should be determined and corrected.

### *Comparison of Time Histories*

The most obvious method for validating a vehicle simulation is by direct comparison of the time histories for an experiment that is both recorded in the field and simulated on the computer. The inputs to the vehicle are measured and used as input for the computer simulation. The time histories of the predicted forces and motions are plotted and overlaid with plots of the measured motions and forces. Time history plots are sensible when the input has some standard form, such as a pothole. However, a comprehensive comparison for a family of inputs can be very time consuming because a large number of plots must be prepared and inspected. Also, vehicle responses to typical road roughness inputs are difficult to evaluate. Therefore, frequency responses are recommended for performing validations when possible.

### *Comparison of Frequency Responses*

Measured time histories can be reduced to yield PSDs and transfer functions. These are plotted and compared with theoretical functions predicted by the vehicle analysis. When linear analyses are used, the frequency-domain plots can be computed directly from the vehicle model parameters and the PSD of the input. For time-domain simulations of potentially nonlinear models, the same frequency analysis applied to measured data is applied to the simulated response data. For example, Figure 6.1-1 compares PSD plots obtained from a nonlinear time-domain model with PSD plots from measured data. The same PSD computation software was used for accelerations measured and accelerations predicted with a simple model.

When frequency-domain comparisons are relevant, they often prove more useful than time-domain comparisons. This is particularly true for the complex motions that occur when vehicles respond to realistic ground inputs. The frequency analysis serves to reduce and organize the information contained in the data (measured or simulated).

Generally, a model is valid over a certain bandwidth. Ideally, that band exceeds the range of interest. A comparison of measured and predicted frequency response curves (PSD or transfer function) shows where the model is valid and where it isn't as a function of frequency. Frequency response plots are useful for identifying modes of vibration.

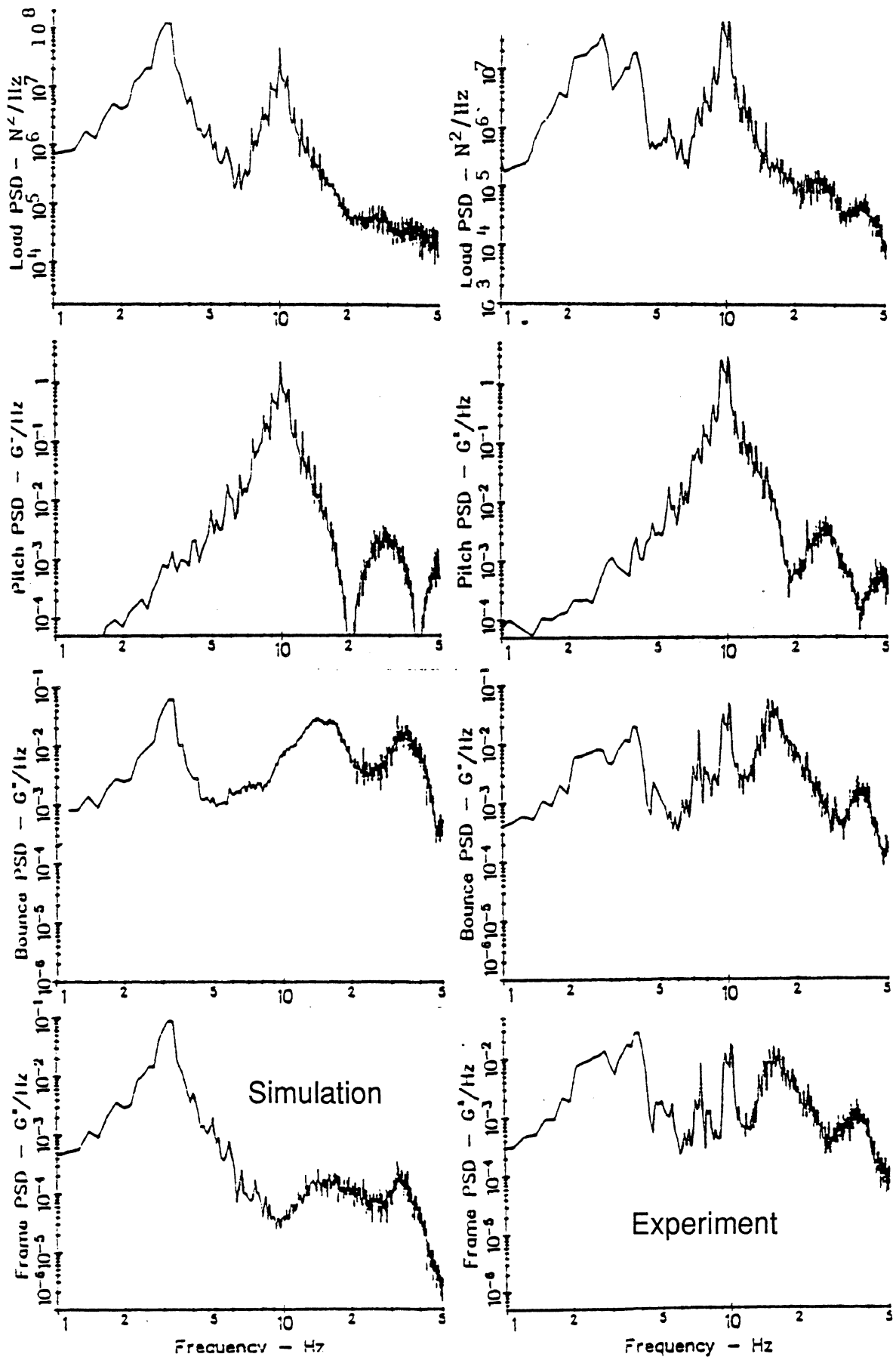


Figure 6.1-1. Comparison of simulated and measured vehicle response PSDs.

## 6.1 Basis for Comparisons

Thus, modes of vibration in the actual vehicle that are not accounted for in the model can be identified.

When the inputs are measured together with the response variables, the frequency response function  $H_{xy}$  can be computed using eq. 2.2-20. The averaging that occurs during processing eliminates the effects of uncorrelated noise which might otherwise confuse the interpretation.

### *Parameter Measurement*

Regardless of how the validation is performed, the parameter values of the test vehicle(s) required by the model must be measured or estimated. For complex models, obtaining the parameter values can be an expensive undertaking that exceeds the cost of the testing. Therefore, validation exercises are usually designed for a very limited number of vehicles. Often, a single vehicle will be tested in several configurations. Most of the parametric data is the same for the different configurations, and just a few parameters are varied, e.g., payload, tire inflation pressure, etc.

## 6.2 Data Recording Requirements

Systems that process and record the signals from the various sensors can be classified as analog or digital. An analog data-acquisition system processes signals using electronic circuits, and stores data signals as continuously varying voltages, using a device such as an FM tape recorder. Analog systems are limited in range and accuracy. Voltages that are too high will saturate operational amplifiers, while voltages that are too low are lost in a background of electronic noise. Thus, users of analog systems must be careful to keep all of the amplifiers set close to the optimum at all stages in the system—from the transducers, to the profile computation, to the tape storage.

Digital systems use one or more components to process data numerically, using arithmetic operations. A digital tape recorder stores a signal as a sequence of numbers spaced at a constant time interval, rather than as a continuously varying voltage. Comparison between theory and experiment inevitably involves processing by digital computer. Thus, the requirements for digitizing the data must be considered for any data acquisition, regardless of how the original signals are originally stored. The digitization can be performed during the testing for immediate storage and/or analysis of the time histories. The requirements for acquiring data are determined by the use that will be made of the data, and also by the frequency content of the data. The choices to make involving the digitization are:

- What frequency should be used to sample the signals?
- What resolution (precision) is required for the numbers?
- What range is required for the numbers?

The choice of sample frequency is determined by the frequency range of interest. When a continuous signal is digitized at discrete intervals, the highest frequency that can be

## 6.2 Data Recording Requirements

recovered through any form of analysis is one-half of the sample frequency. For example, if the interval between samples is 0.002 sec, then the sample frequency is 500 sample/sec and the highest frequency that can be seen is 250 Hz. Higher frequencies in the signal do not go away, but appear “aliased” as lower frequencies. For example, a 300 Hz sine wave cannot be distinguished from a 200 Hz sine wave if they are both sampled at 500 sample/sec. This phenomenon is called “aliasing” or “folding.” Aliasing can result in serious errors, and therefore the signal must not include significant components for frequencies above the “folding frequency” (1/2 of the sampling frequency). For general-purpose digital data acquisition, the sample frequency is set at least four times the maximum frequency of interest, and an analog low-pass filter is used to attenuate frequencies about the range of interest. A low-pass filter used for this purpose is often called an anti-aliasing filter.

When measuring the response of a ground vehicle to road roughness, the maximum frequency of interest is usually in the range of 20 — 50 Hz. Assuming a maximum frequency of 50 Hz, a sample frequency of 200 Hz would be appropriate, together with an anti-aliasing filter with a steep roll-off (say, 24 dB/octave) with a cut-off frequency of 70 Hz. If the anti-aliasing filter has a more gradual roll-off (say, 6 dB/octave), then a higher sample frequency is needed.

The range and resolution of the digitized signal is determined by the specifications of the analog-to-digital converter (A/D) and the scaling of the analog input. A/D hardware is commonly available to produce numbers with the resolutions shown below.

Table 3. Resolution from A/D hardware.

| <i>Binary Digits</i> | <i>Numerical Range</i> | <i>Dynamic Range</i> |
|----------------------|------------------------|----------------------|
| 8-bits               | -128 — +127            | 48 dB                |
| 12-bits              | -2048 — +2047          | 72 dB                |
| 16-bits              | -32,768 — +32,767      | 96 dB                |

In this table, the three columns are showing the same specification expressed in three different units. In theory, an 8-bit digitizer is sufficient for most purposes if the input signal is always scaled to use the full digitizing range. However, this seldom happens. A 12-bit A/D is more practical. A 16-bit A/D offers even more flexibility. Transducer signals usually have a signal/noise ratio of 70 dB or less, so a 12-bit A/D is a reasonable choice if the amplifier gains are set so that the analog signal uses 25% or more of the digitizing range.

Immediate processing can be done conveniently with a real-time spectrum analyzer when the objective of the test is to obtain frequency-domain plots.

A spectrum analyzer or other form of commercial analyzer offers great convenience for two reasons:



## 6.2 Data Recording Requirements

1. These analyzers usually have built-in preprocessing systems to properly digitize the voltage signals from the transducers. Also, most of the signal conditioning hardware is collected into one convenient package.
2. The results are obtained almost immediately. If there are problems in the test setup that cause bad data, they will be noticed in time to correct them.

On the other hand, analyses beyond the built-in capabilities may be difficult or impossible to perform. Another limitation is that most spectrum analyzers handle one or two channels at a time. For comprehensive analyses involving many channels, it is usually necessary to record the data for later processing on a general-purpose computer that can run various analysis programs.

## 6.3 Measurement of Vehicle Response

When instrumenting a vehicle for vibration testing, choices must be made involving what kinds of transducers to use, where to locate them, and how to record the signals. The choice of which dynamic variables to measure in a test vehicle inevitably is the result of a compromise between the variables that can be measured easily and the variables of greatest interest. The transducers normally used for vehicle testing include accelerometers, gyros, rotary and translational potentiometers, LVDTs, speed sensors, and strain gauges. When dealing with vibrational responses, accelerometers are the most commonly used transducers.

Accelerometers are easily attached at various points on the body and suspensions of vehicles. Two or more accelerometers can be used for large bodies to pick up vibration modes. For example, the outputs of two accelerometers spaced along the longitudinal direction can be averaged to obtain a bouncing response and subtracted to obtain a pitching response. Accelerometers spaced laterally can provide roll responses. If flexible body vibrations are involved, several accelerometers can be spaced along the length of the body to discern the beaming modes.

Accelerometers should be placed at practical locations that give meaningful information about the vibration. The locations that are accessible are generally not the same reference locations from the equations of motion for the model. However, the movements of arbitrary points can usually be computed with the vehicle model. Therefore, the model outputs are usually processed to yield accelerations for the actual locations of the accelerometers.

The same considerations apply for other types of transducers—they are usually located at arbitrary points that are accessible on the vehicle, and the model outputs are processed to determine the predicted response of the vehicle at those locations.

## 6.4 Measurement of “True Profile”

The primary vibrational input to a ground vehicle is the profile of the road in each wheeltrack. Measurement of road profiles is a highly specialized area of technology that has been developed mainly to serve the highway community. A variety of equipment has

## 6.4 Measurement of "True Profile"

also been used over the years at universities and in the military. However, it is the systems used for highway applications that have seen the most development and validation. Systems in current use are described below.

Road profile can be measured at highway speeds using Profilometers<sup>©</sup> and other high-speed profiling devices.<sup>1</sup> The high-speed profiling devices are vehicle-mounted instrumentation systems intended to measure vertical deviations of the road surface along the direction of travel. They have been in existence for two decades, and millions of dollars have been spent thus far on their purchase and operation. In recent years, the variety in hardware and design available to the highway community has increased dramatically. These devices are playing an increasing role in the routine evaluation of pavement condition by states, and in federally-coordinated research projects.

The importance of profile measurements has also led to a new interest in measuring profiles manually. Manual measures are appropriate when the scope of the measurement activity is limited and the high cost of obtaining a high-speed system cannot be justified.

### *Manual Methods*

The most obvious method for measuring ground profiles is with a surveyor's rod and level. Although laborious, measurement of a profile by this method is straightforward and contains no surprising sources of error. The accuracy of the measurements is primarily determined by the precision of the level instrument (together with the skill of the survey team) and the interval between measures. Typical land surveying equipment is used for readings of 0.01 ft (3 mm), which is too coarse for all but the roughest pavements. In Brazil, rod and level measures are routinely made on road sites used to calibrate other roughness measuring instruments. The level has a resolution of 1 mm. This resolution was found to be adequate for measuring IRI on all but the smoothest pavements. On very smooth road surfaces, a resolution of 0.5 mm is needed. The sample interval required for computing the correct IRI value is 500 mm if the road has no significant "localized roughness features" (tar strips, potholes, etc) that would not be seen at that interval. A closer spacing of 250 mm is recommended. For analyses other than the IRI, a closer interval may be necessary.

Specification of accuracy and sample interval is trivial for a rod and level measurement. What is not trivial is the actual measurement process. This method is tedious and time consuming, taking several days to measure both wheeltracks for a mile of road. The time required to make the measurement is roughly proportional to the number of samples per mile, so there is a strong motivation to use the longest interval that will give a useful profile. After the measures are made in the field, they must be entered into a computer system. The main problem with the rod and level method is that it requires the manual logging of a large amount of data, such that the chances for human error are high.

---

<sup>1</sup> The name "Profilometer" is often used to refer to high-speed profiling devices. However, the name is copyrighted by K. J. Law, Inc. of Farmington, MI. and technically refers only to the profiling devices manufactured and sold by K. J. Law.

## 6.4 Measurement of "True Profile"

At least two other static profiling methods are in use, based on commercial systems designed to offer greater efficiency and eliminate the manual logging of the measures. One of these is a device developed by the Overseas Unit of the Transport and Road Research Laboratory (TRRL) in England, called the TRRL Beam (see Figure 6.4-1). It consists of an aluminum box beam about 3 m in length supported at each end by a fixed tripod. The beam is leveled by an adjustment at one end, thereby defining a fixed horizontal datum. Measurement of the ground-to-beam distance is made with an instrumented assembly that contacts the ground through a small pneumatic tire, and which slides along the beam on precision rollers. The moving assembly contains a microcomputer that digitizes the signal at pre-set intervals and records the data. After the sliding fixture is moved over the length of the beam, it is picked up and moved down the road such that the new starting position matches the old end position. The TRRL Beam was designed for use in developing countries to calibrate other roughness measuring systems.

Potentially, this design introduces a small random error each time the beam is moved. This error was demonstrated to be negligible when a prototype was used in the 1982 Brazil experiment. In that experiment, the TRRL Beam demonstrated a level of accuracy that is hard to match [19].

A different approach is used for a device called the Dipstick®, shown in Figure 6.4-2. This device is supported by two legs separated by a distance of 1 ft, and held by the operator with long vertical handle. The instrument measures the inclination angle between the feet, thereby providing the difference in elevation. The instrument records the difference in elevation and signals the operator, who then "walks" the device along the road by alternately pivoting it about each leg. This instrument was just recently introduced to the market, hence there are not yet independent reports showing its performance. It was used in a recent demonstration seminar sponsored by the Federal Highway Administration (FHWA) held in Ft. Collins, CO in October 1987, along with other profiling instruments. The results from that project might, when they are made available, provide additional information about the use of the Dipstick.

A potential source of error unique to the Dipstick design is the accumulation of the random error of each measure. It may prove necessary to combine the Dipstick with a rod and level, using the rod and level to establish reference points at long intervals of 100 ft or so to correct "drift" in the profile obtained by the Dipstick. The IRI and other roughness indices are not particularly sensitive to drift, so the corrections may not be necessary if the profile is used solely to compute a roughness numeric.

### *The General Motors Design*

Most high-speed profiling systems are based on a design from the General Motors Research Laboratory that was developed over twenty years ago [29]. In this design, shown in Figure 6.4-3, a vehicle is instrumented with an accelerometer and a height sensor. The accelerometer senses the vertical motions of the vehicle body, relative to an inertial reference. The height sensor follows the road by sensing the distance between the vehicle and the road surface. The signals from the accelerometer and the height sensor are used together to compute the profile of the road. By eliminating the vehicle motions, the

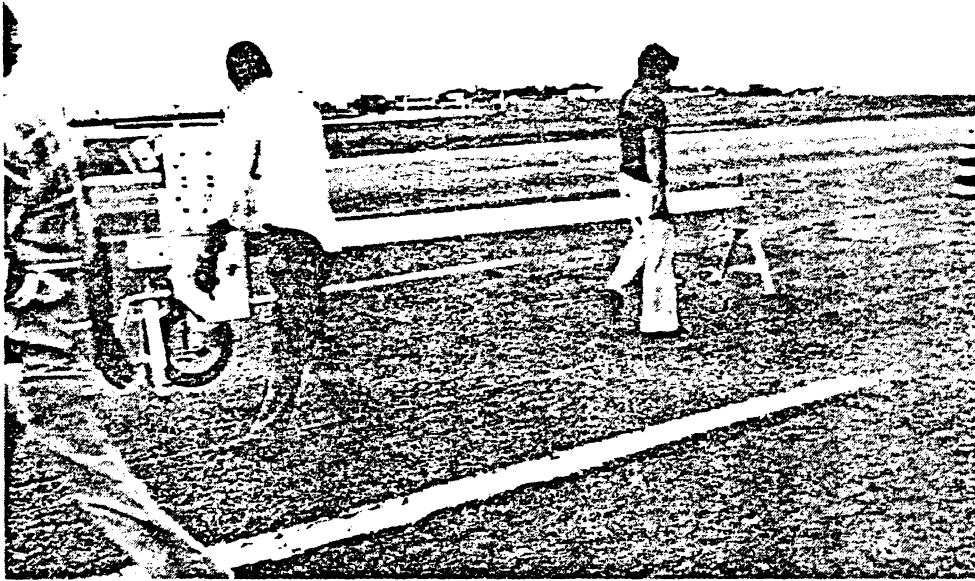


**Figure 6.4-1. The TRRL Beam profiling device.**



**Figure 6.4-2. The Dipstick profiling device.**

GMR profilometer with a noncontact displacement transducer.

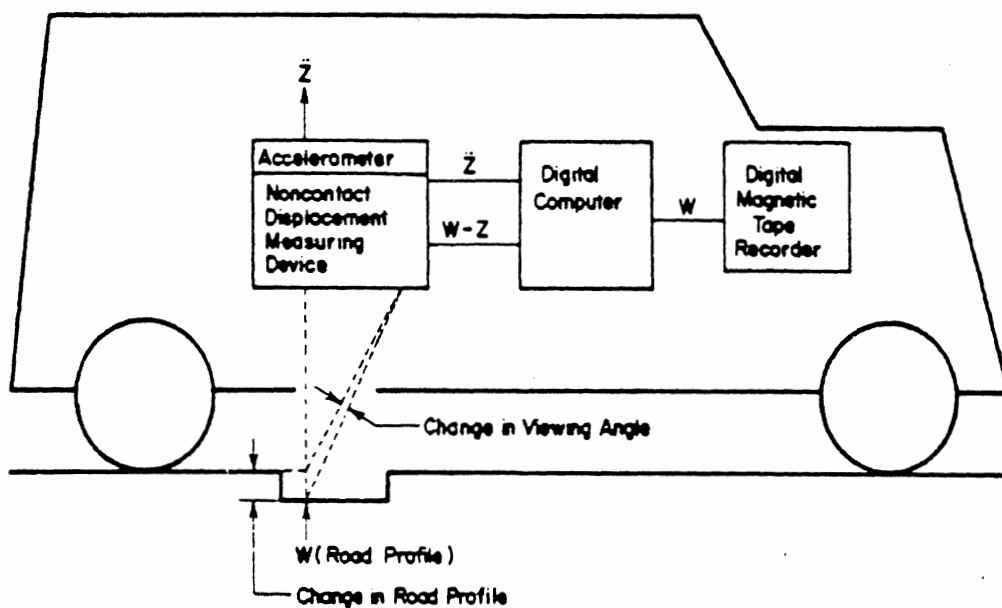


Figure 6.4-3. The GM-type profiling system..

## 6.4 Measurement of "True Profile"

profile obtained is relative to an inertial reference. This profile computation is a form of data processing that is specific to GM-type profilometers, and requires some type of computer capability.

Obtaining the transducer signals for input to the computer requires a data-acquisition system, subject to the considerations mentioned in Section 6.2. The amplitudes in a road profile are approximately proportional to wavelength, such that a profile containing wavelengths over the range of 1-m to 100-m will contain information covering a range of 100 to 1. This allows little margin for error in setting the amplifier ranges in an analog system, especially when considering that roughness varies along the length of a road. Most GM-type systems digitize the transducer signals immediately, so that the profiles are computed and stored in digital form.

The original GM-type Profilometer used a mechanical follower wheel, spring-loaded against the ground. In this design, the position is sensed with a conventional potentiometer, placed between the wheel and the vehicle body. The follower-wheel assembly and tire have dynamic properties that influence the quality of the measurement. This is shown in Figure 6.4-4, which compares PSD functions obtained for profiles measured with a contacting and noncontacting height sensors. Note the large mechanical resonance of the follower wheel assembly at 4 cycle/m. The significance of the resonance depends on the use made of the data—if the frequency range of interest does not extend to wavenumbers above 1 cycle/m, the mechanical system yields the same measure as the non-contacting one.

A problem with a mechanical follower wheel is that it can sometimes bounce when it hits a bump or hole. The result is that the profile obtained will trace the path of the wheel through the air, rather than the surface. The design of follower wheels used on GM-type profilometers has limited their valid measurement range to exclude rough roads, and imposes limits on the operating speed on even slightly rough roads. A more serious problem, from the perspective of the users, is that the mechanical follower wheel is easily damaged. Follower wheels have been replaced in the newer GM-type profilometers by noncontacting sensors which measure height using ultrasound, laser beams, or optical images.

Height can be measured using ultrasound in at least two ways.

1. A speaker emits a short burst of sound, and the time needed for the sound to reach the pavement and be reflected back to a microphone is measured. By knowing the speed of sound through air, the distance can be computed from the time interval.
2. A speaker emits a continuous tone, and the reflected sound is monitored. The height is determined by the phase relationship between the original and reflected sound.

Measuring height with ultrasound requires that a number of problems be solved that have nothing to do with the surface quality, such as effects of wind and changes in air pressure. Surface condition can also challenge an ultrasonic system if it is a poor reflector of sound, such that a detectable sound is not returned to the microphone. Generally, open texture and bumps with sharply sloping surfaces are poor reflectors that cause problems

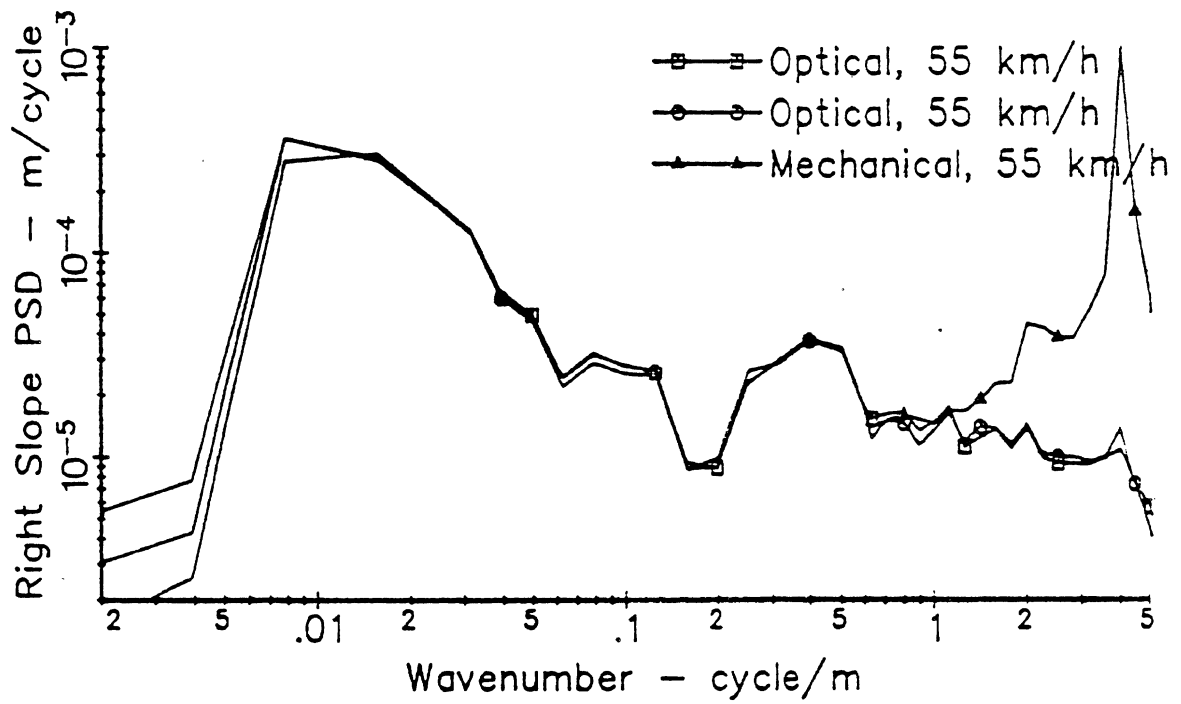


**Figure 6.4-4. Comparison of mechanical and optical road followers in a GM-type system.**



## 6.4 Measurement of "True Profile"

with ultrasonic height sensors. Smooth roads also pose a challenge, because the ultrasound sensors typically have limited resolution—an effect that adds a small amount of roughness to the measurement.

Laser beams are used in other systems to measure vehicle height by triangulation. A laser beam is projected straight down onto the surface resulting in a small, bright spot of light. The spot is seen by a photodetector mounted to the side. Optics and a linear detector are used to relate the light spot location to an angle, from which the distance from the vehicle to the ground is determined. The laser uses a single frequency (monochromatic light), and the detector can include filters to exclude effects of ambient light. Thus the system may be made insensitive to variations in light intensity, both the ambient and that reflected from the laser. One problem that can occur with a laser sensor is that the spot can go into a crack or hole, where it cannot be seen by the detector. Another property of this design is that it may include texture in the measure, which can add a random error to a profile if not properly dealt with in the digital data-acquisition system by anti-aliasing filters.

A commercial laser height sensor sold by the Swedish Selcom Company is shown in Figure 6.4-5. Most of the laser sensors used in profiling systems are manufactured by Selcom. A few other are based on the same design.

Several designs of noncontacting height sensors use conventional light sources (i.e., not laser) to project an image on the ground. An optical noncontact sensor was also developed by Southwest Research using an infrared light beam with two photodetectors viewing the image from an angle. The relative amount of illumination falling on detectors is used to establish the angle to the light spot, and hence the distance from the detector to the road surface. This design is not completely successful at eliminating effects of changes in reflectiveness, although the practical effect is negligible on most pavements.

A more successful optical system has been developed by K.J. Law, Inc. and the Michigan DOT, and is described below.

GM-type profiling systems are in use by agencies other than General Motors. The original GM design was completely analog, used a mechanical follower wheel, and required a constant measurement speed. Most of the newer systems feature on-board computers for digital analysis, noncontacting height sensors, and software that allows a variable measurement speed. The following models are presently in use in North America.

- **The Law 690 DNC.** K. J. Law Engineers, Inc. has commercially manufactured the GM-type profiling system for over 15 years. Originally, the Law version was identical to the GM design and was sold under a patent license. They have since made substantial improvements in the design to include the following:
  - It includes a DEC PDP-11 minicomputer. The processing of transducer signals to yield profile is performed in "real-time" during measurement. Roughness indices are printed during measurement.
  - It uses proprietary optical noncontacting height sensors.

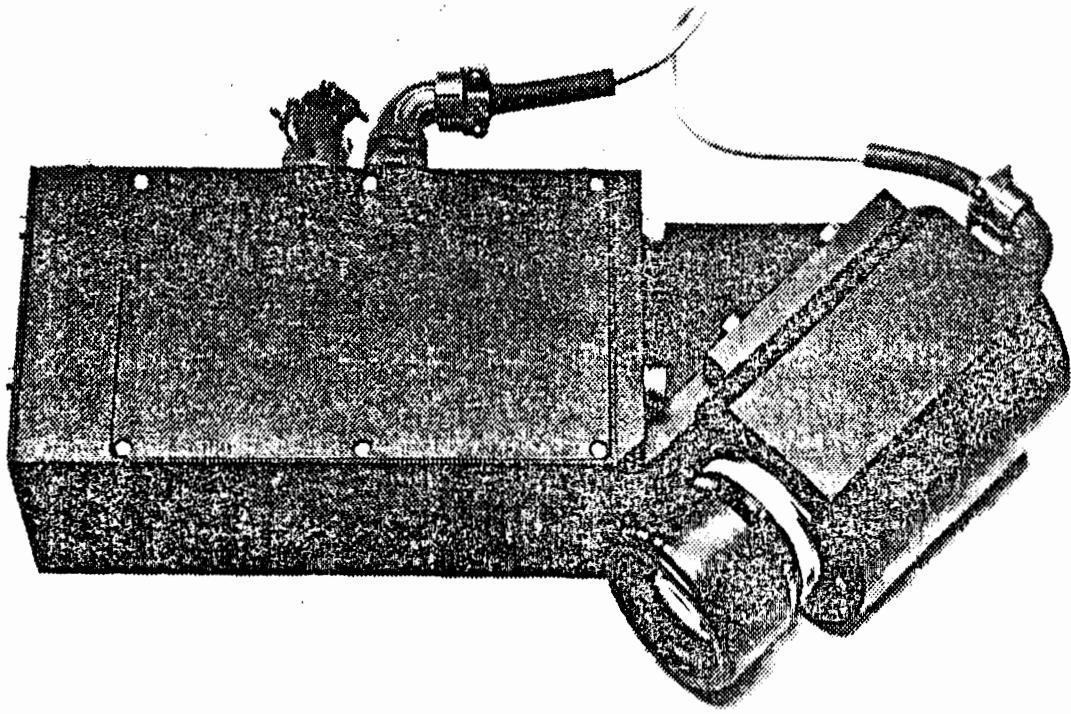


**Figure 6.4-5. The Selcom laser height sensor.**

#### 6.4 Measurement of "True Profile"

- It employs software with patented "spatial" filtering that compensates for speed variations during measurements.
- It measures two wheeltrack profiles, spaced about 1.5 m apart.
- The profiles are stored on 9-track computer tape for later viewing and processing with alternative analyses.
- Numerous profile analysis software packages are available.

The 690 DNC Profilometers measure profile with a very high degree of repeatability on all types of pavement surfaces that were included in the 1984 Road Profilometer Meeting in Ann Arbor. The limits of the system for sensing wavelengths is determined by software. The longest wavelengths included in the measurements are based on a spatial filter whose cut-off properties are specified by the operator. The shortest wavelength is presently limited by a 1-ft moving average filter and a storage interval of 6 in. The moving average attenuates wavelengths shorter than 10 ft, with 2-ft wavelengths reduced by about half, and with 1-ft wavelengths eliminated completely.

The proprietary noncontacting sensor projects a rectangular image of visible light on the road surface. The image is short (1/2 in) and wide (6 in) to precisely define the longitudinal location of measurement, while tolerating normal driver imprecision in the lateral positioning. The angle to the light spot is measured with a system that includes a detector and rotating mirror, designed to eliminate error due to variations in surface reflectivity. This design was shown to be highly effective for all types of pavements that were tested in the 1984 Profilometer Meeting.

The Law 690 DNC is the standard high-speed profiling system to which others are compared in North America. It has been purchased by several states, the Federal Bureau of Standards, and the federal government of Chile. The noncontacting height sensors, critical to the proper measurement of profile, have been shown to operate correctly on all surface types on which they have been tested. Its major limitation in measurement capability is due to the software that controls the storage of profile on tape, which results in the loss of high-frequency (short wavelength) information. A higher bandwidth can be obtained through software.

The criticisms of the system are (1) it is expensive (around \$250,000), (2) it is not "user friendly" to the operator, and (3) it is not robust (minor problems with the computer and optical sensors occur too frequently).

Some of the methods that can be used to eliminate the speed dependency are patented by the inventors of the GM-type design and licensed exclusively to K.J. Law, Inc. [30]. The capabilities of the system are described more fully in Reference [31].

K.J. Law Engineers, Inc.  
23660 Research Drive  
Farmington Hills, MI 48024  
(313) 478-3150

## 6.4 Measurement of "True Profile"

(800) 521-5245

ATTN: Ken Law

- **The Law 8300 Roughness Surveyor.** In 1984 K. J. Law, Inc. introduced a simplified system designed to measure profile-based roughness numerics such as the IRI [32]. It eliminates the expensive components of the 690 DNC model, such as the minicomputer, 9-track tape drive, and optical height sensors. Its major characteristics are:
  - The processing of transducer signals to yield profile is performed in "real-time" during measurement. IRI and other roughness indices are printed during measurement.
  - It uses proprietary software and hardware for ultrasonic noncontacting height measurement.
  - It employs software with patented "spatial" filtering that compensates for speed variations during measurements.
  - It measures roughness in one wheeltrack.
  - Profile cannot be recorded.

Results obtained in the 1984 Profilometer Meeting and subsequent FHWA demonstration projects have shown that the measures from the 8300 are not as accurate as those from the 690 DNC, and that the ultrasonic transducers are not reliable on certain types of surface.

- **The Swedish VTI Laser Road Surface Tester (RST).** The RST was designed by VTI in Sweden [33], and several units are used in North America by Infrastructure Management Services (IMS). The RST has been further developed through collaborative efforts of VTI and IMS. The main features of the RST are the following:
  - It uses an array of laser cameras to measure the transverse profile of the road.
  - The processing of transducer signals to yield profile and other surface properties is performed in "real-time" during measurement. IRI and other roughness indices are printed during measurement.
  - It uses a proprietary version of the Selcom laser height sensor designed for profile measurement.
  - It counts the cracks seen by each laser.
  - Proprietary software compensates for speed variations during measurements.
  - It measures IRI roughness in one wheeltrack.
  - Profile is not recorded.

## 6.4 Measurement of "True Profile"

The RST is not for sale in North America, but is used by IMS to measure road surface characteristics for clients on a cost/mile basis. An early version of the RST participated in the Ann Arbor RPM and was unable to provide valid profile measures at that time. Since then, VTI and IMS have changed both hardware and software to provide profile measuring capability. The RST has participated in several FHWA demonstration projects.

Infrastructure Management Services  
3350 Salt Creek Lane  
Suite 117  
Arlington Heights, IL 60005  
(312) 506-1500  
ATTN: Robert Novak

- **The FHWA PRORUT System.** The PRORUT (profiling and rut-depth) system was designed and built by UMTRI under contract to FHWA [34, 35]. This system is a prototype to demonstrate profiling technology to state agencies to encourage the use of profile measurement in state operations. The main features of the PRORUT are the following:
  - It uses an IBM PC microcomputer to control operation and process data.
  - The design is not tied to a specific height sensor. The prototype uses Selcom laser sensors provided by FHWA.
  - It includes self-calibrating electronics and diagnostics to detect hardware problems. Software encourages daily checking of the system using special hardware, "bounce-test," and distance test.
  - It measures two profiles and average rut depth. IRI is computed for the profiles.
  - Sample distance can be set by the operator to trade-off resolution and storage requirements.
  - It uses anti-aliasing filters for all transducer signals. The filters are set automatically by software for the test speed and sample interval.
  - The measurement, calibration, and analysis capabilities are integrated in a single "user-friendly" program.
  - An interactive plotter shows profiles, rut depth, and roughness profiles with adjustable scales, zooming, and scrolling. Data in files are "random-access."
  - Data are stored on tape cartridges during measurement. Data files can be copied to floppy disks for transfer to other computers.
  - Most components in the system are "off-the-shelf" commercial products available for the PC.
  - Computation of profile is performed after measurement, not in "real-time."

## 6.4 Measurement of "True Profile"

- Variation in measurement speed is corrected by software. The profile computation method might infringe on the K.J. Law patent [30] if a similar system were sold commercially. This has not been tested in court.

The PRORUT system is based on a general-purpose digital data-acquisition system used at UMTRI for a variety of laboratory and field test experiments involving vehicles. The software was developed to customize the system for measuring profile and rut depth. The main design objectives were: (1) to maximize the reliability of the system by using commercial components, (2) to allow the operators to identify hardware problems quickly through an automated daily checking routine, (3) to make the measured data accessible through "user-friendly" graphical presentation, and (4) to provide the highest degree of accuracy possible for the GM-type design.

As a non-commercial prototype, the PRORUT system is not for sale. Its design is in the public domain for use in future systems. The PRORUT system is presently being evaluated by several state departments of transportation in a follow-up to the original FHWA project.

- **The South Dakota ultrasound profiling system.** The South Dakota Department of Transportation (SDDOT) designed and built a novel GM-type profiling system in 1981. SDDOT is providing the plans for the system to other states, and offering help at nominal cost for states wishing to build similar systems. The Nebraska DOT has built a duplicate system, and several other states are considering this option. The SDDOT design features the following:
  - It includes a DEC PDP-11 minicomputer. The processing of transducer signals to yield profile is performed in "real-time" during measurement. Roughness indices are printed during measurement.
  - It uses an ultrasonic road sensor (an instrument grade version of the Polaroid ultrasonic device used for autofocusing in cameras) to measure vehicle height.
  - The operator controls the system using a laptop keyboard with a liquid crystal display.
  - The design of the system allows variable measurement speed.
  - Profile is recorded during measurement on floppy disk or hard disk.
  - Analyses include IRI, profile plots, and RMS indices. The analyses are performed after measurement is complete.

The SDDOT system uses a unique method for computing the profile. The accelerometer signal is sampled at a constant clock rate and double-integrated numerically with a special digital circuit board. Distance to the road, measured by the ultrasonic height sensor, is sampled at regular intervals along the road, as specified by the operator and detected with a wheel pulser. At each sampling position, the relative vehicle height (as measured with the ultrasonic sensor) is

## 6.4 Measurement of "True Profile"

subtracted from the most recent value of the absolute vehicle height to obtain the profile elevation.

The ultrasonic transducer limits the sample frequency because new measures cannot be made until the echos from the previous measure have dissipated. The profile signal is normally sampled at a 305-mm (1.0-ft) interval. Because the limit is based on a time interval, a shorter sample distance can be used when the measuring speed is reduced. The resolution of the ultrasonic sensor is approximately 0.01 ft (3 mm).

The SDDOT system participated in the 1984 Profilometer experiment, where a software bug prevented a complete evaluation of the system. SDDOT has since performed validation testing by measuring profiles with the high-speed system and the Dipstick® static method [36]. They have also participated in several recent FHWA demonstration projects.

Details of the current system status can be obtained from SDDOT.

South Dakota Department of Transportation  
Research Program  
700 E. Broadway  
Pierre, SD 57501  
ATTN: David Huft

- **The Michigan Profiling Systems.** The Michigan Department of Transportation (MDOT) owns and operates a GM-type inertial profilometer that was originally built in-house in the 1960's. Over the years it has been refined and improved, with the main improvement being the replacement of the mechanical follower wheels with noncontacting optical height sensors, also designed and built in-house. A second system was also built in-house.

The MDOT systems are constantly being modified and improved in response to the demands on on-going projects within the state. Therefore, the following descriptions are not as detailed as those for other systems.

- The noncontacting height sensor used by MDOT is similar in design and operation to the K.J. Law sensors.
- Sample interval can be set for various applications.
- Anti-aliasing filters are used. The cut-off frequency is set according to the sample interval.
- The systems can be configured for on-board processing or for post-processing back in the laboratory.
- A standard roughness index called RI is computed at the time of measurement. Other analyses, including PSD and IRI, are available for profile data collected with the systems.

## 6.4 Measurement of "True Profile"

Details of the current system status can be obtained from MDOT.

Michigan Department of Transportation  
Research Laboratory  
P.O. Box 30049  
Lansing, MI 48909  
ATTN: John Darlington

### *The Two-Accelerometer Design*

In a method proposed by Sayers and Gillespie in 1981 [37], the height sensor used in the GM design is replaced by a second accelerometer. One of the accelerometers is placed at the center of an axle, and the second is placed above it in the vehicle sprung mass. The motions of the vehicle are assumed to be largely predictable by a quarter-car model. In a quarter-car model, the vertical accelerations of the sprung and unsprung masses are

$$\ddot{z}_s = \frac{f_s}{m_s} \quad (6.4-1)$$

$$\ddot{z}_u = \frac{f_t - f_s}{m_u} \quad (6.4-2)$$

where  $f_s$  is the suspension force and  $f_t$  is the tire force. It so happens that the vertical tire force is predicted well with only a linear tire spring rate

$$f_t = k_t (z_v - z_u) \quad (6.4-3)$$

where  $z_v$  is the average profile vertical elevation under the left- and right-hand tires,  $z_u$  is the elevation of the unsprung mass (the axle), and the quantity  $(z_v - z_u)$  is an average of the dynamic tire deflections. By combining the above three equations, the average tire deflection can be derived:

$$(z_v - z_u) = \frac{\ddot{z}_u m_u + \ddot{z}_s m_s}{k_t} \quad (6.4-4)$$

By the use of eq. 6.4-4, the two accelerometer signals can be transformed to yield the vertical acceleration of the axle and the height of the axle above the ground. These two signals are then combined in the same way the height signal and accelerometer signals are combined in a GM-type system. The suspension force cancels out of the equations, so friction and other nonlinear suspension properties are not a factor. The method is subject to errors from the following sources:

- The three vehicle parameters  $m_s$ ,  $m_u$ , and  $k_t$  must be measured, and the values should not change with time. Tire stiffness ( $k_t$ ) varies with tire air pressure and temperature; thus the operator must monitor the pressure and always warm up the vehicle before taking data. The sprung mass changes with vehicle load; however, sensitivity analyses have indicated that normal day-to-day changes have a negligible effect.



#### 6.4 Measurement of "True Profile"

- The motions of the axle and body are assumed to derive only from the vertical forces of the tires and suspension. Pitch motions involving excitation from the front wheels are not accounted for. Also, motions of sub-assemblies between body and axle could cause error.
- The vertical tire force is assumed to derive only from the tire deflection and linear stiffness. Forces due to tire nonuniformity can be a problem.

Highway Products International (HPI) manufactures and sells several multi-purpose pavement measuring systems. The ARAN (Automatic Road Analyzer) system is a van-based system built around a computerized logging system controlled by an IBM PC-AT microcomputer. The ARAN is available with many optional capabilities, one of which is measurement and analysis of roughness. The PURD (Portable Universal Roughness Device) is a similar system, with fewer available options, based on a towed trailer. Both the ARAN and PURD are available with the instrumentation needed to measure profile using the above method.

The characteristics of the ARAN and PURD profile-measurement options include the following:

- The measured profile is a point-by-point average of the left- and right-hand wheeltrack profile. That is, it measures the modal vertical profile  $z_v$  described in Sections 3 and 4.
- The software is "user friendly."
- Roughness is computed using the IRI analyses for the vertical profile, and is called HRI (half-car index).
- Profile computation is performed after measurement; that is, it is not performed in "real time."
- Tire nonuniformity is removed by a notch-filter set the specific wavelength corresponding to the tire circumference.

Simple tests conducted by HPI and analyzed at UMTRI show that the design generally functions as intended. However, a thorough evaluation of the sort performed in the 1984 Ann Arbor experiment was not made. The ARAN and PURD systems have participated in the 1987 FHWA demonstration seminar in Ft. Collins, CO.

The ARAN and PURD are marketed by HPI:

Highway Products International  
R.R. #1  
Paris, Ontario N3L 3E1  
Canada  
(519) 422-2261  
ATTN: Don Kobi

## 6.4 Measurement of “True Profile”

### *The French APL Design*

The Longitudinal Profile Analyzer (APL) was developed by the Laboratoire Central des Ponts et Chaussées (LCPC) in France for rapid checking of road unevenness. The APL is a towed trailer, shown in Figure 6.4-6, and described in References [19, 20, 38]. The trailer frame acts as a sprung mass supported by a wheel that follows the road surface. An inertial reference is provided by a horizontal pendulum supported on a Bendix-type bearing. The pendulum is centered by a coil spring and damped magnetically. An LVDT displacement transducer is located between the inertial pendulum and the trailing arm of the road wheel, such that its signal is proportional to profile over the frequency range of 0.5 to 20 Hz as the trailer travels along the road. A digital distance transducer on the road wheel measures the distance traveled and the towing speed.

The APL is designed with dynamic properties that make it insensitive to motion inputs at the hitch point. The response of the trailer is calibrated by placing a dynamic shaker under the road wheel and measuring the output for sinusoidal inputs. The isolation of the system is also checked by placing the shaker at the hitch point, and verifying that no output occurs.

The APL is used routinely at LCPC in two configurations—the APL 25 and APL 72. The two configurations are distinguished by different testing procedures, data storage equipment, and profile analyses. The APL 25 system runs at 22 km/h and produces an average rectified displacement roughness statistic (CAPL 25 value) for each 25-m section of road. It is commonly used to evaluate new construction, before the road is opened to the public. The APL 72 configuration is used for surveying road networks. It is towed at 72 km/h, and the profile signal is recorded on magnetic tape. The profiles are analyzed later in the laboratory, using electronic filters to isolate three wavebands covering long, medium, and short wavelengths. A summary index is accumulated for each of the three wavebands for every 200-m section of road traveled. The APL trailer is also used by the Center for Road Research (CRR) in Belgium. At CRR, waveband analyses of the profile are used to determine a coefficient of evenness known as the CP.

The APL has been used for applications other than the APL 72 and APL 25 analyses, including the measurement of long-wave roughness on airport runways and measurement of IRI in developing countries.

The APL has been compared with other profile measuring methods in several research projects, including the 1982 Brazil experiment and the 1984 Ann Arbor experiment [19, 20]. These experiments have validated its ability to measure profile. The APL performs in mechanical hardware what a GM-type system achieves with a combination of hardware and software. This implies certain differences in operation when comparing the APL to GM-type systems.

- A computer is not required to obtain profile with the APL. The signal from the LVDT is the profile signal. (However, analysis of profile is nearly always performed with a computer, so there is usually a need to digitize the APL signal.)
- The APL profile has the proper amplitude information over the frequency range of 0.5 — 20 Hz; however, some phase distortion exists.

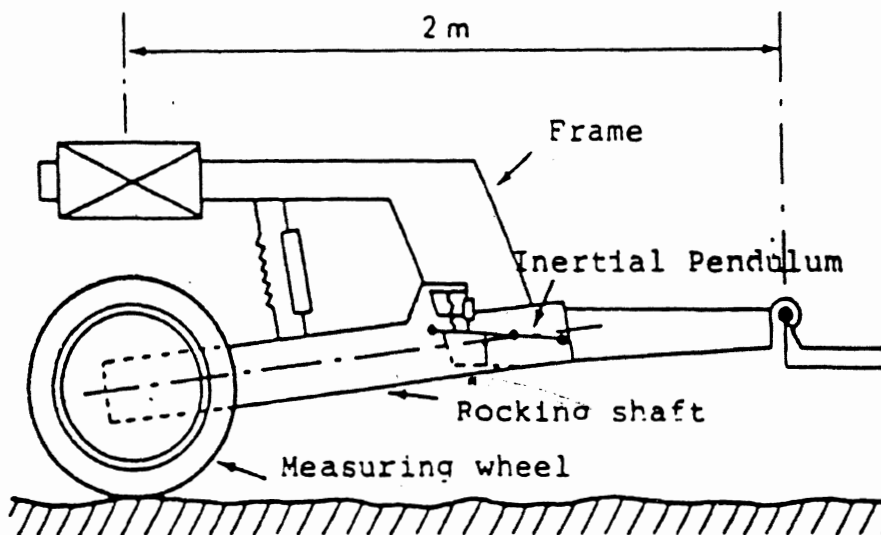


Figure 6.4-6. The French APL profiling system.

## 6.4 Measurement of "True Profile"

- The range of wavelengths included in an APL profile is a function of the measurement speed. At 20 mi/h, the wavenumbers corresponding to the 0.5 — 20 Hz range are 0.016 cycle/ft (64 ft/cycle) to 0.625 cycle/ft (1.6 ft/cycle). At 60 mi/h, the same frequency range corresponds to a wavenumber range of 0.0057 cycle/ft (176 ft/cycl) to 0.22 cycle/ft (4.4 ft/cycle).
- As a towed trailer, the APL is not tied to a particular motor vehicle. It can be crated, shipped, and towed by any available vehicle that can be fitted with a suitable hitch.
- The suspension of the APL trailer is designed to keep the wheel on the ground even on very rough surfaces. Usually, the wheels of the towing vehicle leave the ground before the trailer will. Thus, the system can be used for very rough pavements and unpaved roads.

The APL is commercially available for a cost starting at around \$40,000 and increasing for software options. The device is marketed by MAP.

MAP Inc.  
1825 I Street, NW  
Suite 400  
Washington, D.C. 20006

MAP Sarl  
29 Route d'Ilfurth  
F-68720 Ilfurth, France

### *The British Three-Laser Design*

The Transport and Road Research Laboratory (TRRL) in England has developed a unique laser profiling system [39]. Distance to the road surface is sensed at three points along the length of a trailer. As the trailer progresses forward, road elevation at the leading sensor is referenced to that at the other sensors so that a continuing profile can be developed. The design requires hardware that is much more expensive than the other designs. The positions of the three lasers must be known to a high degree of accuracy, such that thermal expansion within the trailer must be controlled. The system has never been used in North America.

## 7. CONSIDERATIONS FOR AIR FORCE SPECIFICATIONS

This section concludes the report by drawing on the technical material presented in the preceding sections to address the need for durability specifications for ground vehicles operating in the Air Force environment. Although the emphasis is on durability, the same analyses and specified inputs should also be useful for predicting ride quality and dynamic tire loads.

### 7.1 Roughness Scale

A roughness scale such as the IRI offers a simple and universal way to compare and rank surfaces. For example, a roughness scale is useful for showing how a real surface compares in overall roughness to a standard input. No single roughness index is appropriate for every use. Therefore, any standard scale must involve trade-offs to cover a range of applications. The IRI is an obvious choice for this purpose, if it is appropriate for the Air Force environment. Use of the IRI means that software and equipment in use by highway agencies can also be applied to air bases.

One of the main considerations behind the IRI is probably not relevant for the Air Force—that the index be compatible with the response-type system. To most highway agencies, the very concept of roughness is linked to the response-type system. A result of this background is that the IRI is closely linked to “typical” vehicle response, as was shown graphically in Figure 5.3-1.

A roughness index developed from scratch for the Air Force would most likely differ from the IRI in some ways, because acceptance by the highway community and correlation with response-type systems would not be factors. In the case of the IRI, the requirement for compatibility with response-type systems encouraged using the same units (“in/mi” or a metric equivalent such as m/km), the same averaging method (average rectified slope<sup>1</sup>, rather than RMS slope), and an analysis with a simple physical interpretation (quarter-car).

However, any analysis that yields a roughness index that is relevant to vehicle response at speeds near 50 mi/h will share characteristics with the IRI. The analysis must remove wavenumbers from a measured profile outside the band of interest. Also, the profile slope should be summarized (rather than elevation or acceleration), due to the character of real road profiles. Differences in the definition of the filter and method of averaging would affect the implementation and units, but not the essence of how the roughness is defined. The basics of vehicle dynamics and the nature of road roughness require that a roughness index that summarizes relevant vibration amplitudes for a highway-type vehicle will be

---

<sup>1</sup> The method of accumulating displacement in a response-type system is mathematically equivalent to the average rectified (AR) velocity, which is proportional to AR slope for a given travel speed. This is accomplished by various hardware designs, including one-way clutches and counters.

## 7.1 Roughness Scale

highly correlated with IRI. Thus, the IRI is an appropriate index to use when dealing with conventional ground vehicles that will be operated at speeds up to 60 mi/h.

On the other hand, if the index is designed to summarize a narrow waveband, it would be substantially different from the IRI. The same would also be true if an index is developed to describe roughness as seen by (1) a different type of vehicle (e.g., vehicles without suspension other than the pneumatic tire), (2) a much different range of speeds (e.g., speeds less than 30 mi/h), or (3) a different measure of vehicle response (e.g., axle vertical acceleration).

## 7.2 Standardized Road Inputs

Durability specifications should describe standardized inputs that can be used with vehicle models to predict the vibrations and resulting stresses in candidate designs. Those inputs should be realistic. The form of the input descriptions should also be compatible with the various sorts of vehicle models described in Section 2, and also with laboratory road simulators. Much of the work involving vehicle models and road description has been for optimization of ride quality for stochastic inputs of all levels. For durability considerations, it is mainly the inputs that cause the highest stresses that are of interest. Thus, the inputs should be particularly well suited for representing rough roads and pavement features that are the most likely to cause failure.

The roughness features of pavement can be roughly divided into three classes:

1. **Random roughness.** This is roughness caused by so many individual features that the profile resembles a random, stationary, Gaussian, broad-band signal.
2. **Localized roughness.** This is roughness from specific and easily identified features such as potholes and slab misalignment.
3. **Corrugations.** This roughness is the result of a physical cause that is concentrated within a narrow spatial frequency band. This most commonly occurs on unpaved roads when axle vibrations of the vehicle traffic produce a near-sinusoidal pounding of the ground. Once a corrugation is present, it further excites more vehicle responses, increasing the rate of damage. Another source is in certain paving machines that can generate a sinusoidal component at a wavelength corresponding to a characteristic wheelbase of the machine.

Random roughness is the most prevalent on highways, and is the only category well suited for statistical methods. As indicated in Sections 2, 3, and 4, the representation of random roughness is well developed. Most of the roughness input to a ground vehicle will probably fall into this category. However, it may be that the localized roughness is the more critical for causing actual failure. A pavement that is generally smooth might have a single pothole that causes failure for some vehicles. Corrugation roughness can be a problem because the wavelength of the corrugation so often coincides with a lightly damped resonance frequency in the vehicle.

Specified vehicle inputs should cover all three types of roughness. Details of how the input might be defined for each type are covered separately for each type. The design

## 7.2 Standardized Road Inputs

philosophy for using these inputs might be to design the vehicle performance for the random inputs, and use the localized inputs to check for failure analysis of the design. The corrugation input is also mainly for checking a design.

### *Random Roughness*

In this category of input, the roughness properties of two wheeltracks are completely characterized by the PSD function of each, together with the cross-spectral density function. The single-pole high-pass filter used as an example in Section 4.4 is suggested as a shaping filter to develop the proper correlation between two wheeltracks.

The following PSD model for a single wheeltrack is recommended

$$G_{zz}(v) = G_a (2\pi v)^{-4} + G_s (2\pi v)^{-2} + G_e \quad (7.2-1)$$

The selection of the three parameter values in this model defines a standard wheeltrack roughness input. By substituting the transfer function for a one-pole filter (eq. 4.2-4) into eq. 3.2-8, a relation for the cross-spectral density can be obtained:

$$G_{z_L z_R} = G_{zz} \frac{v_1^2}{v_1^2 + v^2} \quad (7.2-2)$$

The squared transfer function in eq. 7.2-2 is obtained with a one-pole low-pass filter with a cut-off frequency  $v_1$ . Based on measurements, a value of  $v_1 = 0.2$  cycle/m is recommended.

The method of adding sinusoids (eqs. 3.3-3 through 3.3-5) or an inverse FFT method [14] can be used to generate profiles. However, the formulation of the PSD model (7.2-1) and the one-pole shaping filter allow the more efficient method described in Section 4.2 to be used (eqs. 4.2-6 — 4.2-10).

In this formulation, the inputs are defined by four parameters: the three coefficients in eq. 7.2-1, and the cut-off spatial frequency for the shaping filter,  $v_1$ . For typical vehicle track widths, measured data are fitted by a cut-off wavenumber of 0.2 cycle/m. For other track widths, more data are needed to determine what the appropriate wavelength should be.

Four random inputs are described below that might be suitable as standard simulation inputs:

1. A normal “moderate” road. This input is representative of most moderately rough roads, and is suggested for preliminary design work.
2. An asphalt road with long wavelengths. This type of road provides much more excitation to the body resonance than the “moderate” road. Vehicle designs should be checked to guard against a design that cannot handle this form of input reasonably.

## 7.2 Standardized Road Inputs

3. A normal “rough” road. This input represents the upper limit of roughness normally seen on public roads. Designers should consider this input and the “moderate” road as representing the inputs seen by a vehicle most of the time.
4. Limit roughness. The input is the maximum level of input that would be caused by pavement roughness. Vehicles designs should be checked to determine that failure does not occur when facing this level of input. This level of input usually corresponds to reduced speeds.

These four inputs are characterized by the coefficients in the PSD model of eq. 7.2-1. Suggested values are shown in the table below.

Table 4. Coefficients for four random roads.

| <i>Description</i>      | $G_s$<br>$m/cycle \times 10^{-6}$ | $G_a$<br>$1/(m \cdot cycle) \times 10^{-6}$ | $G_e$<br>$m^3/cycle \times 10^{-6}$ |
|-------------------------|-----------------------------------|---|-------------------------------------|
| Moderate                | 20                                | 0   | 0                                   |
| Asphalt with Long Waves | 20                                | 7   | 0                                   |
| Rough                   | 100                               | 0   | 1                                   |
| Limit Roughness         | 300                               | 0   | 8                                   |

These values are drawn from measures of the rougher roads in the Ann Arbor area. Note that each case simplifies the PSD model by setting at least one of the coefficients to zero. The “moderate” road simply uses the simple white-noise slope model with a coefficient of  $20 \times 10^{-6}$  m/cycle. The roughness level on the IRI scale is about 2.5 m/km, which is typical of a pavement that is about to require repair. The next road, “Asphalt with Long Waves,” represents the maximum long-wave input that was observed. The third, “Rough,” is characteristic of the rougher roads. It has a higher overall roughness level and includes additional high-frequency roughness. The “Limit Roughness” road is based on a short section of badly damaged pavement that was measured a few weeks before the road was resurfaced. It was so rough that traffic slowed down, as drivers tried to protect their vehicles. It contains a great deal of additional high-frequency roughness.

### *Localized Roughness*

Vehicle damage, when caused by a ground input, is usually the result of a single impact involving a discontinuity. In addition to the random roughness model characteristic of most roads, a simple step input should be used to guard against designs that handle random roughness well but cannot deal with the impact of a pavement discontinuity.

Localized profile features come in a variety of shapes and sizes, including simple steps (due to slab misalignments), potholes, patches, etc. The dynamic response of a particular



## 7.2 Standardized Road Inputs

vehicle to some of these forms of input can involve an interaction between the frequency response of the vehicle with characteristic dimensions of the roughness feature. At some speeds, a vehicle can “tune in” to a particular roughness feature. For example, the worst speed for a vehicle going over a pothole is the speed at which a wheel drops completely into the pothole and reaches a maximum load just as it hits the end. The same pothole would cause less damage for that vehicle at a different speed. A different vehicle would most likely tune in at a different speed.

A step input is one realistic discontinuous profile feature that does not involve “tuning in” of traversing vehicles. A step input is suggested as a standard roughness input, because it is realistic and simpler to apply than other discontinuities. A specification involving a step input would represent the impact loading that is caused by numerous roughness features appearing in pavement.

The ability to roll over a large step once without damage would be one form of a specification. A second form of specification would be the requirement that the vehicle roll over a smaller step size some number of times without damage, to account for fatigue failures. The impact increases with speed up to a point, so the specifications should account for speed.

The size of the step and the speed used in a specification should be related to the type of vehicle. A 2-inch discontinuity occurs on highways, and thus highway vehicles should be able to handle one repeatedly at normal speeds without damage. Occasional encounters with steps of 4 or 5 inches also occur, and therefore surviving a 4-inch step at 50 mi/h might be a reasonable design specification. However, a specification to that effect would be clearly inappropriate for a cart with 6-inch wheels.

### *Corrugations*

Corrugated pavements cause problems when a vehicle “tunes in” to the frequency of the corrugation. This only happens for vehicles with a lightly-damped resonance. If frequency-domain vehicle analyses are used in the design process, such behavior should be obvious. However, frequency analyses may not be convenient if the bulk of the analysis work is performed with time-domain simulation. Even if frequency analyses are performed, nonlinear behavior of the vehicle can invalidate the analyses.

To guard against a vehicle design with poor performance on corrugated surfaces, a standard corrugation is suggested. The following model provides a sinusoidal with changing wavelength, centered at a wavelength  $\lambda$ .

$$z_{cg}(\xi) = A \sin \left( \frac{2\pi\xi}{\lambda} \left[ \frac{3}{4} + \frac{\xi}{2L} \right] \right) \quad (7.2-3)$$

where  $z_{cg}$  is the corrugation profile,  $\xi$  is the distance along the road,  $A$  is the amplitude of the corrugation,  $\lambda$  is the nominal wavelength of the corrugation, and  $L$  is the length of the profile. This model defines a sinusoid whose frequency ramps to cover a one-octave waveband, centered at  $1/\lambda$ . A value of  $\lambda = 2$  m matches data from Ann Arbor and Brasilia, and is suggested.

## 7.2 Standardized Road Inputs

The corrugation profile should be added to the “moderate” random profile defined above. Vehicle designers should use this input for a range of speeds to ensure that the vehicle does not overreact to corrugations.

## 7.3 Validation and Measurement

Validation requirements depend on the form of the analysis and the uses made of its predictions. In Section 7.2, three types of standard inputs were suggested for random roughness, localized roughness, and corrugations. Frequency-domain methods are appropriate for validating predictions of vehicle response to random inputs and corrugations. Predicted responses to step inputs should be validated through comparison of predicted and measured time histories. Comparison of summary amplitude indices such as RMS levels or histograms is necessary, but this comparison alone is not adequate for validation purposes. (It is all too common for incorrect models to predict correct RMS levels for certain combinations of vehicle parameters and road input conditions.)

### *Validation Criteria*

The interpretation of the frequency-response plots and time-history plots is ordinarily performed subjectively. Reducing this process to a specific criterion is not trivial, and it may not be appropriate. The considerations for comparing transient time-history plots include the following:

- The time-history plots should be selected to show the behavior of interest. Usually, this means short sections with a high-amplitude response to a localized roughness.
- The predicted and measured peak values should be compared.
- The predicted and measured transient responses should be compared.

Evaluating graphs of transient time histories is usually more difficult than frequency-response plots. The transient response is unique for each input. Evaluation of long tests is difficult because the entire time history must be examined. In contrast, a single frequency plot can summarize a long test, or even a set of tests.

The considerations for comparing frequency plots such as PSD functions computed from experimental and simulated data include the following:

- Only the frequency range that contributes significantly to the mean-square variables of interest should be evaluated. This range is most easily seen by preparing a plot of the PSD using linear scaling. For example, the plot in Figure 2.2-1 shows that contributions to vertical acceleration are essentially limited to the frequency range of 0 to 15 Hz.
- The frequency analysis of the data should be appropriate to the form of input. Different methods are used for the continuous vibrations due to random roughness and the transient response due to a step or impulse input.

### 7.3 Validation and Measurement

- There should be a one-to-one correspondence between the major resonances predicted by the model and those observed in the test data. The frequencies and amplitudes should agree approximately.
- Predicted summary statistics such as RMS values should agree with the measurements.
- If measures of inputs and outputs can be synchronized, coherence functions and transfer functions can be used to determine the transmission properties of the vehicle.

#### *Measurement of Vehicle Response*

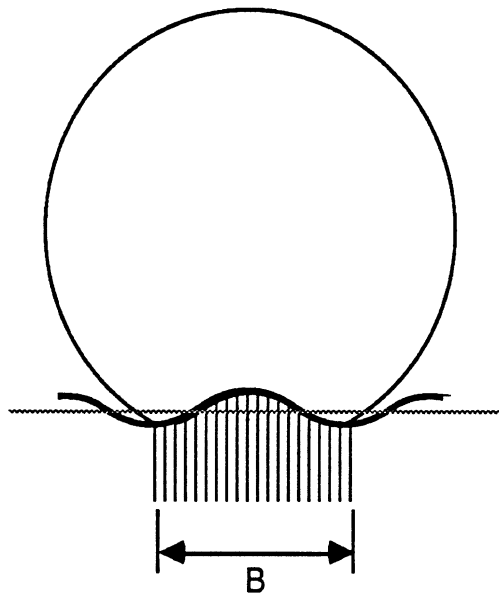
The measurement requirements are determined by how the measures will be used. The major forces in a ground vehicle are closely tied to the large motions of the sprung masses. Movements of the axles can reveal how the ground inputs are transmitted through the vehicle. The following variables are often measured when studying vehicle response to roughness.

- Accelerometers and/or rate gyros should be installed in the sprung mass(es) to discern pitch, bounce, and roll motions.
- Vehicle speed should be measured continuously and recorded with other data channels.
- Axle motions can be sensed using accelerometers, potentiometers, LVDTs, or rate-sensitive transducers.

Data can be recorded for later analysis using analog or digital systems. If analog systems are used, the signals should be scaled to make maximum use of the dynamic range of the recording medium. The frequency bandwidth should extend at least to 50 Hz, and 100 Hz or higher is recommended. Filters applied to the transducer signals should not attenuate their response below 50 Hz. Phase distortion in the signal processing or the recording method should be noted, because it will influence the recorded transient time histories.

When the data are digitized, the sample frequency must be no less than 100 Hz, and 200 Hz or higher is recommended. Anti-aliasing filters must be used for accelerometer signals. The specifications for the anti-aliasing filters depend on the sampling frequency. With much higher sampling frequencies (400 Hz), an attenuation of 6 dB/octave is adequate; however, higher-order filters are recommended. A 24 dB/octave filter with an 80 Hz cut-off frequency, together with a sampling frequency of 200 Hz is probably adequate for most work. The digitizing resolution should be at least 12-bits.

The above discussion is based on experience with highway-type vehicles. A fundamental characteristic of the highway vehicle is the pneumatic tire, which attenuates high-frequency inputs through its vertical compliance and through a mechanism called "enveloping." The compliance attenuates high frequencies via the dynamic transmissibility of the vehicle, as characterized by a transfer function (see Figures 2.2-2 and 5.3-1). The tire enveloping effect, shown conceptually in Figure 7.3-1, is independent of speed.



Area is unaffected by the variation  
when the averaging baselength = wavelength

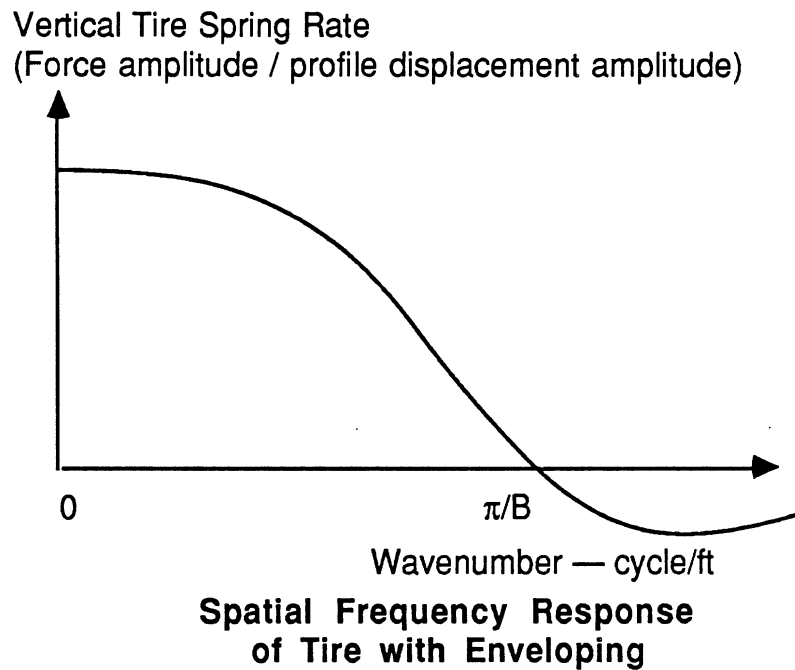


Figure 7.3-1. Conceptual overview of tire enveloping.

### 7.3 Validation and Measurement

Changes in profile that occur in a very short space are “enveloped” by the tire and are not transmitted to the vehicle. For highway vehicles, the tire enveloping acts approximately as a 1-ft moving average or a low-pass filter with a cut-off frequency corresponding to a 2-ft wavelength. At 65 mi/h, the tire enveloping approximates a low-pass filter with a 50 Hz cut-off.

Ground vehicles that deviate from the design of a highway vehicle may have a different frequency response that extends well beyond 50 Hz. Vehicles with small tires, or rigid wheels would transmit more of the high-frequency roughness to the vehicle. Specifications for data acquisition should be set according to the relevant frequency range of the vehicle.

#### *Measurement of Profile*

Measurement of road profile is necessary for any form of detailed or comprehensive validation activity. The techniques and methods used for this are not yet well known, and were therefore covered in Section 6.4. The choice of which system to use depends on several factors. Once again, the main factor is the intended use for the data.

Most of the high-speed profiling systems are capable of measuring wavelengths longer than needed for inputs to ground vehicles. If the vehicle speeds are below 80 mi/h, the lowest wavenumber of interest is about 0.015 cycle/m (67-m wavelength). The highest wavenumber of interest is generally limited by the tire-enveloping behavior, mentioned above.

The profiling devices developed for highway applications are suitable for measuring inputs to highway-type vehicles, but are in some cases not capable of sensing the very short wavelengths that could be relevant for vehicles with smaller tires or solid wheels. Very briefly, the limits for the devices described in Section 6.4 are the following:

- The K.J. Law 690 DNC Profilometer applies a 1-ft moving average to the data before storage on tape. Thus its profile measures have a high-wavenumber limit appropriate for measuring inputs to highway vehicles, but not for vehicles responsive to higher frequencies. The capabilities can be extended by revising the software in the system.
- Measures from the ARAN and PURD systems are subject to tire-enveloping from the tires on the profiling systems. The upper wavenumber range cannot be extended beyond the limit of an ordinary passenger car tire.
- Measures from the APL trailer are limited by the dynamic response of the system, which is nominally 20 Hz, and by the enveloping properties of the motorcycle-type tire. The wavenumber range of the system is determined mainly by the speed at which it is towed. It is not possible to simultaneously sense very long wavelength (67 m) and very short wavelengths (0.2 m) with this design, although repeat runs at different speeds will produce different “views” of the profile, covering different wavebands. Due to the small contact patch of the APL tire, the enveloping is probably less of a factor than for a passenger-car tire.

### 7.3 Validation and Measurement

- Ultrasonic systems are generally not capable of sensing the small-amplitude, short-wavelength profile features.
- Laser systems are capable of capturing short wavelengths well beyond the range required for vehicle analysis.

There are no accepted methods for specifying profile accuracy. PSDs of road profiles show elevation amplitudes that increase with wavelength. For measures involving long wavelengths, errors are larger than for measures involving short wavelengths. Some of the profiling systems are capable of sensing changes of profile of 0.5 mm or less, but they cannot hold that level of accuracy over much distance. Presently, the only usable measures of profile accuracy are obtained by comparing summary indices computed from profiles measured by different systems. For example, IRI has been used as a basis for specifying profile accuracy. If a different roughness index (or family of indices) is developed for Air Force use, it (or they) would be a rational measure of profile accuracy.

Unfortunately, determining the accuracy of a profiling device is an extremely expensive undertaking. A problem is that repeatability is limited by the operator's ability to position the system exactly over a specified wheeltrack profile, and start the recording at the proper instant. A practical specification is that the profile is "good enough" if the repeatability of the instrument is better than the repeatability of the operator. This is the case for most of the systems described in Section 6.4.

### 7.4 Recommendations

This report has attempted to describe the technical issues that are relevant to the measurement, description, and specification of ground inputs to vehicles. The next step is to apply this knowledge to prepare specifications and procedures that can be provided to contractors who design and build ground vehicles for Air Force use.

#### *Roughness Index*

A roughness index by itself is not sufficient for specifying inputs for vehicle models. However, the use of a standard road roughness index such as the IRI can simplify the description of roughness, and allow contractors and others to place the specification into perspective with other roads. If the roughness index should be relevant to overall vehicle vibration inputs for speeds up to about 60 mi/h, the IRI is recommended. If a different criterion is more important (e.g., vehicles used only at low speeds), a roughness index should be defined to match the criterion. If a new index is developed, it should be relevant and reproducible, as is the IRI. However, the compatibility with response-type systems and traditional highway roughness measures would not be necessary. If a new index is developed, RMS-type averaging is recommended for 100% compatibility with PSD analyses.

## 7.3 Validation and Measurement

### *Standard Inputs*

To eliminate the large costs associated with profile measurement, and to reduce the uncertainty involved when contractors choose their own test sites, it is recommended that a family of standard inputs be prepared by the Air Force that would be provided to contractors for use with computer simulations and laboratory testing. These inputs could be made available in several forms:

1. Profiles would be prepared and made available as computer files. The files would consist of elevation values spaced at a constant interval of about 100 mm (3.9 in). Pairs of profile would be generated for random roads having specific roughness properties, such as the four defined in Table 4. Also, the current profiles of roads that are used for validation testing should be made available to contractors, to enable comparisons of computer predictions with measurements. At least one road should be included that shows “washboard” corrugations. The profiles would be of sufficient length (about 1 mile) for most computer applications.
2. Software for generating “random” profiles would be prepared, documented, and made available to contractors. The software would be used when the needs of the contractor are not perfectly satisfied by the form of the computer files described above (option 1). The software should allow valid profiles to be generated for arbitrary roughness parameters, intervals, and duration. A possible option would be the specification of IRI roughness (or a similar summary statistic) and a surface category (asphalt, dirt, etc.) as the only required inputs. Profiles produced by the software should be reproducible on different computers. The profiles described above (option 1) could be generated with this software to provide complete consistency. One possible use of the software would be to provide inputs to laboratory road simulators, for durability testing. The software should be provided in the form of Fortran source code for portability.
3. Analytic descriptions of roughness would be provided, in the form of PSD functions (e.g., eqs. 7.2-1 and 7.2-2) and roughness parameters.

### *Validation of Computer Predictions*

Validation experiments at a test track can turn into very expensive undertakings, particularly when road profile measures are required. Therefore, it is recommended that experimental work be kept to a minimum by using established computer simulations and/or laboratory road simulators for all conditions and sensitivity studies, and performing only a few key tests to validate the computer results. Usually, the computer results are either correct for all “normal” conditions, or incorrect for all. Arrangements should be made to select a small number of pavements that are accessibly throughout the year and under control of the Air Force. The profiles of these roads should be measured periodically by the Air Force, so that the profiles can be used as inputs to the computer models.

### *7.3 Validation and Measurement*

#### *Pilot Study*

It is recommended that a pilot study be performed to establish the criteria to be used for determining the level of agreement needed between measurements and computer prediction. Considerable effort can be saved if a vehicle is used which has been adequately modeled and which has known parameter values. The pilot study might be coordinated with a contractor that has recently delivered a vehicle and has already gone through the modeling effort. Several pavements at Wright-Patterson should be profiled, using Air Force equipment or outside (leased) profiling equipment.

The study would compare the measured vehicle response on the test sites with the response predicted from the model. If possible, the suitability of any standard input profiles should also be evaluated from various viewpoints (contractors, Air Force engineers, etc.)



## APPENDIX A—PSD COMPUTATION

This appendix describes the basic steps that are required to transform a series of discrete measures of a variable into a series of discrete PSD values. The method requires the use of the fast Fourier transform (FFT), which is available in many forms for most computers.

There are a few special considerations for computing PSD of road profiles, and these are noted. The following steps summarize the data-processing method that has been used at UMTRI for several large-scale research projects involving road profiles measured by a variety of methods.

1. The profile is measured, digitized, and entered into the computer as a sequence of  $n_e$  elevation values

$$x_i, i = 1, 2, \dots, n_e \quad (\text{A-1})$$

Adjacent samples are separated by constant sampling interval,  $\Delta\xi$ . The details for performing this step are specific to the method used to obtain the profile. If an analog signal is digitized, an anti-aliasing filter should be used.

2. The elevation profile is converted to a slope profile, by taking the difference between adjacent elevation values and dividing by the sample interval:

$$x'_i = \frac{x_{i+1} - x_i}{\Delta\xi}, i = 1, 2, \dots, n_s \quad (\text{A-2})$$

$$n_s = n_e - 1 \quad (\text{A-3})$$

This step is taken for several reasons. Because only a finite length of the wheeltrack is measured, there is an effect on the PSD computation due to the abrupt start and end of the profile. (This effect is called a “window” in textbooks, because the analysis is viewing a theoretically infinite signal through a finite window.) The transitions are much greater for elevation profiles than for slope profile, and therefore the influence of the transitions in the computations is reduced. (If the profile includes a hill, the PSD computation can be corrupted by the large triangular shape of the static slope.) A second reason is that a profile slope has a more or less uniform PSD, and as a result numerical round-off and truncation errors are minimized during the FFT calculations. A third reason is that the PSD functions are desired in the form of a slope PSD, and the transformation from elevation to slope must be performed at some stage of the processing anyway.

By performing this step, weighting of the signal to account for “windowing” is not required. The need for trend removal is also eliminated.

(NOTE: If the signal being processed is *not* an elevation profile, this step should be omitted.)

3. The mean value of the slope profile is computed and subtracted from the signal:

$$\bar{x}' = \frac{1}{n_s} \sum_{i=1}^{n_s} x'_i \quad (\text{A-4})$$

$$\hat{x}'_i = x'_i - \bar{x}' \quad (\text{A-5})$$

4. The signal is padded with zeros until it contains a number of samples that is a power of two. The sequence is stored as the vector  $\mathbf{x}$ , with dimension  $n_t$ .

$$\mathbf{x} = (\hat{x}'_1 \ \hat{x}'_2 \ \hat{x}'_3 \ \dots \ \hat{x}'_{n_t})^T \quad (\text{A-6})$$

$$\hat{x}'_i = \begin{cases} x'_i - \bar{x}' & i \leq n_s \\ 0 & i > n_s \end{cases} \quad (\text{A-7})$$

The power of two is computed with the following equations:

$$\alpha = \frac{\ln n_s}{\ln 2} \quad (\text{A-8})$$

$$\mathbf{k} = \begin{cases} \alpha & \alpha \text{ is an integer} \\ \alpha + 1 & \alpha \text{ has a fractional part} \end{cases} \quad (\text{A-9})$$

$$n_t = 2^k \quad (\text{A-10})$$

For example, if the original signal contains 6000 samples ( $n_e$ ), the slope signal contains 5999 samples ( $n_s$ ), the exact power of two is 12.550506 ( $\alpha$ ), the next higher power of two is 13 ( $k$ ), and the total number of points in the vector  $\mathbf{x}$  is 8192 ( $n_t$ ).

5. The  $\mathbf{x}$  vector is transformed by the fast Fourier transform (FFT) into the frequency (wavenumber) domain to yield a vector  $\mathbf{X}$  containing a sequence of  $n_t/2$  complex Fourier coefficients. The coefficients contain phase and amplitude information that could be used to reconstruct the profile with a series of sinusoids. The Fourier transform vector is scaled to compensate for the zeros added in the previous step.

$$\mathbf{X} = \sqrt{\frac{n_t}{n_s}} \text{FFT}(\mathbf{x}) \quad (\text{A-11})$$

The first element of  $\mathbf{X}$ ,  $X_0$ , corresponds to the square of the mean value, which is identically zero due to the bias removal in step 3. The other elements correspond to wavenumber according to the relationship

$$v_i = \frac{i}{\Delta\xi n_t} \quad (\text{A-12})$$

6. The amplitudes of the  $n/2$  coefficients are squared and scaled to yield PSD units:

$$G_i = \frac{\Delta\xi n_t}{2} |X_i|^2 \quad (\text{A-13})$$

(NOTE: If a transform is being made that involves two signals, e.g., a cross-spectral density, both signals are processed identically up to this point. Eq. A-13 is replaced with

$$G_i = \frac{\Delta\xi n_t}{2} X_i^* Y_i \quad (\text{A-14})$$

where  $X_i^*$  is the complex conjugate of  $X_i$ , and  $Y_i$  is the Fourier transform of the second signal.)

7. Adjacent PSD values are averaged to obtain smoothed PSD functions for wavenumbers in a specified sequence,  $v_j$ .

$$G(v_j) = \frac{1}{q+1-p} \sum_{i=p}^q G_i \quad (\text{A-15})$$

$$p = \text{nint} \left( \Delta\xi n_t \sqrt{v_{j-1} v_j} \right) \quad (\text{A-16})$$

$$q = \text{nint} \left( \Delta\xi n_t \sqrt{v_j v_{j+1}} \right) \quad (\text{A-17})$$

where *nint* is a function that returns the nearest integer to its argument. (e.g.,  $\text{nint}(3.2)=3$ ;  $\text{nint}(3.8)=4$ .)

The figures in this report were prepared using wavenumbers at 1-octave intervals for long wavelengths (each wavenumber is twice the previous value), 1/3-octave intervals for medium wavelengths (the wavenumbers increase by a factor of  $2^{1/3} = 1.26$ ), and 1/6-octave intervals for short wavelengths (the wavenumbers increase by a factor of  $2^{1/6} = 1.1225$ ). These wavenumbers are spread evenly on the log scale normally used for plotting PSD functions. Before averaging, the PSD values ( $G_i$ ) occur at wavenumbers that are equally spaced on a linear axis. Thus, there is a great deal of averaging at the higher wavenumbers, and relatively little at the low wavenumbers.

The compensation for additional zeros used in eq. A-11 applies for a broad-band signal (such as a road profile), but gives an error for a pure sinusoid or a single pulse.

Various FFT subroutines may scale their output differently. The scaling shown in this appendix assumes the mean-square of the FFT output sequence equals the mean-square of the input sequence. If an FFT routine is used that produces a different scaling, the scaling in eq. A-13 should be adjusted accordingly.

## APPENDIX B—SOURCE OF ROAD DATA

The profile and PSD data shown in this report were drawn from two recent research projects involving the measurement of road roughness. The first, called the “International Road Roughness Experiment”(IRRE), was held in Brasilia, Brazil in 1982 to determine correlations and calibration methods for roughness measuring equipment. As a part of the experiment, the profiles of both traveled wheeltracks in a lane were measured for 49 test sites, each 320-m long. The measures were made manually, using rod and level instruments, with a vertical resolution of 1 mm and a longitudinal sample interval of 0.5 m. The second experiment was held in Ann Arbor, Michigan in 1984 to validate profile measuring instruments. Twelve systems were used to obtain profiles on a variety of public roads and roads at the General Motors Proving Grounds. In addition, test sites at the proving grounds were also measured with a rod and level. Several of the systems were demonstrated to provide valid and accurate profile measures for wavelengths ranging from 0.3-m up to wavelengths exceeding 100-m. (The systems can measure longer wavelengths, but the rod and level measures were reliable only for wavelengths up to 100-m.)

The measures from the Brazil and Ann Arbor experiments constitute a particularly valuable resource for the purpose of determining statistical descriptions of pavements for several reasons:

- All roads were measured independently by several methods (including static rod and level), allowing the quality of the profile measures to be determined. Without this check, unknown response properties of a single measuring system can introduce systematic errors into the data.
- The roads included a full spectrum of pavement type and roughness condition. (The Brazil roads even include unpaved surfaces.)
- Profiles were measured for both travelled wheeltracks for all of the roads.

The data set for paved roads includes profile measures from 13 asphaltic concrete roads and 12 surface treatment roads from the Brasilia experiment, 16 asphalt and surface treatment roads from the Ann Arbor experiment, and 11 Portland Cement Concrete (PCC) roads from the Ann Arbor experiment. All of these roads had similar roughness levels in the right- and left-hand wheeltracks. They also had roughness distributed fairly uniformly over length such that they are similar to stationary random signals.

Other test sites include unpaved roads (12 gravel and 12 earth), and several non-stationary features (bridge crossing, railroad crossing, etc.).

## REFERENCES

- [1] Press, W. et al. *Numerical Recipes: The Art of Scientific Computing*. Cambridge Univ. Press, 1986, 700 p.
- [2] *ADAMS Users Manual*, Mechanical Dynamics, Inc., Ann Arbor, MI.
- [3] *DADS User's Manual Rev. 4.0*, CADSI—Computer Aided Design Software, Inc., Oakdale, Iowa, 1986
- [4] McClelland, W. A., and Klosterman, A. L., "NASTRAN for Dynamic Analysis of Vehicle Systems." International Conference on Vehicle Structural Mechanics: Finite Element Applications to Vehicle Design, SAE Report 740326, SAE, New York, 1974, pp. 95-107.
- [5] Kane, T. R., and Levinson, D. A., *Dynamics: Theory and Applications*, McGraw-Hill series in mechanical engineering, 1985.
- [6] Greenwood, D. T., *Principles of Dynamics*. Prentice Hall, New Jersey
- [7] Bendat, J. S., and Piersol, A. G., *Engineering Applications of Correlation and Spectral Analysis*. John Wiley and Sons, New York, 1980.
- [8] Franklin, G., Powell, J. and Naeni, A., *Feedback Control of Dynamic Systems*. Addison Wesley Publishing Co., 1986.
- [9] Rill, G. "The Influence of Correlated Random Road Excitation Processes on Vehicle Vibration," 8th IAVSD Symposium on the Dynamics of Vehicles on Roads and on Railway Tracks, Cambridge, Mass., Swets & Zeitlinger B.V., Lisse, 1984 pp. 449 - 459.
- [10] Robson, J. D., "The Role of the Parkhilovskii Model in Road Description," *Vehicle System Dynamics* 7 (1978), pp 153-162.
- [11] Dodds, C. J., and Robson, J. D., "The Description of Road Surface Roughness," *Journal of Sound and Vibration*, October/November 1973, pp. 175 - 183.
- [12] Heath, A.N, "Evaluation of the Isotropic Road Roughness Assumption." Proceeding of the 10th IAVSD Symposium on the Dynamics of Vehicles on Roads and Railway Tracks, Prague.
- [13] Sayers, M. W., "Characteristic Power Spectral Density Functions for Vertical and Roll Components of Road Roughness." Proceedings, Symposium on Simulation and Control of Ground Vehicles and Transportation Systems, American Society of Mechanical Engineers, Anaheim, Calif., December, 1986, pp 113 - 129.
- [14] Cebon, D. and Newland, D. E. "The Artificial Generation of Road Surface Topography by the Inverse FFT Method," 8th IAVSD Symposium on the Dynamics of Vehicles on Roads and on Railway Tracks, Cambridge, Mass., Swets & Zeitlinger B.V., Lisse, 1984 pp. 29 - 42.

- [15] Anon. "Proposals for Generalized Road Inputs to Vehicles," ISO/TC 108/WG9 draft 3e, May 1972.
- [16] Houbolt, J. C. "Runway Roughness Studies in the Aeronautical Field," ASCE Trans. paper N3364, V127, Pr. IV, 1962, pp 427-448.
- [17] Van Deusen, B. D. and McCarron, G. E. "A New Technique for Classifying Random Surface Roughness," SAE Trans. 670032, 1967.
- [18] La Barre, R. P., Forbes, R. T., and Andrews, S. "The Measurement and Analysis of Road Surface Roughness," MIRA Rept. No. 1970/5, Dec. 1969.
- [19] Sayers, M. W., Gillespie, T. D., and Queiroz, C. "The International Road Roughness Experiment: Establishing Correlation and a Calibration Standard for Measurements," World Bank Technical Paper No. 45, The World Bank, Washington DC, January 1986, 453 pp.
- [20] Sayers, M. W. and Gillespie, T. D., "The Ann Arbor Road Profilometer Meeting," FHWA Report FHWA/RD-86/100, July 1986, 237 pp.
- [21] Smith, C. C. et al. "The Prediction of Passenger Riding Comfort from Acceleration Data. Research Report 16, Council for Advanced Transportation Studies, University of Texas at Austin, 1976, 107 pp.
- [22] Carey, W.N., and Irick, P. E., "The Pavement Serviceability-Performance Concept." *Bulletin 250*, HRB, National Research Council, Washington, C. C., 1960.
- [23] ASTM E 867-82
- [24] Gillespie, T. D. Sayers, M. , and Segel, L. "Calibration of Response-Type Road Roughness Measuring Systems." NCHRP Report No. 228, December 1980, 88 pp.
- [25] Hudson, W. R. et al., "Root-Mean-Square Vertical Acceleration as a Summary Roughness Statistic," *Measuring Road Roughness and Its Effects on User Cost and Comfort*, ASTM STP 884, T. D. Gillespie and M. Sayers, Eds., American Society for Testing and Materials, Philadelphia, 1985, pp 3-24.
- [26] Gorski, M. B., "The implication of the International Road Roughness Experiment for Belgium." 65th Annual Meeting of the Transportation Research Board, Washington DC, January 1986.
- [27] "Analyseur de Profil en Long - APL 72." Bulletin 1BAC76, Laboratoire Central de Ponts et Chaussees, 58 Boulevard Lefebvre, 75732 Paris Cedex 15, France.
- [28] Sayers, M., T. D. Gillespie, and W. D. Paterson, "Guidelines for Conducting and Calibrating Road Roughness Measurements," World Bank Technical Paper No. 46, The World Bank, Washington DC, January 1986, 87 pp.
- [29] Spangler, E., and Kelly, W. "GMR Road Profilometer—A Method for Measuring Road Profile." HRR121, Highway Research Board, 1966.
- [30] U.S. Patent No. 4,422,322, issued Dec. 27, 1983.

- [31] Spangler, E., and Kelly, W. "Integration of Inertial Profilometer in ODOT Pavement Management System." Final Report, Surface Dynamics, Inc. Bloomfield Hill, MI. May 1987, 122 p.
- [32] "Descriptive Specification for the Model 8300 Road Roughness Surveyor." K. J. Law Engineers, Inc., Farmington, Michigan, November 1983.
- [33] P. Arnberg, "The Laser Road Surface Tester." Swedish National Road & Traffic Research Institute, Report No. 255A, 1983.
- [34] Gillespie, T.D., and Sayers, M. W., "Methodology for Road Roughness Profiling and Rut Depth Measurement." Federal Highway Administration, Report No. FHWA/RD-87/042, July 1987, 50 pp.
- [35] Sayers, M. W. and Gillespie, T.D., "User's Manual for the UMTRI/FHWA Road Profiling (PRORUT) System." Federal Highway Administration, Report No. FHWA/RD-87/043, July 1987, 66 pp.
- [36] Huft, D.L. et al. "Status of the South Dakota Profilometer." TRR 1117, *Pavement Evaluation and Rehabilitation*, Transportation Research Board, 1987, pp. 104 - 113.
- [37] Sayers, M. W. and Gillespie, T.D., "An Overview of Road Meter Operation in Measuring Pavement Roughness, with Suggested Improvements." Transportation Research Record 836, 1981, pp. 29-35.
- [38] Lucas, J., and Viano, A., "Systematic Measurement of Evenness on the Road Network: High Output Longitudinal Profile Analyser." LCPC Report No. 101, June 1979.
- [39] Still, P. B., and Jordan, P. G., "Evaluation of the TRRL high-speed profilometer." TRRL Laboratory Report 922, Crowthorne, UK, 45 pp.

